الجمهورية الجزائرية الديمقراطية الشعبية

République Algérienne Démocratique et Populaire

Ministère de L'Enseignement Supérieur et de la Recherche Scientifique

Université Ferhat ABBAS Sétif 1

UNIVERSITÉ FERHAT ABBAS - SETIF1

FACULTÉ DE TECHNOLOGIE

THÈSE

Présentée au Département de Génie Civil
Pour l'obtention du diplôme de

DOCTORAT

Domaine : Sciences et Technologie

Filière : Génie Civil **Option : Structures**

Par

TAMRABET Abdelkader

THÈME

Effet de la porosité sur le comportement mécanique des plaques sandwiches épaisses en matériaux à gradient fonctionnel

Soutenue le 12/11/2024 devant le Jury:			
KEBICHE Khelifa	**Professeur**	**Univ. Ferhat Abbas Sétif 1**	**Président**
BOUHADRA Abdelhakim	**Professeur**	**Univ. Abbes Laghrour Khenchela**	**Directeur de thèse**
MENASRIA Abderrahmane	**MCA**	**Univ. Abbes Laghrour Khenchela**	**Co-Directeur**
MANSOURI Mouloud	**MCA**	**Univ. Ferhat Abbas Sétif 1**	**Examinateur**
MESSAI Abderraouf	**MCA**	**Univ. Ferhat Abbas Sétif 1**	**Examinateur**
BELARBI Mohamed Ouejdi	**MCA**	**Univ. Mohamed Khider Biskra**	**Examinateur**

Dedications

This thesis is dedicated to the people who have supported me throughout my education.

"There is nothing noble about being superior to another man;
the true nobility lies in being superior to your previous self."

Acknowledgments

First, I'm so grateful to Allah for blessing me with this work and for giving me the power to make this research possible.

I would like to acknowledge the support, assistance, and contribution given to me by my beloved parents. Warmest thanks to my friends, brothers, and sisters for their great encouragement and all those people who have stood by my side in very hard moments.

My deep and sincere gratitude and special thanks to my teachers and supervisors, **Pr. Bouhadra Abdelhakim** and **Dr. Menasria Abderrahmane**, for their valuable direction, support, and helpful instructions; without them, this work could not see the light.

I would also like to thank the board examiners for devoting their time to reading and evaluating my research work.

Also, I express my respect and deep appreciation to all my teachers and professors for the priceless knowledge they gave me during the long Carriere in the university.

Without forgetting the department staff for the help they provided.

CONTENTS

Contents

LIST OF TABLES

list of tables

LIST OF FIGURES

List of figures

CHAPTER I

CHAPTER II

CHAPTER III

CHAPTER IV

CHAPTER V

LIST OF NOTATIONS

List of notations

z	Thickness direction coordinate.	$\gamma_{xz}, \gamma_{yz}, \gamma_{xy}$	Transverse shear strains.
a, b, h	Dimensions of the plate.	C_{ij}	Elastic constants.
k	Power-law index.	δU	total strain energy.
V_c	Volume fraction of ceramic.	$N_x, M_x^b, M_x^s, N_z, S_{xz}$	Force and moment components
E	Elastic modulus.	$U_{mn}, V_{mn}, W_{mn}, X_{mn}, \Phi_{mn}$	Unknown parameters
ν	Poisson's ratio.	ζ	porosity coefficient
u_0, v_0, w_0, θ and ϕ_z	Unknown displacements	Ω	Load coefficient
$f(z)$	*S*hape function	E_c	Young's modulus of ceramic
$g(z)$	Derivative of the shape function	E_m	Young's modulus of the metal
n, m	Real numbers	L_{ij}	variable parameter
k_1, k_2 A', B'	Coefficients	D_c	Reference bending rigidity
$\varepsilon_x, \varepsilon_y, \varepsilon_z$	Normal strains.	η, η^*, γ	Foam coefficient

ABSTRACT

Abstract

The main objective of this thesis is to study the effect of porosity on the mechanical behavior of thick functionally graded sandwich plates resting on various boundary conditions under different in-plane loads. The formulation is made from a developed sandwich plate using a functional gradient material based on a modified power law function of symmetric and asymmetric configuration. Four different porosity distributions are considered and varied in accordance with material propriety variation in the thickness direction of the face sheets of the sandwich plate; metal foam is also considered in this study on the second model of sandwich, which contains metal foam core and FGM face sheets. A new quasi-3D high shear deformation theory is used for this investigation; the present kinematic model introduces only six variables with stretching effects by adopting a new indeterminate integral variable in the displacement field. The stability equations are obtained by the virtual work's principal and then solved by the Navier-type method for the supported plate. The effect of Pasternak and Winkler elastic foundations is also included here. The present model validated with those from the literature, then the effect of different parameters: porosity parameters, foam cell distribution, boundary conditions, elastic foundation, power law index, ratio aspect, side to thickness, and different in-plane load on the variation of the buckling behavior are demonstrated.

Keywords: Buckling; sandwich plate; functionally graded materials; porosity; plate theory

RESUME

Résumé

L'objectif principal de cette thèse est d'étudier l'impact de la porosité sur le comportement mécanique d'une plaque sandwich épaisse en matériau fonctionnellement graduée, qui repose sur diverses conditions aux limites sous différentes charges dans le plan. La formulation est destinée à un matériau à gradient fonctionnel basé sur une fonction de loi de puissance modifiée de configuration symétrique et asymétrique. Quatre distributions de porosité distinctes sont considérées et variées en fonction de la variation des propriétés du matériau dans le sens de l'épaisseur des feuilles de face de la plaque sandwich. Le deuxième modèle de sandwich contenant un noyau en mousse métallique et des feuilles de face FGM est également examiné dans cette étude. Cette étude utilise une nouvelle théorie de déformation par cisaillement élevé quasi-3D. Le modèle cinématique actuel introduit seulement six variables avec effet d'étirement en utilisant une nouvelle variable intégrale indéterminée dans le champ de déplacement. Le principe des travaux virtuels est utilisé pour obtenir les équations de stabilité, qui sont ensuite résolues par la méthode de type Navier pour une plaque simplement appuyée. Il y a également l'effet des fondations élastiques de Pasternak et Winkler. Le modèle actuel a été validé avec des données de la littérature, puis il a été démontré que divers paramètres, tels que les paramètres de porosité, la répartition des cellules de mousse, les conditions aux limites, la fondation élastique, l'indice de loi de puissance, l'aspect de la ration, le côté d'épaisseur et différentes charges en plan, ont un impact sur la variation du comportement au flambement

Mots clés : Flambement ; Les plaque sandwiches ; Les matériaux à gradient fonctionnel ; la porosité ; Théories des plaques.

ملخص

ملخص

الهدف الرئيسي من هذا البحث هو دراسة تأثير المسامية على سلوك لوحة الساندويتش السميكة المتدرجة وظيفيا والتي ترتكز على ظروف حدودية مختلفة تحت أحمال مختلفة على المستوى. تم تصنيع الصيغة للوحة شطيرة مطورة حديثًا باستخدام مادة متدرجة وظيفية تعتمد على وظيفة قانون الطاقة المعدلة للتكوين المتماثل وغير المتماثل. تمت دراسة أربع توزيعات مختلفة للمسامية وتنوعت وفقا لاختلاف المواد في اتجاه سماكة الصفائح السطحية للوحة الساندويش، كما تم في هذه الدراسة أخذ الرغوة المعدنية في الاعتبار على النموذج الثاني للساندويتش الذي يحتوي على قلب رغوي معدني وصفائح الوجه .FGM يتم هنا استخدام نظرية تشوه القص العالي شبه ثلاثية الأبعاد الجديدة في هذا البحثquasi-3D HSDT ؛ يقدم النموذج الحركي الحالي ست متغيرات فقط ذات تأثير تمديد من خلال اعتماد متغير تكاملي جديد غير محدد في مجال الإزاحة. تم الحصول على معادلات الاستقرار من خلال مبدأ هاميلتون) (Hamilton ثم تم حلها بطريقة نافي) (Navier للوحة المدعومة ببساطة. تأثير أسس باسترناك وونكلر المرنة يشمل هنا أيضًا. تم التحقق من صحة النموذج الحالي مع تلك الواردة في الأدبيات، ثم تأثير المعاملات المختلفة: معاملات المسامية، توزيع خلايا الرغوة، الظروف الحدودية، الأساس المرن، مؤشر قانون الطاقة، الجانب التمويني، الجانب إلى السُمك والاحمال المختلف داخل الخطة على تباين يتم إظهاره على سلوك الاتواء.

الكلمات الرئيسية: التواء؛ لوحة شطيرة مواد متدرجة وظيفيا. المسامية؛ نظرية اللوحة.

GENERAL INTRODUCTION

Introduction

Composite materials technology is new enough that many working engineers have had no training in this area. So, research in composite materials mechanics should be useful not only for the education of new engineers but also for the continuing education of practicing engineers.

Composite materials consist of two or more constituent materials that, although remaining separate and distinct on a macroscopic level in the final structure, have considerably differing physical or chemical properties. There are two phases of this unique family of composites: a matrix phase and a reinforcing phase. Graphite, glass, ceramic, or polymer fibers are commonly used as the reinforcing phase, whereas polymers, though they can also be ceramic or metal, are commonly used as the matrix. Composites are often found in the natural world. The best examples include exoskeletons of insects, wood, bone, and other minerals. Furthermore, composites are taking the place of conventional engineering materials in a wide range of applications related to infrastructure, transportation, architecture, recreation, and industry.

Functionally graded materials (FGMs) are a new sort of composites and more advanced, were developed to overcome the composites' limitations[1]. Bever and Duwez[2] originally proposed FGMs. FGMs, generally made of ceramic and metal, have two main properties: stiffness and high-temperature resistance. These unique properties make them more attractive for engineering applications than conventional composite materials, which are prone to delamination. [3]

The functionally graded material (FGM) is a kind of composite material made from a mixture of metals and ceramics. Then, FGM can have several advantages from two materials, such as increasing stiffness in high temperatures and toughness of metals, so it is useful for structures working in high-temperature environments. In most cases, the term “functionally graded material” denotes a material having changeable properties along one of the linear dimensions, for instance, as a result of a continuous change in its chemical composition, morphology, or structure. The gradient of a given feature of a given material should be understood as a systematic change in this feature observed along the direction determining the behavior of the material during its use.

The earliest FGMs were introduced by Japanese scientists in the mid-1980s as ultra-high temperature-resistant materials for aerospace applications. At the introduction of FGMs, most of the essential concepts and information about the materials were largely unknown outside of Japan. The first book of FGMs written in English was published in London, UK. It contained comprehensive explanations of fundamentals, manufacturing processes, design, and the current applications of

FGMs, which were useful and available for general researchers outside of Japan M. Niino and his colleagues [4].

FGM is widely used in various structural applications in civil and mechanical systems, including thermal systems such as; fiber reinforced polymer (FRP) is another application of FGMs for reinforcing concrete materials as used in bridges cause the FRP materials improve the corrosion resistance of the steel and enhance the life cycle of the material strength, aerospace application to sustain high thermal barrier coating such as rocket nozzle (TiAl - SiC), heat exchanger panels, engine parts (Be-Al), wind tunnel blades, spacecraft truss structure, thermoelectric generators, wear-resistant linings, diesel and turbine engines, etc.), extended to commercial and industrial application such as automotive (combustion chambers (SiC-SiC), engine cylinder liners (Al-SiC) and diesel engine piston (SiCw/Al)… etc.). As the FGM becomes more widely used, more accurate plate theories are needed to predict the FG plate's response[5, 6].

Therefore, it is essential to have the most efficient and precise means of possible calculation, which respect the laws of physics in order to study the behavior of thermal, mechanical, and thermomechanical bending of FGM structures and deduce the evolution of the displacements, deformations, and normal and tangential stress. The determination of the stress (normal and tangential) in beams is usually made from the hypotheses on the shape of the displacement field in the thickness of the model chosen. These theories are designed as an approximation of the reality for one dimension. We know that there can be several differences between them (the CBT, the FSDT, and the HSDTs) in terms of the precision approximation on which they are based.

With the development in the manufacturing process, the FGMs are considered in the sandwich structures industries when the problem of stress concentration between the layers is very important. Hence, the key of this material was the use of a smooth gradient between the two materials, this makes it capable of minimizing the concentration stress between two sandwich layers and the propagation of cracks. FG sandwich plate with designed three-layered forms, core layer combined with top and bottom designed face sheets[7]. During the manufacturing process and due to the restriction in fabrication technique, microvoids can be scattered inside the FGM structure, which perhaps can reduce the resistance of the material, so there are few papers focusing on this phenomenon of the effect of porosity on the behavior of FG structures [8]. Porous gradient materials are multi-functional, with a high weight-to-performance ratio and impact resistance. However, it is important to remember that porosity causes a local loss of stiffness.[9-11].

The objective of this work is to study the effect of porosities on the mechanical behavior of FG sandwich plates resting on various boundary conditions, which takes into account the effect of transverse shear deformation and to get the realistic variation of transverse shear stress across the thickness of the beam. Only three unknown movement functions are used in this theory, while four or more in the case of the other theories of shear deformation. To achieve this objective, our thesis will be structured around five chapters.

The first chapter presents the evolution of composite materials, their effective properties, the history of their development, and their constituent and especially sandwich structures.

The second chapter illustrates synthetic materials with gradient properties, the history of development, and their field of application. As well as the different homogenization methods used to calculate their effective properties.

The third chapter collects a bibliographic study of the different theories used to examine the mechanical behavior of isotropic and sandwich plates, which are equivalent single layer theory, 3D-elasticity theory, zig-zag theory, and layer-wise theory.

The fourth chapter is reserved for analytical modeling of the effect of porosity on the mechanical behavior of thick functionally graded sandwich plates resting on various boundary conditions under different in-plane loads. Their properties are gradually distributed across the thickness according to the power law. Four different porosity distributions are considered and varied in accordance with material property variation in the thickness direction of the face sheets of the sandwich plate; metal foam is also considered in this study on the second model of the sandwich, which contains metal foam core and FGM face sheets.

The last chapter will be dedicated to the result of the comparison and parametric studies carried out and the comment on the result.

A general conclusion closes all of this work, allowing us to review the important results put forward and who’s considering perspective for future work.

CHAPTER I

COMPOSITE MATERIALS AND SANDWICH STRUCTURES

Chapter I: composite materials and sandwich structures

I.1. Introduction:

Emerged in the last century, the new material called composite materials is one of the hotspot research fields in modern technology because of their special characteristics and properties, which provide a highly attractive combination of stiffness, and toughness with lightweight and corrosion resistance, reason to make them suitable in various applications area as mechanical and civil engineering.[12].

The name of composite materials can elaborate the meaning that it's a composition of materials that consists of two or more component materials having totally different physical and chemical properties, typically the composite is an amalgamation of two materials: base material is also called matrix to surround a filler material or reinforcement, this combination produces a new material with unique characteristics Frome the one element constituent.[13, 14]. The concept of composite is well shown in nature, such as wood and bone; on the other hand, composite has been used since antiquity, in the Mongolian arcs when the compressed part was made of corn and the stretched parts made of wood and cow tendons glued together. [15].

I.2. Definition:

The architecture of composite materials usually consists of two or more distinct constituents with different chemical and physical properties, which creates a new material that is enhanced. Most constituent composites are typically made in two main categories: matrix material and reinforcing material. The matrix materials are generally continuous and enclose and protect the reinforcement from deleterious environmental conditions such as harmful chemicals. The reinforcement material may be embedded within the matrix, which will make the composite materials more rigid and strong. Common examples of composite materials are concrete reinforced with steel and epoxy reinforced with graphite fibers.[16].

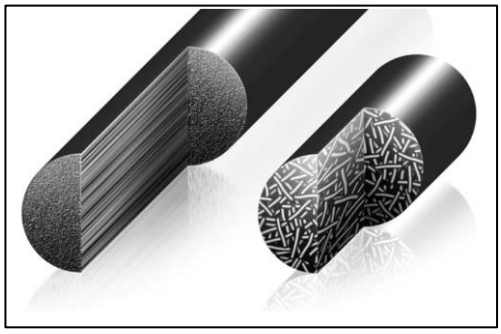

Figure I. 1: composite material

I.3. Isotropic and Anisotropic Materials

The materials can be classified as isotropic, anisotropic, and orthotropic; However, isotropic materials are materials that have the same properties when tested in different directions. Also, normal loads are made only with normal strain; isotropic materials are different from anisotropic materials when the mechanical properties vary in different directions at a point in the body; examples of isotropic materials are glass, plastics, ceramic and metal when the fiber-reinforced Materials such as composite are anisotropic materials show an excellent performance compare with isotropic materials. [17].

I.4. Composite material constituents

Composite materials consist of two main constituents, matrix and reinforcement; these constituents work together to create the desired properties of the composite. The matrix materials surrounding the reinforcement take their relative position and can be introduced to the reinforcement before or after the reinforcement material; the reinforcement is added to impart their special mechanical and physical properties to enhance the matrix characteristics.

I.4.1. Reinforcements

In the conception of composite materials, the reinforcement phase plays an important role in providing the strength and stiffness of composite structures. The reinforcement shape can be shown in the two most common types of fibers and particles:

The reinforcement provides the strength and stiffness of the composite. Increasing the amount of reinforcement increases the strength and stiffness of the composite in the direction parallel to the reinforcement [18].

I.4.1.1. Fibers reinforcement

Fibers are usually used in early composite structures, which are characterized by high-strength materials, low density, and long and slenderness. Currently, the fibers can be made of various materials such as carbon-based fiber, glass-based fibers, and syntenic polymeric fibers. The fibers need to be aligned under loading.[18]

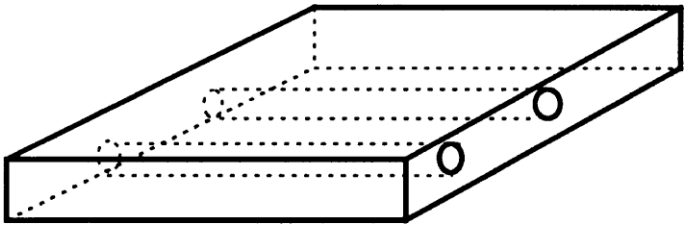

Figure I. 2: fiber reinforcement

I.4.1.2. Carbon-based fibers

Carbon-based fibers (CBFs), which are high-strength and lightweight carbon materials that possess excellent mechanical, electrical, and thermal properties, are mainly used in combination with other materials to create a composite material such as resins or polymers for example, plastic reinforced with carbon fiber, carbon fiber reinforced cement[19]. These carbon fibers are made in several steps, which involve subjecting the suitable precursor material, such as pitch or polyacrylonitrile, to high temperatures in an oxygen-free environment. These types of fibers are the most commonly used in composite materials that provide lightweight and strong materials such as energy construction, sports equipment, aircraft, and biomedicine [20].

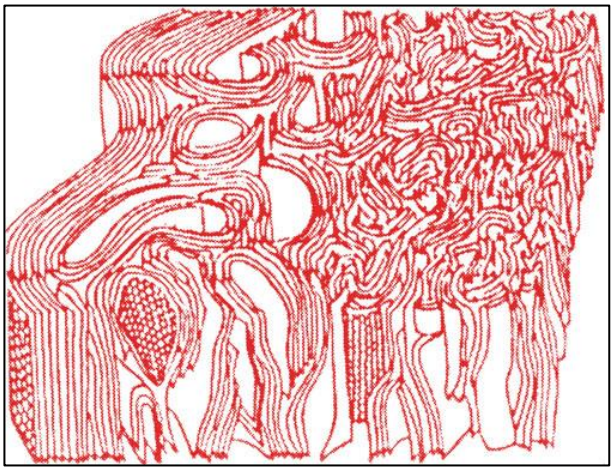

Figure I. 3: Three-dimensional representation of PAN-based carbon fiber

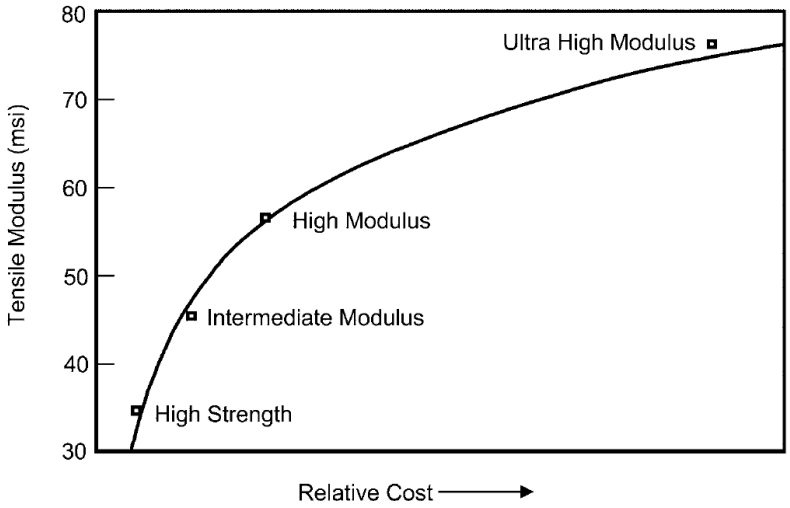

Figure I. 4: Carbon fiber cost increases with the heat treatment used to obtain a higher modulus

I.4.1.3. Glass-Based Fibers

Glass-based fibers are used widely in composite materials because of their excellent tensile strength, stiffness, and weight, which helps to produce suitable materials where weight reduction is critical, such as aerospace and automotive. Furthermore, glass fibers are used in chemical environment attacks because of their high corrosion resistance, in electrical insulation, and under high thermal stress. Compared with carbon fibers, glass fibers have a specific strength and stiffness and are more brittle[21]. The manufacturing process of the glass fibers is classified according to the uses of the composite materials, such as injection molding, filament winding, pultrusion, sheet molding, and hand layup.[22]

Figure I. 5 : Continuous glass fibers (cut from a spool) obtained by the sol–gel technique

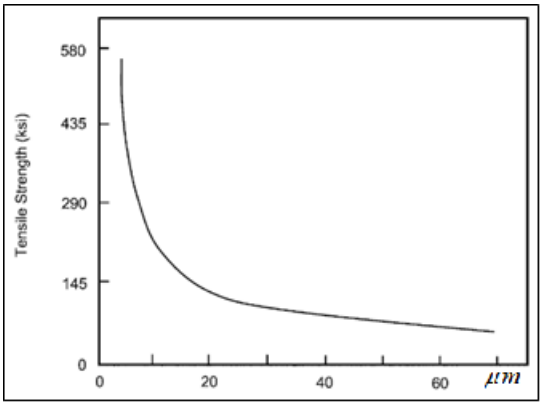

Figure I. 6:Effect of fiber diameter on strength of glass fibers[17]

I.4.1.4. Polymeric Fibers

Polymer fibers are thin and long, made up of plastic or synthetic materials combined with matrix materials, such as a polymer resin or a metal, for reinforcing and improving the composite's mechanical behavior. Furthermore, polymer fiber exists in several types, which are Polyester fibers, Nylon fibers, Polypropylene fibers, acrylic fibers, and Aramid fibers, as shown in (Table I. 1). polymeric fibers may be used in various applications because of their desirable properties, including strength, durability, flexibility, and lightweight nature [23]

Polymeric fibers	Uses
Polyester fibers	This type is commonly used in the textile industry because of its excellent properties (strength, abrasion resistance, and low moisture absorption)
Nylon fibers	This type is a popular polymer widely used in clothing fabrication, ropes, and fishing nets. It has high tensile resistance and good elasticity.
Polypropylene fibers	Polypropylene is commonly used in geotextile carpeting and other industrial fabrication due to its resistance to moisture, mildew, and staining. It has an excellent chemical resistance.
Acrylic fibers	This type is used in clothing, blankets, and carpets because of its softness and warmth.
Aramid fibers	For example, Kevlar and Nomex are used in ballistic protection and aerospace components because of their high heat resistance and strength-to-weight ratios.

Table I. 1: fibers and their uses

I.4.1.5. Particles reinforcement

Particle reinforcement usually enhances the strength, stiffness, toughness, wear resistance, and other desired properties of the composite materials by adding a different material with several shapes,

sizes, and compositions to the matrix; maybe the particle reinforcement is not effective like long fibers, but they are used in various field as ceramic, metal and organic particles. The distribution and the dispersion of these reinforcements determine the properties of the composite materials. Concrete and aggregates are the simplest examples of composite materials with particle reinforcement when the cement is the matrix, and the aggregates provide strongness and stiffness.[24]

I.4.2. Matrix

The matrix is the continuous phase in composite materials that surrounds and binds the fibers or the particle reinforcement. On the other hand, the matrix acts like a support structure that holds the reinforcement and, at the same time, transfers the loads between the reinforcement. The matrix material can be a polymer, ceramic, or metal.[25]

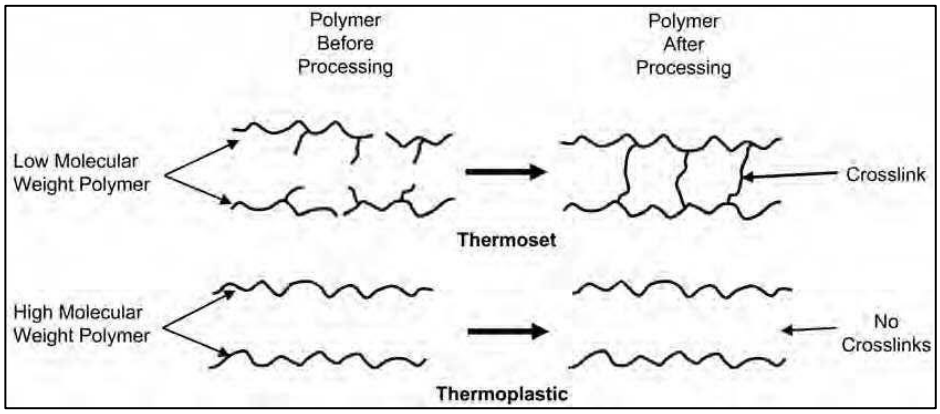

Figure I. 7 : Comparison of thermoset and thermoplastic polymer structures[17]

I.4.2.1. Thermosets

The thermoset is the common polymer matrix used in composite structures, which cannot be melted and reformed many times. Crosslinking is the most common process for manufacturing thermosets; the polymer is subjected to chemical additives in a temperature environment, producing three-dimensional structures. This type of matrix, based on its characteristics, perhaps can be used in applications requiring high strength, durability, and resistance to heat and chemicals. The most frequently used thermosetting matrices are cited in the table (Table I. 2).[25]

Polyesters	Used for continuous and discontinuous composite, it is relatively inexpensive with processing flexibility.
Vinyl Esters	Similar to polyesters with better moisture resistance
Epoxies	Have a better high-temperature resistance than Polyesters and Vinyl Esters, have a high-performance matrix system for primary continuous fibers.

Bismaleimides	High-temperature resin matrices are for use between 275–350 °F with epoxy-like processing.
Cyanate Esters	High-temperature resin matrices for use between 275–350 °F with epoxy-like processing.
Polyimides	Very-high-temperature resin systems for use between 550–600 °F. Very difficult to process.
Phenolics	Have a high-temperature resin system with fire and smoke resistance, used for aircraft interiors.

Table I. 2: Relative characteristics of thermoset resin matrices[17]

I.4.2.2. Thermoplastics

Thermoplastics are another type of matrix polymer in the form of linear chains, which can be reformed many times without decreasing their properties. The manufacturing processes of thermoplastics are passed through many stages; firstly, they are heated, then formed by injection, extrusion, molding, or thermoforming, and cooled to get their last shape. Thermoplastics can be made as flexible as rubber, as rigid as metal or concrete, and as transparent as glass. Due to their excellent properties, which are high thermal and electrical insulators, high corrosion resistance, and other environmental effects, the thermoplastics can be used in various applications. In contrast, the thermoplastics materials act as binders and support; the fibers enhance the mechanical properties of the composite materials.[25]

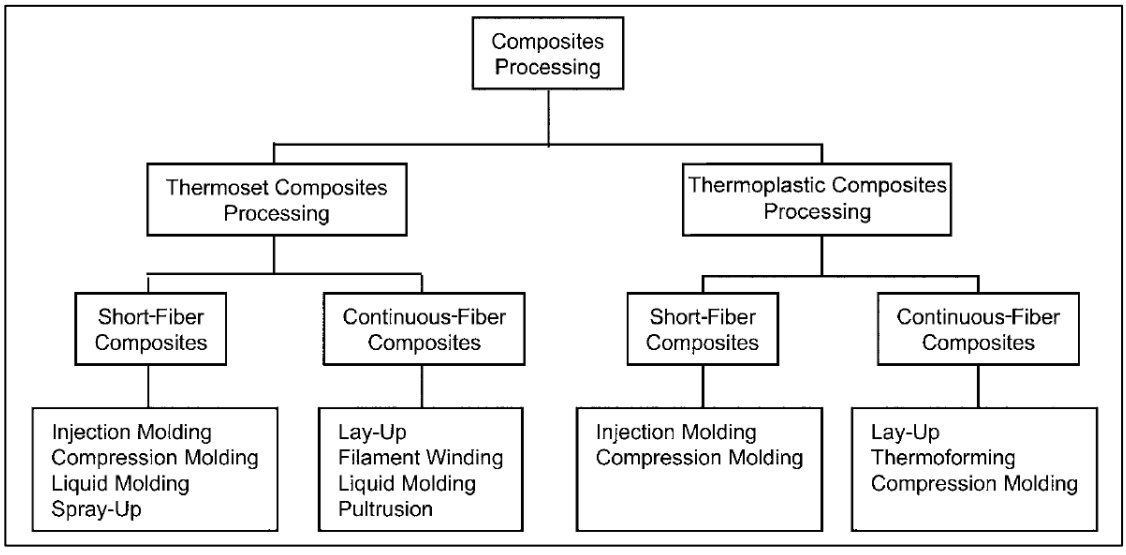

Figure I. 8: Major polymer matrix composite fabrication processes [17]

I.4.3. Interface

An interface in composite materials is the region of the contact between two or more different material parameters such as density, elastic modulus, coefficient of thermal expansion, etc.… The

interface has an important role in determining the overall performance and properties of the composite materials cause some reinforcement may not be compatible with the matrix, which causes premature failure of the composite; an example of interface ultrahigh molecular weight polyethylene (UHMWPE) fibers have poor wettability with epoxies so the materials chosen for the composite should have compatible properties to ensure good adhesion and bonding at the interface, [26].

I.4.4. Gelcoat

Gelcoat or 'Gel Coat': During the manufacturing process of composite materials, the gel coats are used to the mold surface before the reinforcements are added, specifically in fiberglass reinforced or epoxy resins; the most common gel coats are thermosetting polymers based on epoxy or unsaturated polyester resin chemistry. The gelcoat layer becomes an important part of finishing the composite structures by protecting the outer layer underlying the laminate for the composite from UV radiation, moisture, and chemicals to assure the durability, longevity, and also aesthetic quality of the composite materials, Many marine craft and some aircraft are manufactured using composite materials with an outer layer of gelcoat [27]

Figure I. 9: Gelcoat (from SIKA France)

I.5. Composite materials processing

Several suitable methods of manufacturing composite materials are available today; here some of these methods are listed:

I.5.1. Laminating Process

Laminating is a process of bonding or fusing multiple layers of material to create a single composite structure. The purpose of laminating is to enhance the properties of the base material or to combine different materials to achieve specific characteristics. [28-30]

Figure I. 10: Robot system lays thermoset, thermoplastic or dry fiber[31]

I.5.2. Filament-winding Process

Pipe bends and other non-axisymmetric composite pieces can be made with the help of winding. As seen in the image, continuous prepreg sheets, roving, and monofilament are driven by multiple pulleys and made to flow through a resin bath and gather over a revolving mandrel. Following the application of enough layers, the mandrel with the intended product shape is next prepared for room-temperature curing.[32]

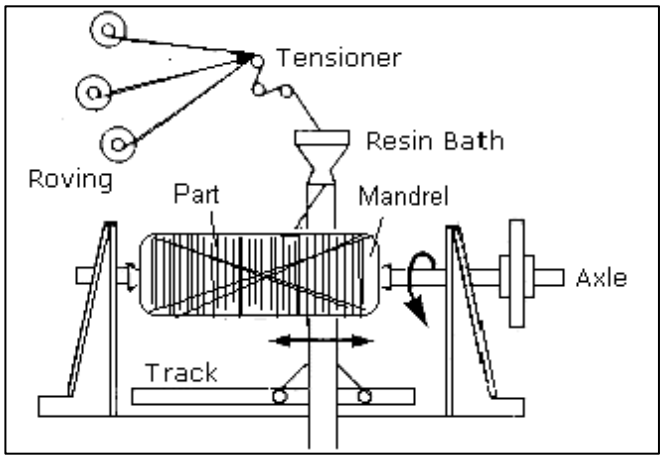

Figure I. 11: Filament winding. [33]

I.5.3. Pultrusion Process

The fiber bundles are continuously transported through a resin matrix bath during the pultrusion process, after which they are dropped into a heated die or series of dies. Following the curing process, the pultrusion is saw-cut to the required length, transforming the component from a wet saturated reinforcement to a solid par. Parts having intricate shapes, like tubing, channels, I-beams, Z sections, and flat bars, are produced by this method. The pultrusion method for composites is similar to that of metal extrusions, with the exception that the part is pulled during the pultrusion process from the die's exit end.[34].

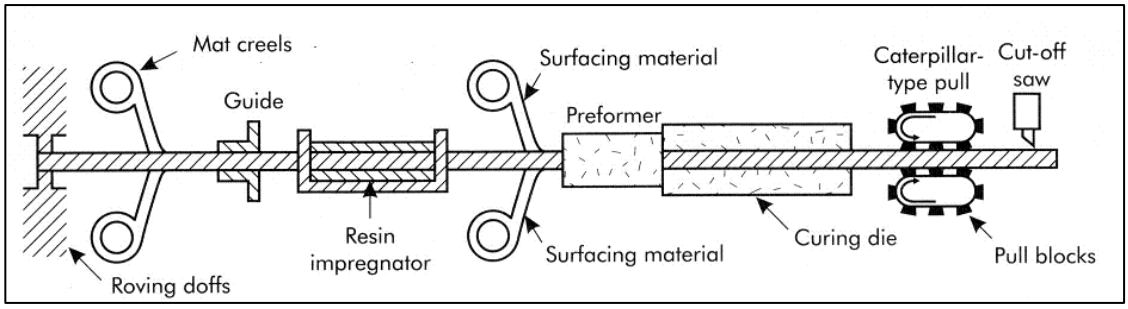

Figure I. 12: Pultrusion process.[33]

I.5.4. Resin Transfer Molding Process

Resin transfer molding (RTM) is a closed-mold composite manufacturing process that produces finely detailed, well-made products with accurate measurements and a smooth surface. It is widely used in the marine, automotive, and aerospace industries to make components with remarkable strength-to-weight ratios.[30, 31]

I.5.5. Injection molding process

Injection molding allowed for the extremely accurate and quick cycle time production of composite products. As seen in Figure I.11, a typical injection molding process entails putting pelletized fiber composites through a hopper and then transporting them using a heated barrel and screw. Once the required amount has melted in a barrel, the material is injected into the mold by the screw using a nozzle, where it cools and assumes the proper shape.[35]. Injection molding for thermoplastic encapsulations of electronic devices utilized in the medical field has been shown to be highly effective. [36]. Surface treatment of biocomposites results in enhanced fiber-matrix compatibility and consistent fiber dispersion inside the matrix material. [37].

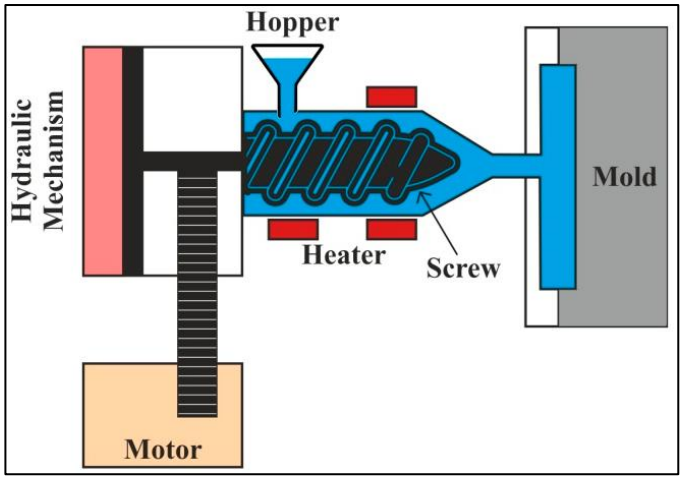

Figure I. 13: Injection molding process.

I.5.6. Additive manufacturing process

The innovative technique of additive manufacturing, commonly referred to as 3D printing, creates three-dimensional items layer by layer using digital design data. Technologies for additive manufacturing come in a variety of forms, each with a distinct procedure.[38]. Given its broad range of options for selecting fiber volume and orientation, additive manufacturing (AM) is one of the most advanced technologies in the composites industry. It is perfect for prototype and customization since it can swiftly translate design concepts into the finished product without wasting materials or cycle time.[39].

I.6. Structural Composite Materials

I.6.1. Laminates

Laminate composite structures are composed of layers or laminae with different materials cemented together, such as the orientation of the fibers, which vary with each successive layer. The laminates are oriented in a specific manner to get a high property, and it's worth mentioning that the laminate's response depends on the properties of each lamina and the order of each one. Due to their high strength-to-weight ratio and high mechanical properties, these structures may be used in various industries as aerospace and automotive; the vast majority of the laminated structure is the modern ski [40]

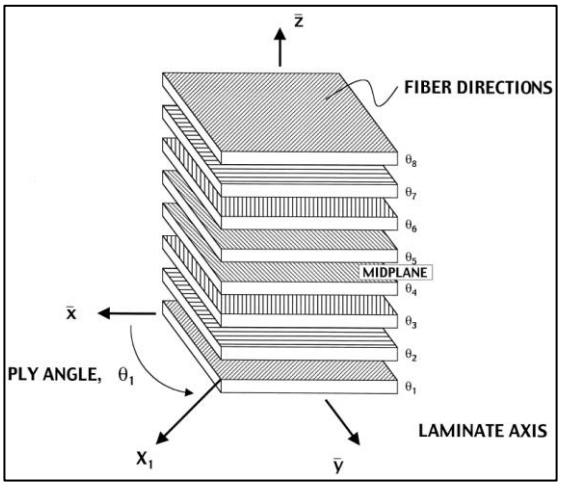

Figure I. 14: Laminates composite structures

I.6.2. Sandwich panels

Sandwich composite materials are specially engineered structures made up of three layers: attaching two face sheets to a lightweight material core which is made of low-density and low-strength material, providing the thickness between the sheets and the distribution of the loads, and

enhancing the bending stiffness, while the face sheets are usually fabricated by high strength materials as glass fiber, Carbon fiber or metal fiber which can protect the core from damage. The sandwich structures are widely used in various fields, including aircraft panels, turbine blades, civil engineering structures… etc.[41].

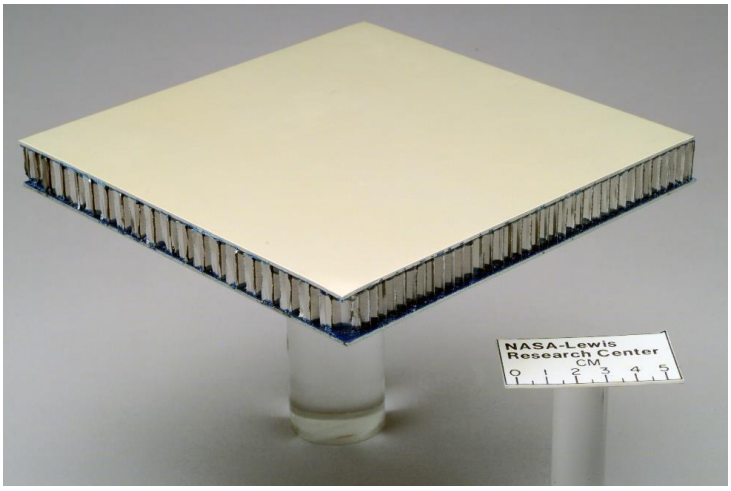

Figure I. 15: sandwich panel

I.6.2.1. Properties of sandwich structures

The strength of the composite material is dependent largely on two factors:

- The outer skins: The bending moment will cause shear stress in the material if the sandwich is supported on both sides and then strained by a force applied in the center of the plate. The top skin is compressed while the bottom skin is in tension as a result of the shear stress. These two skins are separated from the core substance. The composite is stronger, and the core material is thicker. This principle functions similarly to that of an I-beam.[42]
- The contact between the skin and the core: The adhesive layer experiences some shear force as well since the shear stresses in the composite material change quickly between the two. The most likely outcome will be delamination if the adhesive link between the two layers is sufficiently weak. [42]

I.6.2.2. Layout of a sandwich composite

I.6.2.2.1. Core

The low-strength, low-density material is called the core, and its main function is to maintain the distance between the outer faces so that the moment of inertia of a cross-section of the sandwich skin and its flexural rigidity is large.[43]

The core of a sandwich structure can be almost any material or architecture. Still, in general, cores fall into four types, as shown in Figure I.15: (a) foam or solid core, (b) honeycomb core, (c) web core, and (d) corrugated or truss core.

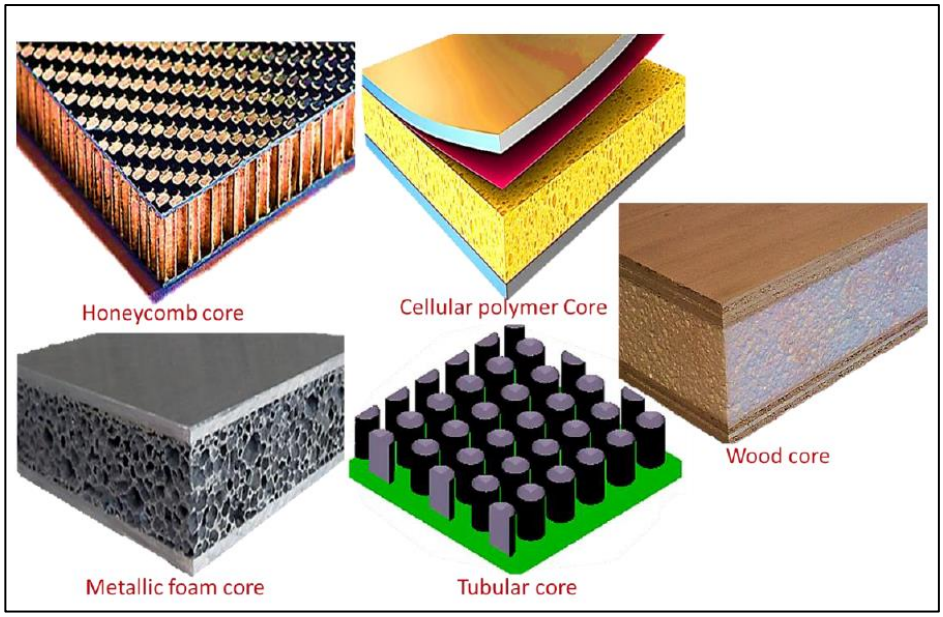

Figure I. 16: Various cores of sandwich

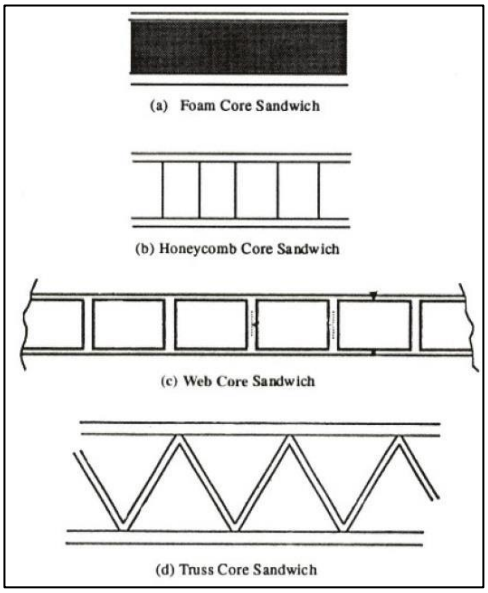

Figure I. 17: Types of core sandwich

I.6.2.2.1.1.Cellular Polymer Foam Core

A cellular polymer foam sandwich core is another type of low-density composite material used in different industries. This type of material has key features such as low cost, easy production, impact energy absorption, and good thermal and acoustic insulation. The sandwich structure containing polymer foam core has excellent thermal and mechanical properties, such as shock wave

absorption, blast mitigation, and good insulation. Various types of polymer foam, such as polyurethane, polyethylene, or polystyrene [44, 45].

I.6.2.2.1.2. Metallic Foam Core

A metallic foam sandwich core is an innovative and unique material that combines the properties of metal with the benefits of a cellular foam structure. This type of material has the advantage of better energy absorption, retaining the thermal and electrical conductivity of the base metal, as well as acoustic and thermal insulation. The sandwich structure containing a metal foam core with composite face sheets has high blast resistance and crashworthiness; the metallic foam core performs better than the perfect density core. Nonetheless, the development of these materials makes them capable of use in various industries, such as civil engineering constructions.[46]

I.6.2.2.1.3. Honeycomb Core Sandwich Structure

Another important and effective type of sandwich core is honeycomb structures, which are versatile and valuable composite materials that have revolutionized many fields by providing better shock wave propagation, high stiffness, and sound damping. Aluminum and polymers such as Nomex have been included as honeycomb cores. The sandwich composite structure containing a honeycomb core structure is a specific type of composite structure. Moreover, this combination creates a lightweight, strong, and performance material with a wide range of applications in various industries such as Aerospace, Marine, Construction, and Wind Energy.[47]

I.6.2.2.1.4. Wood Core-Based Structure

The wood sandwich core is another type of material used as the central core enclosed between two outer composite faces, usually glass fiber-reinforced polymer or carbon fiber-reinforced polymer. The wood core sandwich has been used for thermal stability and design engineering.[48]

I.6.2.2.2. Skins (faces)

These are the outer layers that provide protection and carry the tensile and compressive stress in sandwich structures. The face sheets are usually made of steel, stainless steel, and aluminum with fiberglass, carbon fiber reinforced, or other high-strength materials.[43]

I.6.2.2.3. Adhesive

An adhesive is a method used to join two or more components; in sandwich structures, it's used to create a strong bond between the face sheet and the core material when the concentration of the stress is very important. Hence, the adhesive layer is the critical factor to achieve the desired

mechanical properties of the sandwich structure. The most common types of adhesives used in sandwich composite materials are Epoxy Adhesives, Polyurethane Adhesives, Acrylic Adhesives, and Film Adhesives. [43]

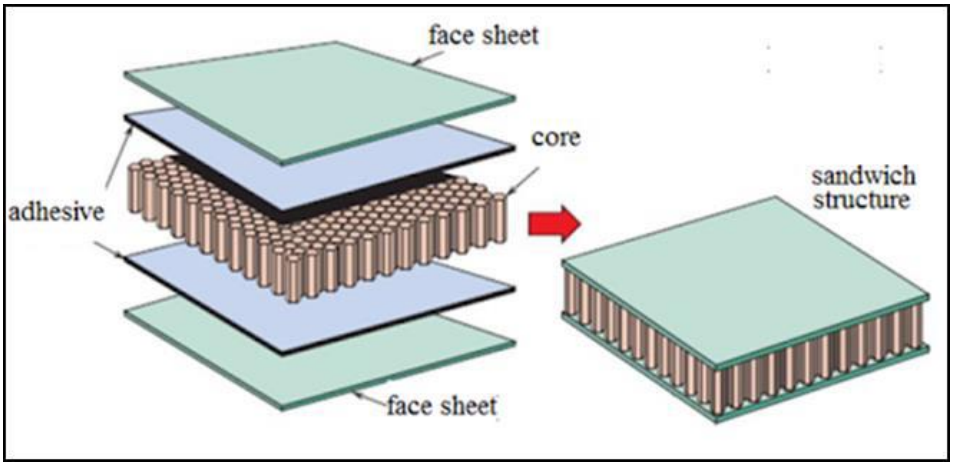

Figure I. 18: Layout of a sandwich composite

I.6.2.3. Design optimization

a) Strength

The concept of sandwich structures provides higher bending strength and stiffness with a lightweight core surrounded by high-modulus skins that resist tensile and compressive stress. Therefore, these properties have increased the usage of sandwich structures in various areas in the last few years. [49].

b) Stiffness

The core material in sandwich structures plays an important role in offering high bending and torsional stiffness, making it resistant to deflection and rotational loads at low weight. [49]

c) Weight

With the use of lightweight core material such as foam or honeycomb, the sandwich structure could be strong and rigid while reducing its weight[49]

d) Economic considerations

Due to the complexity of the manufacturing of sandwich structures, the production costs could be more expensive, but, on the other hand, these structures' enhanced durability and reduced maintenance can lead to the lifetime of the sandwich structures [49]

I.7. Advantages of Composites in Structural Design

The composite structure added numerous advantages to the structural design, which is cited below.

I.7.1. Flexibility

Composite materials are specific materials containing two or more different constituents, such as fiber and matrix, to create a product with unique characteristics not present in any single material, as well as flexibility. The fiber, usually made from carbon or glass, guarantees the strength and stiffness of the composite. They are included in a matrix material such as a polymer or epoxy, which acts as a load transducer between the fibers, so the composite can be produced to offer the maximum stiffness and rigidity to highly stiffness and pliable. The flexibility of composite materials is related to many factors, such as the type of fiber, fiber orientation, and the properties of the matrix…. Etc. This advantage makes the composite able to be used in various fields.[24]

I.7.2. Simplicity

The simplicity of composite materials is related to their special properties and Versatility, which are design flexibility, lightweight construction, corrosion resistance, and ease of repair. These characteristics, despite their engineering, reduce costs and enhance the performance of composite components in various applications.[24]

I.7.3. Efficiency

The efficiency of composite materials stems from their ability to be performance, strong, lightweight, easy in manufacturing processes, and low costs; these properties contribute to increasing their efficiency and enhance the ability to use them in even broader applications.[24]

I.7.4. Longevity

The long-term structural integrity of composite materials is provided by their Resistance to Corrosion, Fatigue Resistance, Environmental Stability, Design Flexibility, Maintenance Requirements, Manufacturing Quality, and Continuous Improvements. These characteristics make composites a suitable choice for applications that require longevity structural. [24]

I.8. Applications of Sandwiched Composite Structures

I.8.1. Aerospace Structures

Sandwich composite structures have been used in the aircraft sector; however, only certain structures have shown good performance. Success has been achieved with the honeycomb core made of aluminum, aluminum alloy, and Nomex. Aluminum alloys and composites made of carbon, Kevlar, or glass fiber have been utilized as face sheets or skin for aerospace sandwich panels.

Typically, face sheets are developed with a thickness of less than 2 mm. Sandwich composites, both symmetrical and asymmetrical, have been used in the building of airplanes and spacecraft.[50]

I.8.2. Automotive

The car industry has experimented with a number of cutting-edge production techniques and structural designs to produce lightweight, higher-performing cars. Sandwich composite structures have replaced conventional metallic materials such as steel and aluminum. High flexural strength, stiffness, impact resistance, thermal insulation, and energy absorption are characteristics of sandwich constructions used in cars. For use in automotive applications, manufacturing procedures for sandwich composite structures with different geometries have been devised.[51]

I.8.3. Energy Application

Energy absorption characteristics have been incorporated into engineering constructions in addition to load carrying, fatigue resistance, and high-pressure tolerance qualities. Sandwich structures are one type of engineering structure that has been successfully used to the importance of energy absorption. Different core/face materials, geometries, and manufacturing procedures have been used to build engineering structures based on sandwich composites. The sandwich constructions need to be lightweight, energy-absorbing devices. When there is a dynamic event, like a crash impact, ballast, or high strain rate, the sandwich structures may absorb energy.[52]

I.9. Conclusion

The biggest advantage of modern composite materials is that they are light and strong. By choosing an appropriate combination of matrix and reinforcement material, a new material can be made that exactly meets the requirements of a particular application. Composites also provide design flexibility because many of them can be molded into complex shapes. The downside is often the cost. Although the resulting product is more efficient, the raw materials are often expensive. Composites know their main applications in transport, construction, aerospace, etc. These applications need knowledge of thermophysical properties and methods of measuring these materials, which is the subject of the next chapter.

CHAPTER II

FUNCTIONALLY GRADED MATERIALS

Chapter II: Functionally graded materials

II.1. Introduction:

The traditional composite materials offered higher properties to single materials, such as specific strength and stiffness, which made them able to be used in specific applications such as aircraft and space structures; in another way, the traditional composite material failed, the point of failure is usually at the same level where two different materials are joined together to create a weak area in the material when higher stresses are concentrated. The interface between discrete materials can result in large plastic deformation and propagation of cracks in the material.

To overcome the problem of the interface in traditional composite materials, several researchers proposed new composite materials technology In the 20th century; Bever and Duwez in 1972 [2] originally proposed functionally graded materials and then developed by Japanese scientists in mid-1982 in which material properties such as Young modulus, mass density, and Poisson's ratio usually vary continuously across the thickness direction to optimize the performance of the materials for specific applications[53].

The breakthrough of modern high technology requires more recent materials with extra special properties and functions to resist complicated environments such as thermomechanical loads.[54]. FGM is made from two components, usually ceramic and metal, ceramic with high-temperature resistance and metal for high mechanical loads; the material changes gradually from one to the other based on volume fraction.

II.2. History of FGM

The general idea of structural gradients first was advanced composites and polymeric materials in 1972 by Bever and Duwez [2, 55]. In 1984, Japanese researchers were the first to look to treat the problem of concentration stress at the interface in a multi-layer panel at the National Aerospace Laboratory. In 1985, the continuous texture was proposed to increase the strength of the ceramic coating and eliminate thermal stress.[56]. The control of the property could be extended to another concept, which is to propose new properties and functions to any material by gradually changing in texture or constituents[57]. The term functionally gradient materials was first known in 1986, and it soon became abbreviated as FGM. It was realized that as FGMs are not uniform materials, extensive research would be required in design approach, theoretical modeling, processing, and evaluation in order to produce them. Thus, "Fundamental Studies on the Relaxation of Thermal Stress by Tailoring Graded Structures," a five-year research program, was started in Japan in 1987.[58]. The program's

main goal was to create FGMs that could withstand high temperatures and be employed in a hypersonic spacecraft. The outcomes of these research and development initiatives have been shared globally since 1989 through conferences, publications, papers, and exchange initiatives. Every two years since 1990, a worldwide symposium on functionally graded materials (FGM) has taken place in various cities across the world, including Sendai, San Francisco, Lausanne, Tsukuba, and Dresden. The FGM idea is currently used globally in many different material industries. Following a discussion at the Third International Symposium on FGMs in Lausanne in 1994, the whole name was changed in functionally graded materials in 1995 since it is grammatically and descriptively more correct.

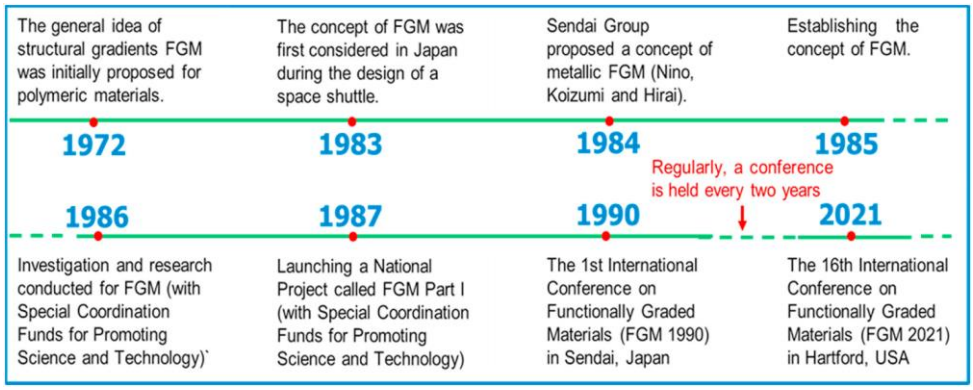

Figure II. 1: Historical overview of relevant milestones in the research and development of FGMs

II.3. Definition:

The metal-ceramic reinforced-based FGM is an advanced engineering material that is able to survive in high-temperature environments by exploiting the combination of the properties of both materials; ceramic has a good resistance in high temperatures, while metallic has a good mechanical resistance. Functionally graded materials (FGMs) are designed with changing properties of one material to the other across the thickness of the material, which helps to increase performance and eliminate the problem of concentrated stress.[59]

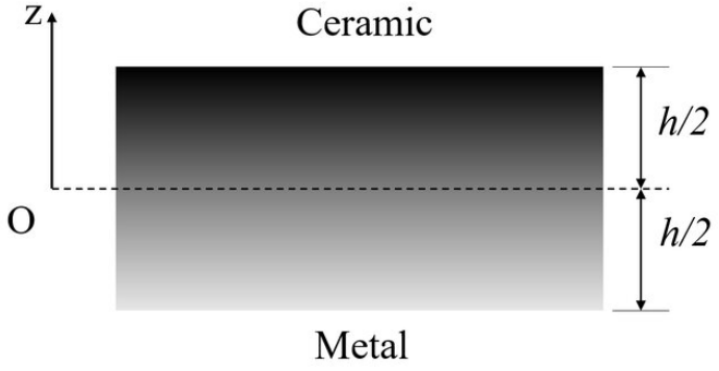

Figure I. 19: A functionally graded material layer[60]

II.4. Types of Functionally Graded Materials

Functionally Graded Materials are fabricated by taking into account the gradient in composition, properties, and microstructure to achieve high-performance material, the different types of FGM are illustrated here:

II.4.1. Compositionally Graded Materials:

Compositionally graded materials (CGMs) are advanced composite materials that vary gradually in chemical composition at the microscale or nanoscale level from one element to another to achieve a specific property, such as mechanical and thermal resistance and electrical conductivity. Powder mixing, powder metallurgy additive manufacturing (3D printing), chemical vapor deposition, and other specialized processes for fabricating the CGMs and controlling the composition gradient [61].

II.4.2. Structurally Graded Materials:

Structurally graded materials (SGMs) are advanced composite materials that vary gradually in their microstructure when parameters such as grain size, crystallographic orientation, and porosity are controlled to achieve the required properties. The SGMs are obtained by various processes such as powder consolidation, heat treatment, or additive manufacturing methods[62].

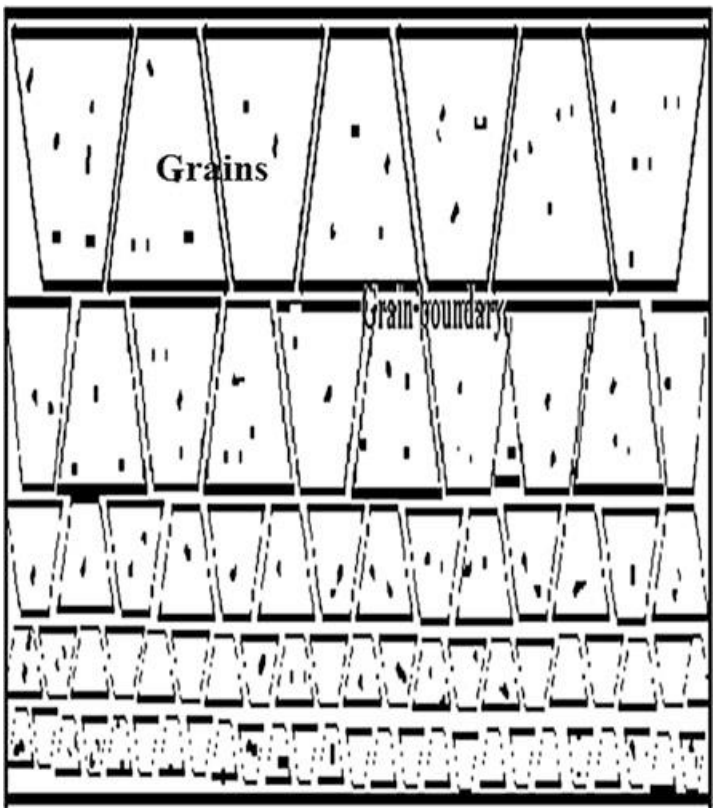

Figure II. 2: Structurally graded materials

II.4.3. Functionally Graded Coatings:

Functionally graded coatings (FGCs) are advanced materials that vary gradually in chemical composition, microstructures, and properties across their thickness. The FGCs are designed to enhance wear resistance, corrosion resistance, and thermal resistance, and the coated material also provides an optimal performance of the coated surface. The FGCs were obtained by using the powder metallurgy method, electro-position method, and thermal spray method. The ceramic, metal, and polymer coating have been used in various areas of applications such as aerospace, automobile, microelectronics, and biomedical fields.[63]

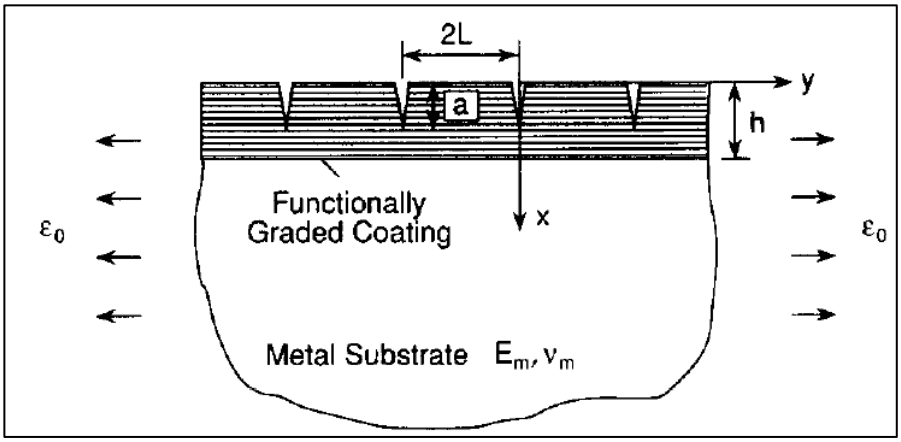

Figure II. 3: Functionally graded coatings

II.5. Classifications of FGMs

II.5.1. According to the state during FGM processing

Based on the state of FGM processing, methods can be broadly classified into solid-state processes, liquid-state processes, and deposition processes, Deposition methods represent highly advanced technologies that are used for high accuracy and small products, solid-state-based FGMs are utilized for highly stressed thermo-mechanical components and Liquid-state processes are usually used for large products of relatively lower property control. [64]

II.5.2. According to the FGM structure

Based on the structure of FGM, it can be classified as continuous and discontinuous graded material. At first, one is when the zone of separation is not clear, while in the second one, the material ingredients change in discontinuous gradation. Furthermore, the continuous and discontinuous can be classified into three groups, is shown in Figure II.4. The dental is the most common field of application of discontinuous graded material, the outer and inner part of the tooth has different work, the outer parts has a sure-resistance when the inner part is produced ductile to absorb the shock and

make it stronger in fatigue life. So, the different properties of the teeth in each layer will create a discrete gradient structure. When the concentration of the stress between two different layers (interface) is avoided, the continuous graded material is used; for example, the sound is reflected if the interface between two layers of the sound-absorbing materials is different [64].

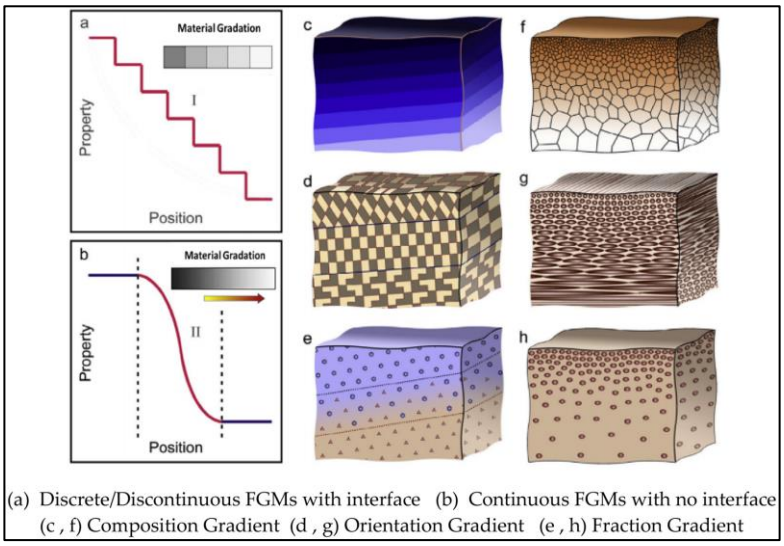

Figure II. 4: FGM structures

II.5.3. According to the type of FGM gradient

Functionally graded materials can be classified into three bands, as shown in Figure II.5; functionally graded composition (FGC) seems to materials have a gradual change in composition across the bulk volume of material, and the behavior of FGC is specified to resist under thermal and mechanical loading such as a wear resistance[65]. Functionally graded porosity (FGP) is material that has gradual variation in pore structure across the volume, which can change their mechanical properties such as mechanical strength, thermal conductivity, and permeability[66]. Material with varying microstructures across the bulk volume (SGMs) could be achieved by controlling some parameters like grain size, and crystallographic orientation[67].

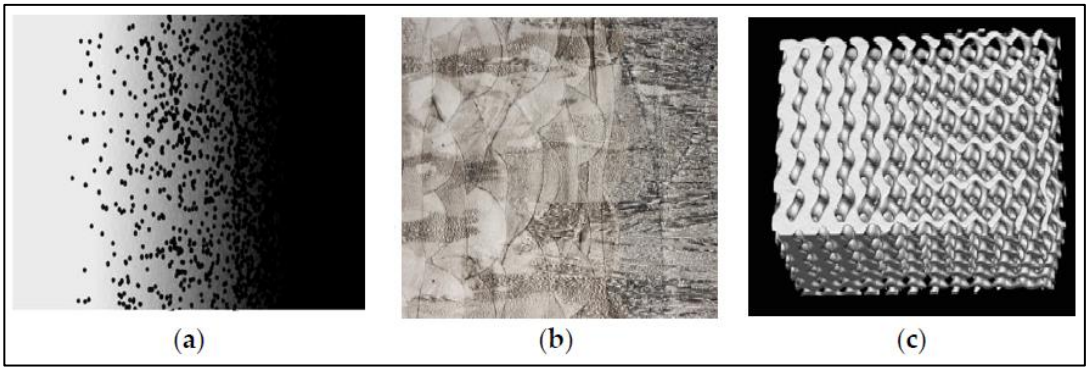

Figure II. 5:Classification of functionally graded material (FGM) according to (a) composition[68]; (b) microstructure[67]; (c) porosity[69].

II.5.4. According to the FGM scale and dimensions

Functionally graded materials may be classified into two groups according to their dimensions: thin FGM and Bulk or thick FGM. Thin FGM has a gradual change in composition and properties in small thickness based on different process methods like physical vapor deposition (PVD), thin FGM ranges between 5nm and 500nm, while thick FGM can cover 5-350 mm, and is manufactured by different methods as powder metallurgy to be a gradient in over a significant portion of the material's thickness. [70].

II.5.5. According to the nature of the FGM gradation process

Another classification of FGM is the nature of the gradation process, which is divided into FGM based on constructive methods and transport-based methods. The first processes are technologically and economically feasible, especially for prototypes and small batch production, using powder sintering techniques, vapor deposition techniques, and additive manufacturing techniques to produce the design gradients and properties[71]. The second process is the appropriate method based on natural transport phenomena to produce compositional and microstructural gradients of FGM using mass transport technique, settling and centrifugal technique, and thermal technique[72].

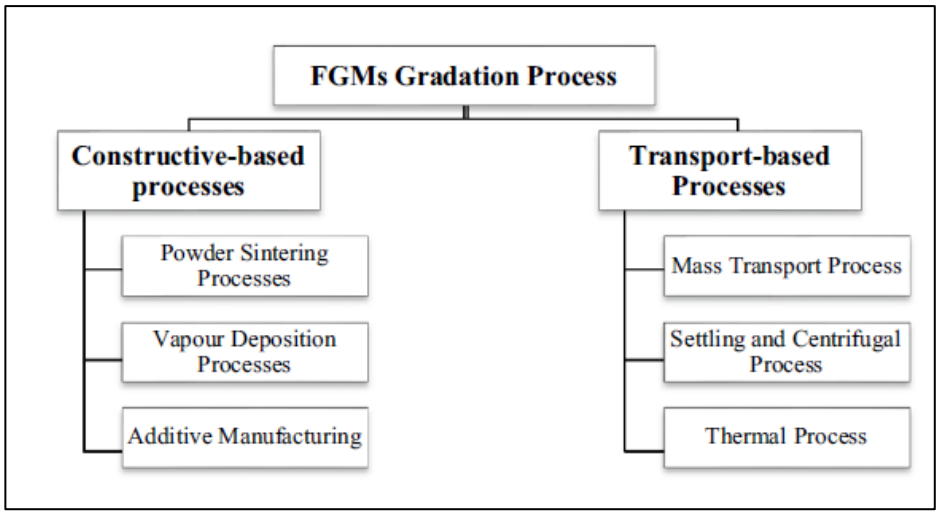

Figure II. 6: FGM gradation process

II.5.6. According to the field of application

Functionally graded materials (FGMs) have diverse applications across various fields due to their unique property gradients. Here are some notable application areas of FGMs:

- ***Aerospace Industry:***

Functionally Graded Materials (FGMs) offer several potential applications in spacecraft due to their ability to tailor material properties to meet specific engineering requirements [73]. FGMs

offer unique opportunities to enhance the performance, reliability, and functionality of both spacecraft and aircraft across a wide range of applications, from thermal protection and structural reinforcement to radiation shielding and optical instrumentation. As advancements in materials science and manufacturing technologies continue, FGMs are likely to play an increasingly important role in the aerospace industry. [74].

Figure II. 7: FGMs pieces in aerospace applications.

- ***Automotive Engineering:***

FGMs can be used in cylinder liners to improve their thermal conductivity and wear resistance. FGMs can enhance engine performance and durability by optimizing attributes like hardness and thermal expansion by grading the material composition from the inner to the outer surface. FGMs can also be used to enhance heat dissipation and wear resistance in valve seats and guides. FGMs can survive high temperatures and pressures encountered during engine operation by customizing the material properties along their length or thickness, which results in longer service life and less maintenance[75].

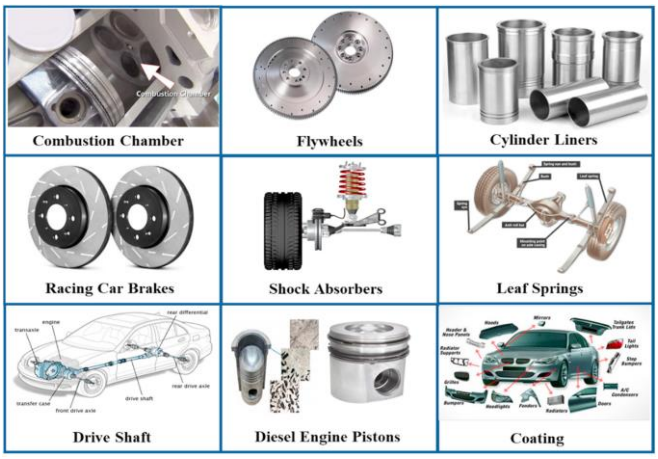

Figure II. 8:FGMs pieces in automotive applications.

- ***Biomedical Devices:***

Apart from the domains above, FGMs, including gradient structures, have significant promise for applications in energy, electronics, and optoelectronics. FGMs can be incorporated into the electrodes and electrolytes to improve the longevity and performance of batteries and fuel cells. FGMs can be designed to increase energy density, cycle life, charge/discharge rates, and ion conductivity by incorporating graded porosity, electrochemical activity, and these properties. FGMs can also be used to improve light absorption, charge transport, and photovoltaic efficiency in solar cell materials. FGMs have the potential to improve solar energy conversion by optimizing light harvesting and electron-hole separation through the customization of material composition and bandgap along the layers of the solar cell[76].

- ***Energy and Electronics:***

In addition to the previous fields, the FGMs with gradient structures present high potential for energy and electronics as well as optoelectronic applications. FGMs can be used in electrodes and electrolytes for batteries and fuel cells to enhance their performance and durability. Engineering FGMs with graded porosity, ion conductivity, and electrochemical activity can improve charge/discharge rates, cycle life, and energy density. FGMs can also be applied in the development of solar cell materials to optimize light absorption, charge transport, and photovoltaic efficiency. By tailoring the material composition and bandgap along the solar cell layers, FGMs can enhance light harvesting and electron-hole separation, leading to improved solar energy conversion. [75]

- ***Civil Engineering:***

The application of FGMs can restore buildings, tunnels, and other aging infrastructure. FGMs can effectively strengthen and repair deteriorating structural parts, such as concrete beams, columns, and decks, by developing them with graded mechanical properties. FGMs can be used in slope stabilization, foundation strengthening, ground reinforcement, and other soil stabilization and ground improvement approaches. FGMs can improve the soil's bearing capacity, settlement resistance, and shear strength by adding them to soil-cement or soil-grout combinations. FGMs can be used in smart constructions as sensing and actuating materials for vibration control and structural health monitoring. Graded electrical, mechanical, or optical qualities allow FGMs to be engineered so that they can react to and sense changes in structural parameters like vibration, deformation, and strain. [77, 78]

II.6. Processing Methods of Functionally Graded Materials

II.6.1. Deposition based methods

Deposition methods represent highly advanced technologies that are used for high accuracy and small products.

II.6.1.1. Vapor deposition methods

II.6.1.1.1. Physical vapor deposition method

PVD techniques are simple processes used to produce thin films and coatings, which are highly pure materials, by deposing the desired material at the atomic state based on high-temperature vacuum evaporation. It's widely used in electronics, optical, and in various decorative industries[79]. PVD is one of the different approaches to obtain the gradient structures FGM by a mixture of ceramic and metal; the chemical variation is controlled using one or more electronic guns[73]

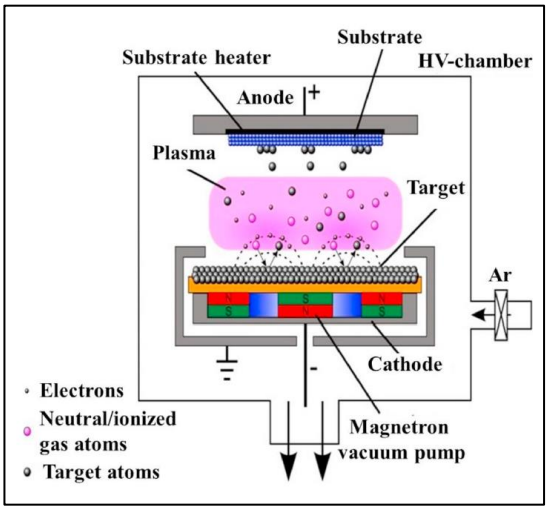

Figure II. 9: Schematic diagram of PVD process[73]

II.6.1.1.2. Chemical vapor deposition method

Dissimilar to Physical Vapor Deposition (PVD), which uses the physical transfer of material, CVD depends on chemical reactions by controlling the composition and microstructures to produce the desired material based on a vapor processing route, highly pure coating at low temperature. CVD

is widely used in various industries, such as semiconductor device fabrication, integrated into advanced materials like coating and metallic film .[80]

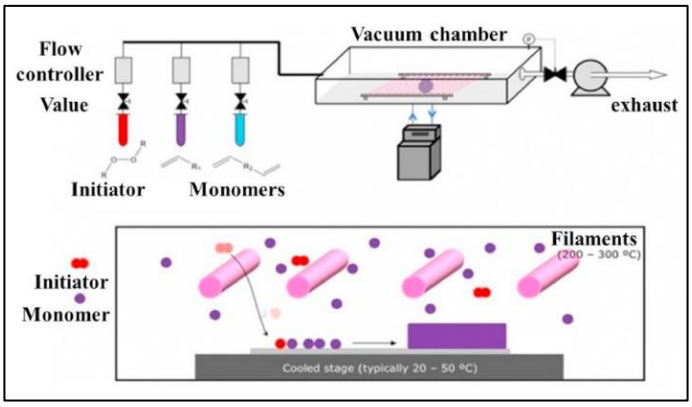

Figure II. 10: Schematic diagram of CVD process

II.6.1.1.3. Electrodeposition methods

The two procedures that make up the electroplating method, also known as electrodeposition, are deposition and electrophoresis, which are based on the motion of suspended particles in an electric field. Since G.M. Bose created this technique in a liquid siphon experiment in 1740, it may be used to build the functionally graded materials and desired qualities. It can also be utilized to generate a gradient material in micro-scale and complicated geometry at a low cost. [81].

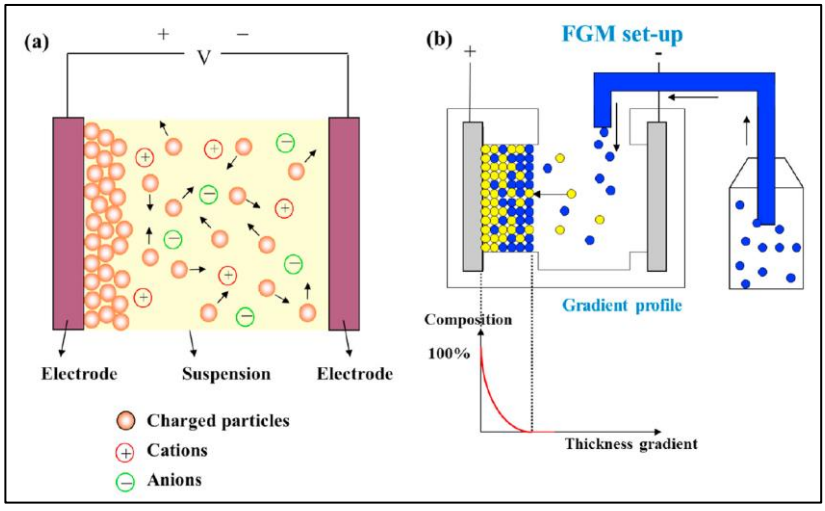

Figure II. 11: Schematic diagram of electrodeposition process

II.6.1.1.4. Thermal spray method

The thermal spraying process (TSP) is an important coating method used to produce coatings in different supports. Relating the process to FGM preparation, the coated materials will be FGM, which is used to produce a coating with varying composition and properties. The coating material is electrically or chemically heated.[82]

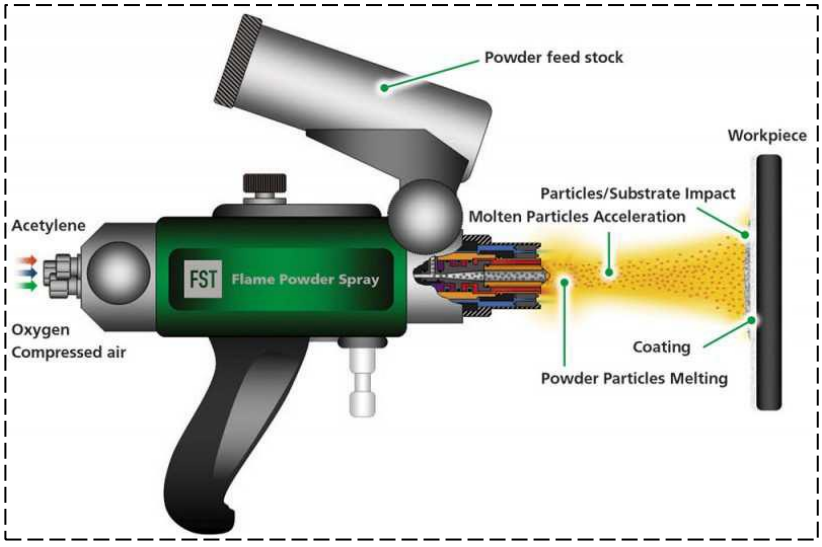

Figure II. 12: Thermal spraying process

Furthermore, the coating material is heated to a molten or semi-molten condition using these power sources. Process gases or atomization jets accelerate and direct the heated particles toward a stationary surface. A connection is made with the body at impact, and when more particles strike, thickness accumulates, and a lamellar structure is formed. As illustrated in Fig. II.10, three primary deposit kinds can be thermally sprayed during the thermal spray process.

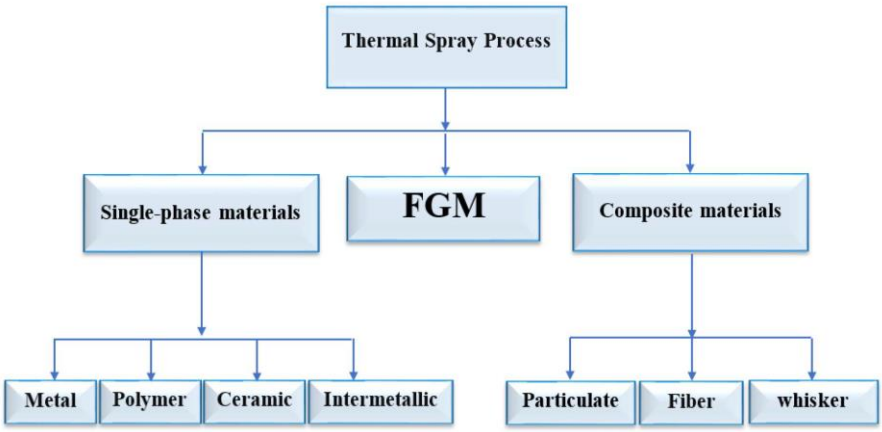

Figure II. 13: three basic types of thermal spray method

II.6.1.2. Solid state methods

solid-state-based FGMS are utilized for highly stressed thermo-mechanical components

II.6.1.2.1. Powder metallurgy method

Powder metallurgy PM is one of the popular techniques of FGM fabrication[54] and all engineering parts including the basic steps: mixing, which is the powder preparation (precis the weigh, confirm the distribution of the materials in the mixture), the second step is stacking or putting the mixture in the die, the third is the pressing by using a controlled load to give shape to the materials

and make it ready to the next step by applying controlled heating to the compact materials in the sintering method pressure assisted hot consolidation[83, 84].

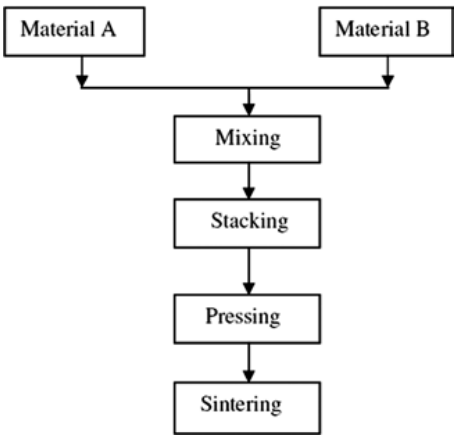

Figure II. 14: powder metallurgy method

A good production process for fabrication engineering components, FGM, and several kinds of gradient structures, like porosity gradients, chemical composition gradients (ceramic/metal), and volume content gradients, is powder metallurgy or ceramic technology. [85].

II.6.1.2.2. Additive manufacturing methods

Layer upon layer of material is added in Additive Manufacturing (AM) processes. This is a quick way to create and display new material prototypes based on 3D-CAD, a tool for performance optimization that uses sliced files to determine the geometry of each layer and orders the fabrication setup to deposit a layer according to that geometry.[86].

Many types of deposition methods are similar in the mechanical, thermal, and chemical ways of fabrication which are Laser-based methods, Stereolithography process, Material jetting process, and Fused deposition modelling[87].

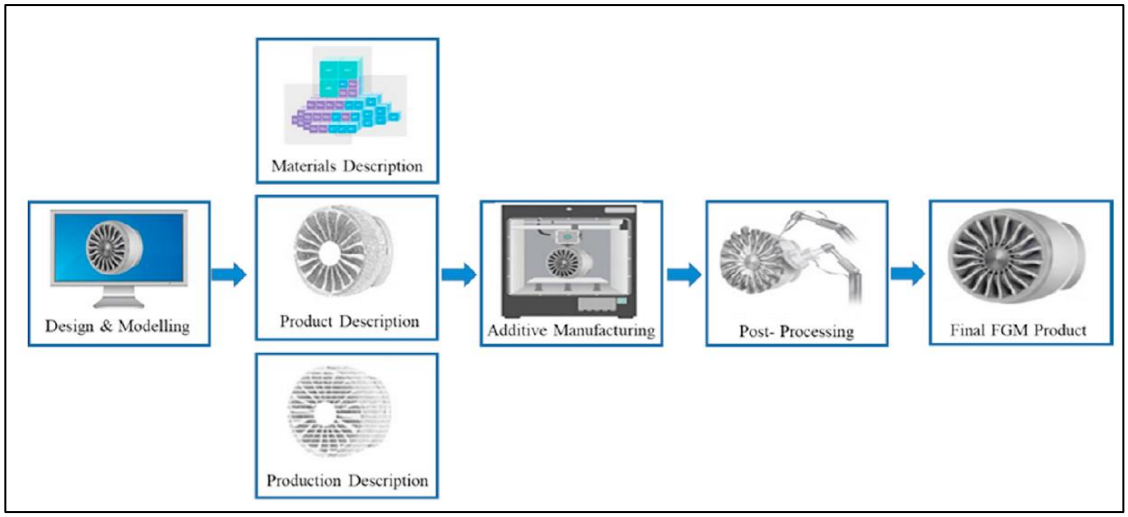

Figure II. 15: Concept of functionally graded additive manufacturing method[88]

II.6.1.2.2.1. Laser-based methods

One reliable kind of metal additive manufacturing is laser-based technology. It is also in most cases, compared to polymer processing techniques, a more sophisticated regulating setup is needed. A bed of powdered chosen material feeds the fabrication chamber during this operation. A roller sometimes referred to as a coater, supplies the metal powder ingredients to the fabrication site.[89]. Similar to other AM procedures, a computer design file will provide each layer's geometry, and an integrated laser head will read the G-codes and follow the predetermined routes. The materials that came into contact with the laser after each pass will melt, leaving the remaining powder particles unaltered.[90]

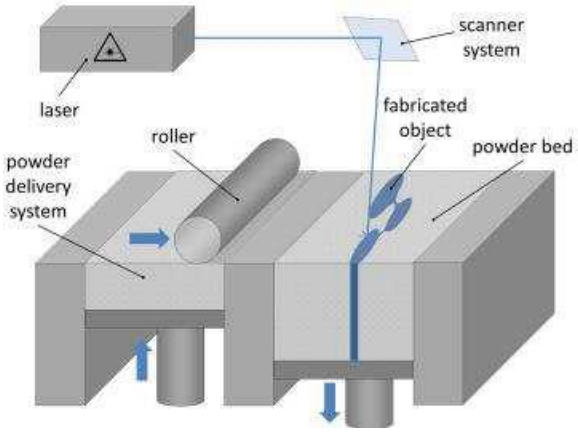

Figure II. 16: Laser-based methods[89]

II.6.1.2.2.2. Stereolithography process

One of the most used forms of AM is stereolithography (SLA). In this process, the feedstock is liquid, and each layer is formed and solidified once it is struck by a light beam (laser, UV, etc.). This procedure is known as the SLA curing stage. As the materials are cemented by light curing, the

thickness of each layer cannot pass a certain value that depends on feedstock material qualities and the intensity of light emitted. Additionally, a material's reflectivity is crucial to the production process.[91]

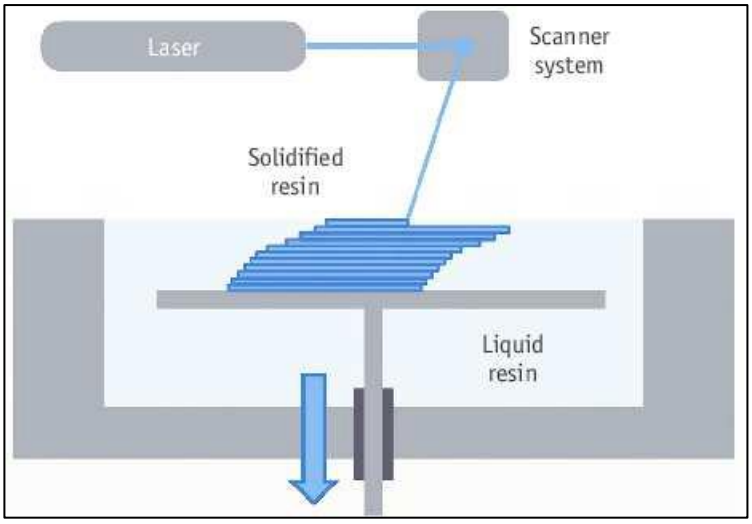

Figure II. 17: Stereolithography method[91]

II.6.1.2.2.3. Fused deposition modeling

One method of additive manufacturing of polymers without the use of a laser is fused deposition modeling or FDM. This setup has a computer-controlled nozzle head that forms layers on a surface by depositing semisolid materials onto it. Since the hard polymers are semisolid before deposition, this method is frequently utilized for their deposition.[92].

Depending on the state of the nozzle head, the deposited materials exist in a filament mode with varying diameters and shapes. Once more, the fabrication is done layer by layer. Similar to LTP, a milling head cuts the surface to modify the thickness and surface finish of the layers after each layer is deposited.[93].

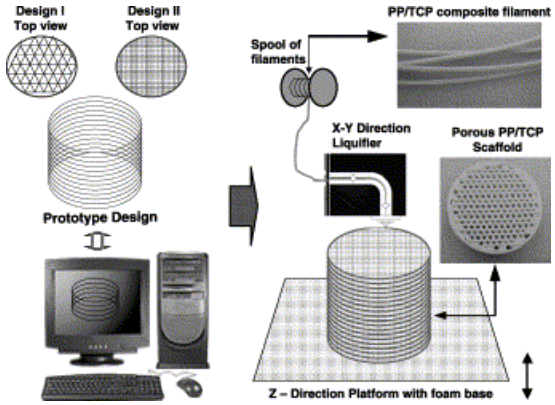

Figure II. 18:Fused deposition modeling[92]

II.6.1.3. Liquid state methods

Liquid-state processes are usually used for large products of relatively lower property control.

II.6.1.3.1. Centrifugal force methods

Centrifugal force methods, sometimes referred to as centrifugal casting or centrifugal processing, or manufacturing processes, control the distribution of materials and create desired forms by using the force created when a mold or substrate is spun. These techniques are frequently applied to the casting of metals, polymers, and composite materials in many different sectors.[94].

II.6.1.3.2. Centrifugal casting methods

A manufacturing technique called centrifugal casting is used to produce cylindrical or tubular parts with a high degree of structural integrity. It works by evenly dispersing molten material inside a spinning mold using centrifugal force. This process works especially well for creating hollow pieces with a consistent wall thickness and a dense, void-free microstructure, such as pipes, tubes, and rings.[94].

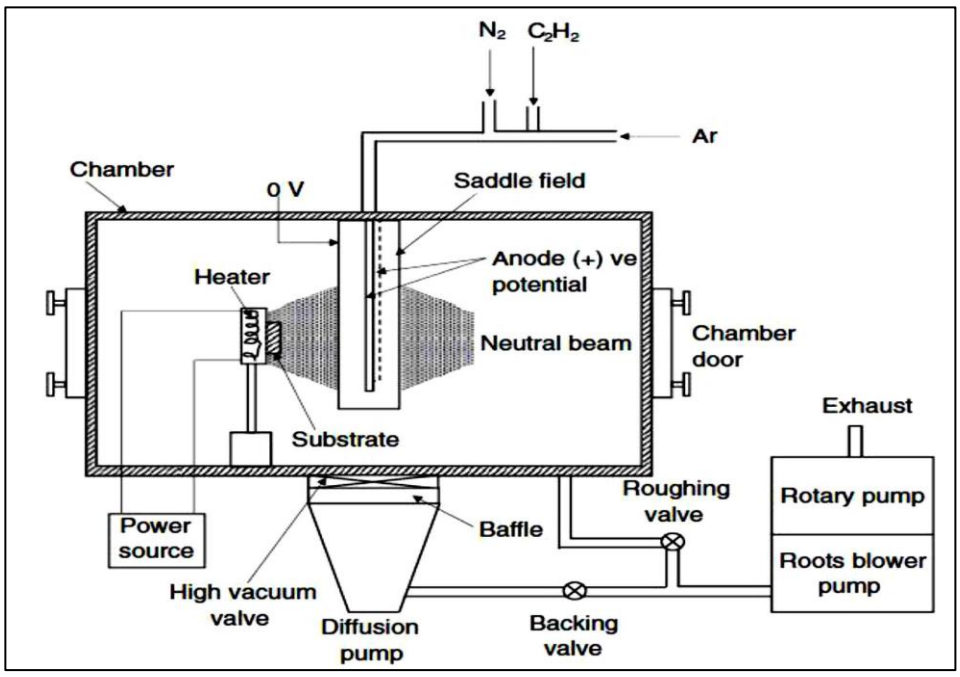

Figure II. 19:The centrifugal casting process

II.6.1.3.3. Centrifugal slurry pouring method

A variation on centrifugal casting that is especially useful for producing components made of composite materials, “metal matrix composites (MMCs) and ceramic matrix composites (CMCs),” is the centrifugal slurry pouring method. With this technique, a mold is rotated as a slurry containing reinforcement particles—like fibers or particles—suspended in a liquid matrix material is

simultaneously poured into the mold. Centrifugal force pushes the slurry towards the inner surface of the mold as it rotates, creating a composite part with improved mechanical qualities.[95].

II.6.1.3.4. Centrifugal pressurization methods

II.6.1.3.4.1. Centrifugal mixed-powder method

The centrifugal mixed-powder method uses centrifugal force to disperse solid reinforcement particles within a metal matrix in order to create composite materials, namely metal matrix composites (MMCs). To make a composite material with better mechanical qualities, this process combines metal particles with ceramic, metallic, or other reinforcing powders. The combination is then subjected to centrifugal force.[96]

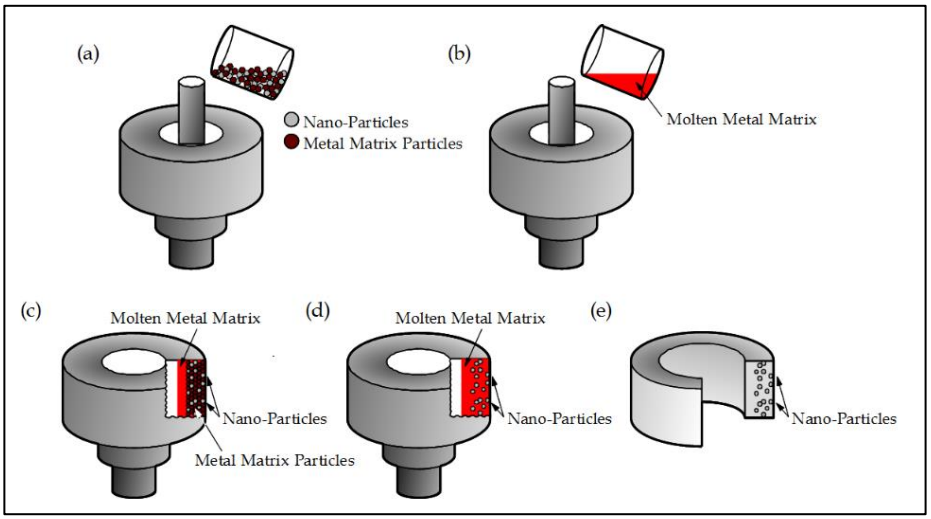

Figure II. 20: centrifugal mixed-powder method.[96]

II.6.1.3.5. Slip casting method

Generally, the slip casting process is a colloidal and cost-effective method to fabricate the engineering ceramics, composites, and FGMs in aqueous suspension by using the porous mold and draining water from the slurry of a green body ready for the sintering process[97]. In this process, in order to fabricate the products with high performance and density, the most significant concern factors such as particle size, distribution of particles, particle shape and morphology, volumetric solids content, inter-particle force, pH values and slurry stabilization using desirable type and amount of dispersant must be controlled and optimized[98].

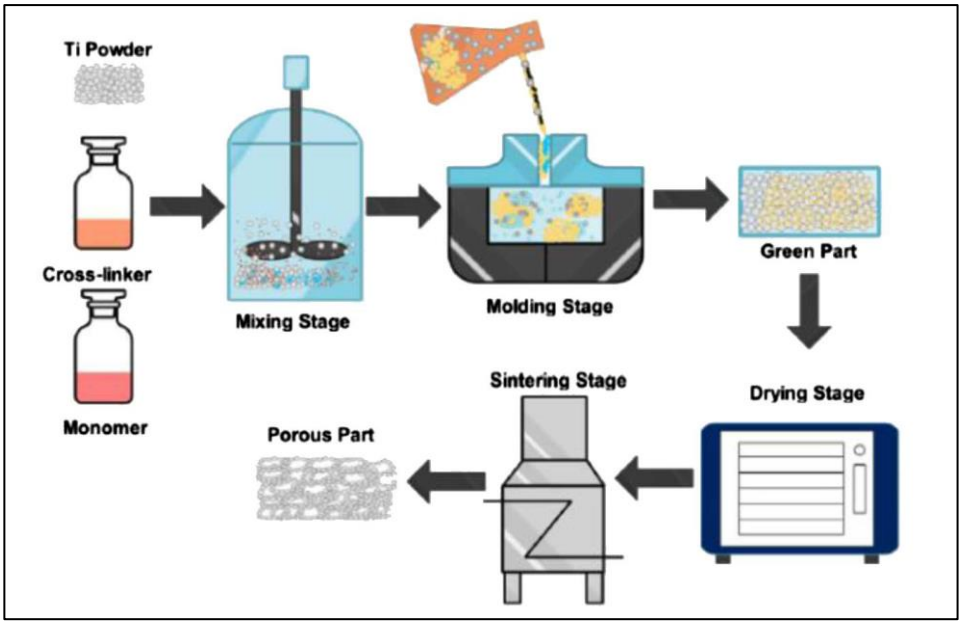

Figure II. 21: Slip casting process

II.6.1.3.6. Tape casting method

In the middle of the Second World War, in the 1940s, Howatt pioneered the tape casting technique (TCP) in an effort to create thin piezoelectric materials. A doctor blade, or other carefully controlled blade, is used to spread the slurry over a surface during the tape casting process, which is also frequently referred to as the doctor-blade process. An outline of the tape-casting procedure is shown in Figure II.22.[99]

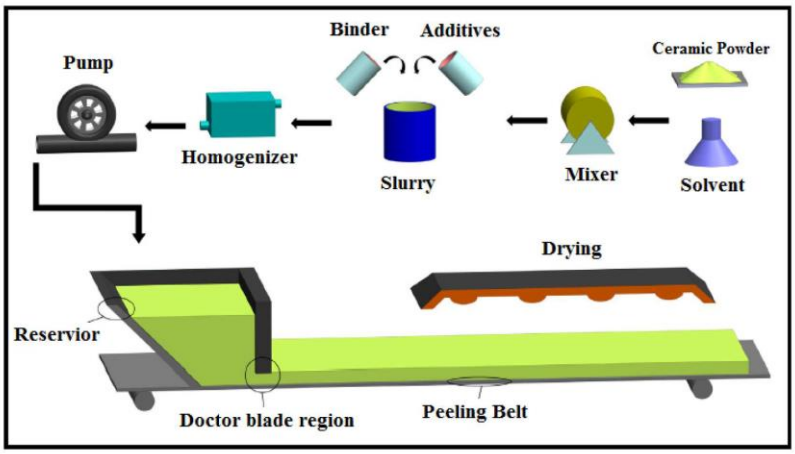

Figure II. 22: Tape casting process

The most important choice that needs to be made in this procedure, aside from the ceramic powder being a necessary component, is choosing a binder or plasticizer to increase the dried tape's or de-feculent system's flexibility. The binder/plasticizer must be a long-chain polymer and a "film-former" after drying from a solvent system in order to create a flexible tape-cast result.[100]. Because

they regulate the rheological behavior of the ceramic slurry, these factors have a significant impact on the final qualities of the tapes. [101].

II.6.1.3.7. Infiltration method

The process by which fluid on the ground surface precipitates into the soil is known as infiltration, or to use the proper scientific terminology, hydrology. Either capillary action or gravity is the force that drives this process. The ease of fluid entrance, transmission rate through the soil, and storage capacity of the soil all affect the rate of infiltration. The infiltration technique was developed to prepare the shape of some complex FGCs. This manufacturing process requires faster reaction kinetics and little to no bulk shrinkage. Making sure there is no bulk shrinkage is difficult since molding is often accomplished by heating the powder to a temperature higher than the liquid phase.[102]

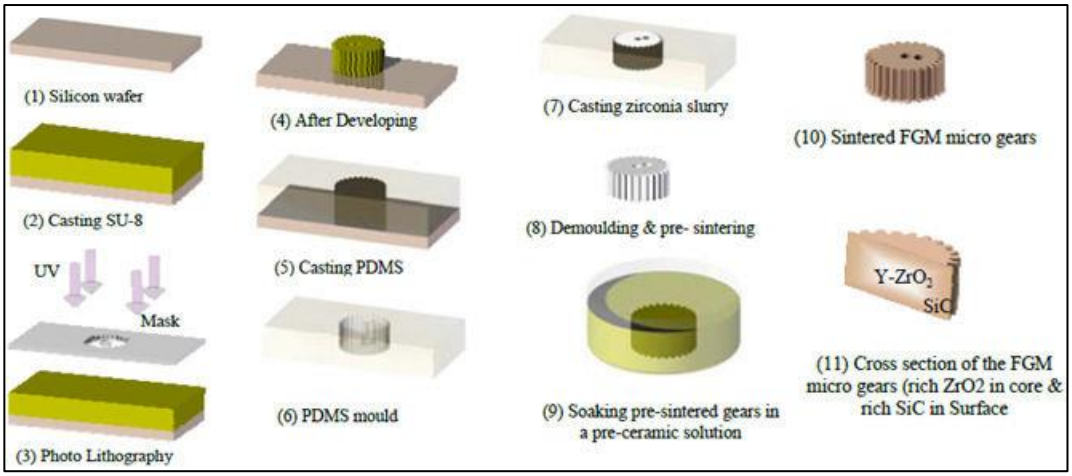

Figure II. 23: Infiltration method

II.7. Material properties of FGM structures

The mechanical properties of FGMs vary smoothly and continuously from one surface to the other. Typically, these materials are made from a mixture of ceramic and metal or a combination of different materials. The most distinct features of an FGM are the non-uniform microstructures with continuously graded macro properties. An FGM can be defined by the variation in the volume fractions; some of the micromodels are presented in figure II.24 below.

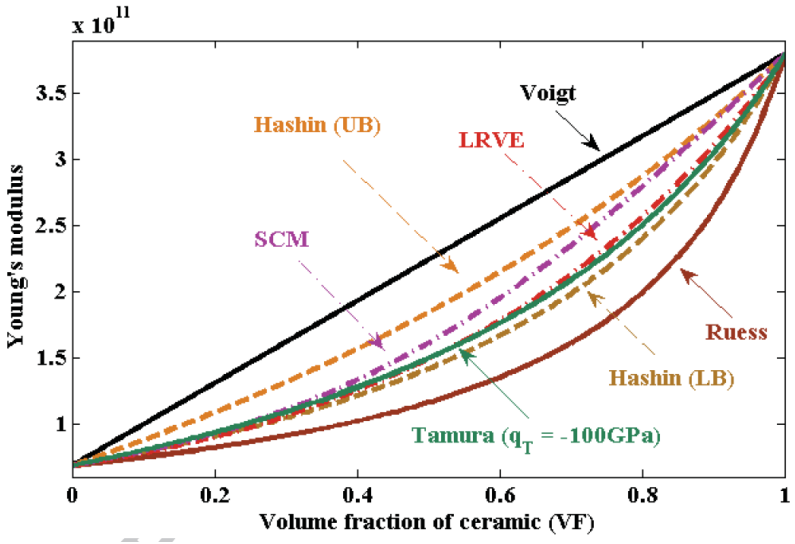

Figure II. 24:Effective Young's modulus as a function of volume fraction of ceramic for several micromechanical models

II.7.1. Voigt model

Voigt model, originally developed by Voigt[103]. This model is known as a rule of mixtures used in most FGM as a simple one to estimate the Young's modulus of functionally graded material and assumes the equivalent modulus of two different materials change across the thickness direction in most cases, where their approximation is not less than the value of the modulus of the composite. [104]:

$$E(z) = E_c V_c + E_m (1 - V_c) \tag{01}$$

Where:

E_c and E_m are Young's modulus of ceramic and metal, respectively, and Vc is the volume of the fraction.

II.7.2. Reuss model

Reuss proposed the first hypothesis of this model[105]. It is also known as the inverse rule of Voigt when the materials are considered homogonous at a macroscopic scale under uniform stress. [106]. The effective properties of this model are obtained as[107]:

$$E(z) = \frac{E_c E_m}{E_c (1 - V_c) + E_m V_c} \tag{02}$$

Where:

Ec and Em are Young's modulus of ceramic and metal, respectively, and Vc is the volume of the fraction.

II.7.3. Tamura model

Tamura model proposed and developed for the linear rule of mixture, introducing an empirical fitting parameter known as “stress-to-strain transfer”[104]:

$$q = \frac{\sigma_1 - \sigma_2}{\varepsilon_1 - \varepsilon_2} \tag{03}$$

The Tamura model is dependent on the value of, and the FGMs usually should have a range of these values, the effective properties vary in the thickness direction, and the young modulus is found as [108]:

$$E(z) = \frac{(1-V_c)E_m(q-E_c)+V_cE_c(q-E_m)}{(1-V_c)(q-E_c)+V_cE_c(q-E_m)} \tag{04}$$

For q=0 correspond to the Reuss rule and with q=100 to the Voigt rule, stay invariant to the consideration of which phase is matrix and which one is fiber[109].

Where:

Ec and Em are Young’s modulus of ceramic and metal, respectively, and Vc is the volume of the fraction.

II.7.4. Description by a representative volume element (LRVE)

Local representative volume elements (LRVE) are obtained by the hypothesis that the microstructure of the heterogeneous materials is known; Young’s modulus is expressed as follows by the LRVE method[106]:

$$E(z) = E_m\left(1+\frac{V_c}{FE-\sqrt[3]{V_c}}\right), \qquad FE = \frac{1}{1-\frac{E_m}{E_c}} \tag{05}$$

Where:

Ec and Em are Young’s modulus of ceramic and metal, respectively, and Vc is the volume of the fraction.

The model uses local representative volume elements (LRVE) and is based on a “mesoscopic” length scale which is much larger than the characteristic length scale of particles (inhomogeneities) but smaller than the characteristic length scale of a macroscopic specimen[110]

The input for the LRVE for the deterministic micromechanical framework is usually the volume average or ensemble average of the descriptors of the microstructures.

II.7.5. Mori-Tanaka model

Mori-Tanaka scheme is a model of homogenization and usually is applicable to predict the effective properties for two or more different materials, especially to the regions of the graded microstructure that have a continuous matrix and discontinuous particles, based on Mori-Tanaka model, the effective Bulk Modulus (K) and the effective shear modulus (G) are given by[111, 112]:

$$K(z) = K_m + \frac{V_c(K_c - K_m)}{1+(1-V_c)3(K_c - K_m)/(3K_m + 4K_c)}$$
$$G(z) = G_m + \frac{V_c(G_c - G_m)}{1+(1-V_c)(G_c - G_m)/(G_m + f_1)} \quad (06)$$
and
$$f_1 = \frac{G_m(9K_m + 8G_m)}{6(K_m + 2G_m)}$$

The overall modulus of elasticity:

$$E(z) = \frac{9K(z)G(z)}{3K(z) + G(z)} \quad (07)$$

The effective Young's modulus (E) in terms of constituents is given by[113]:

$$E(z) = E_m + (E_c - E_m)\left(\frac{V_c}{1+(1-V_c)(E_c/E_m - 1)(1+v)/(3-3v)}\right) \quad (08)$$

Although FGMs are usually considered combinations of metal and ceramic, they can be made from different dissimilar materials. Here, the variations of materials are assumed to be in the thickness direction of the microbeam. The volume fraction of reinforcements is changed in the z-direction according to three different models: (a) power-law (P-FGM), (b) Sigmoid (S-FGM), and (c) exponential (E-FGM) models, that is:

II.7.6. P-FGM model

The volume fraction of the P-FGM is assumed to obey a power-law function[114]:

$$V(z) = \left(\frac{z + h/2}{h}\right)^k \quad (09.a)$$

where p is the material parameter, and h is the thickness of the beam. Once the local volume fraction g(z) has been defined, the material properties of a P-FGM can be determined by the rule of mixture[114]:

$$E(z) = E_m + (E_c - E_m)V(z) \tag{09.b}$$

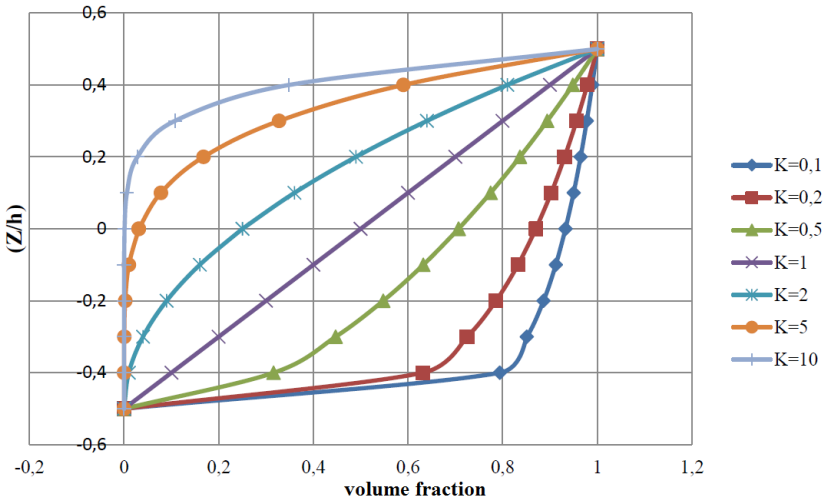

Figure II. 25: The variation of Volume Fraction in a P-FGM plate

The variation of volume fraction in the thickness direction of the P-FGM beam is depicted in Figure II.21, which shows that the Youngs modulus changes rapidly near the lowest surface for p < 1 and increases quickly near the top surface for p > 1.

II.7.7. S-FGM model

In the case of adding an FGM of a single power-law function to the multi-layered composite, stress concentrations appear on one of the interfaces where the material is continuous but changes rapidly[63, 115]. Therefore, Chung and Chi (2001) defined the volume fraction using two power-law functions to ensure smooth distribution of stresses among all the interfaces[116]. The two power-law functions are defined by:

$$V(z) = \frac{1}{2}\left(\frac{\frac{h}{2}+z}{\frac{h}{2}}\right)^p, \; For -h/2 \le z \le 0$$
$$V(z) = 1 - \frac{1}{2}\left(\frac{\frac{h}{2}+z}{\frac{h}{2}}\right)^p, \; For \; 0 \le z \le h/2 \tag{10.a}$$

By using the rule of mixture, the Youngs modulus of the S-FGM can be calculated by:

$$E(z) = V_1(z)E_1 + \left[1 - V_1(z)\right]E_2, \; For - h/2 \le z \le 0$$
$$E(z) = V_2(z)E_1 + \left[1 - V_2(z)\right]E_2, \; For \; 0 \le z \le h/2 \qquad (10.b)$$

Figure II.26 shows the variation of Young's modulus in Eqs. (10a) and (10b) represents sigmoid distributions, and this FGM plate is thus called a sigmoid FGM plate (S-FGM plates).

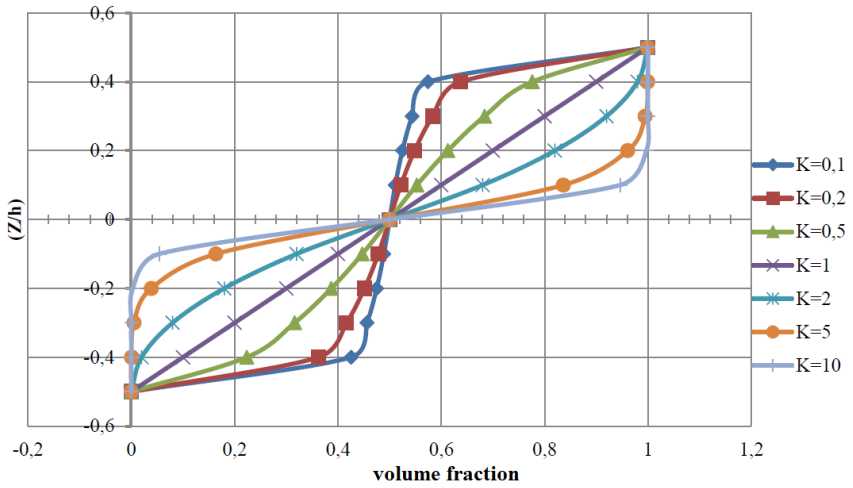

Figure II. 26:The variation of Volume Fraction in a S-FGM plate

II.7.8. E-FGM model

Many researchers used the exponential function to describe the material properties of FGMs as follows[117]:

$$E(z) = E_2 e^{B(z+h/2)}$$
$$and \qquad (11)$$
$$B = \frac{1}{h}\ln\left(\frac{E_1}{E_2}\right)$$

The material distribution in the thickness direction of the E-FGM beams is plotted in Figure II.23:

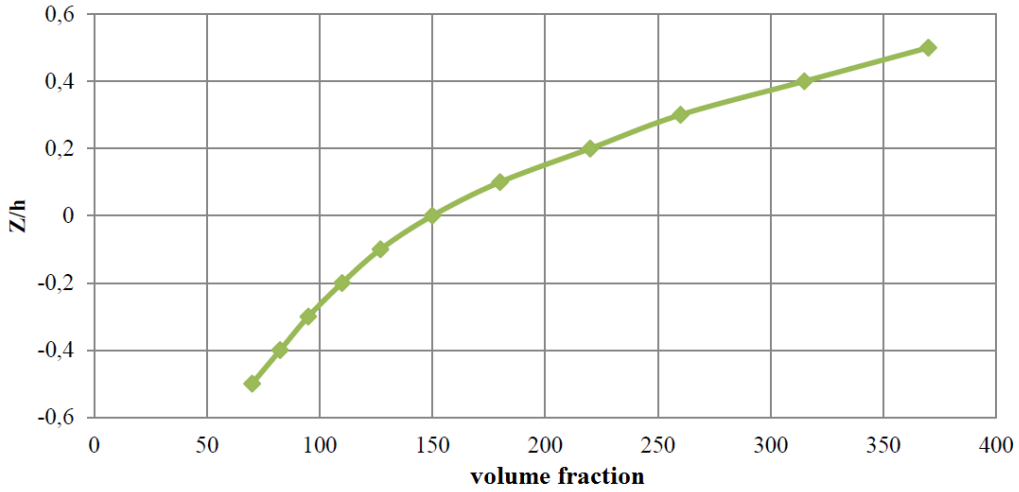

Figure II. 27: The variation of Volume Fraction in an E-FGM plate

II.8. CONCLUSIONS

This chapter defines "FGMs" as materials with a gradient of properties, as well as the types, production processes, fields of use, classifications, and laws that control how the material properties of FGM plates vary. Innovative structures that can be utilized in various disciplines of civil engineering unique structures are made possible by the spatial and progressive alteration of the properties of gradient materials.

CHAPTER III

OVERVIEW OF FUNCTIONALLY GRADED PLATE DEFORMATION THEORIES

CHAPTER III: OVERVIEW OF FUNCTIONALLY GRADED PLATE DEFORMATION THEORIES

III.1. Introduction:

The plate made from functionally graded materials is the most common structure used in a diversity of civil engineering, mechanical engineering, naval/marine, and aerospace because of their material properties, which can be tailored to different applications and working environments. The development of FGM led to the development of different theories to study their responses. However, the behavior of FGM plates can be analyzed using Equivalent Single Layer (ESL) theories, which include classical plate theories which is based on love-Kirchhoff assumptions.[118], first-order shear deformation theory based on Reissner-Mindlin [119, 120] Assumption and high shear deformation theory, which proposed the reason of the limitation of the uses of classical plate theories (CPT) and first-order shear deformation theory (FSDT) [121], furthermore, the 3D elasticity theory, layer-wise theory, and zig-zag theory are also important in predicting the response of the FGM plate. In the present chapter, the different theories and the most applicable one are discussed in detail. The modeling of FGMs is currently an active research area, and over the years, different approaches have been introduced to investigate the mechanical performance of FGM structures.

III.2. Equivalent Single Layer theories

Equivalent Single Layer (ESL) theories are a mathematical model used to study the behavior of composite structures and sandwich panels (heterogeneous laminated plates, shells, or beams) by the simplification of the complex three-dimensional behavior of these structures into a single-layer representation. The ESL is developed based on the assumptions that the displacement field is at least C^1-continuous (the function and its derivative are continuous) through the thickness of laminate[121]. The ESL theories include the classical laminated theory, first-order shear deformation theories, and higher-order shear deformation theories.

III.2.1. Classical plate theory (CPT)

The classical plate theory developed based on the love-Kirchhoff hypothesis[118], used as a simple model to analyze the behavior of thin plates under various loads and boundary conditions where the normal and transverse deformation ε_{zz} and γ_{xz}, γ_{yz} are neglected. The theory assumes that the plane sections which are perpendicular to the neutral layer before bending remain plane and perpendicular to the neutral layer after bending. This means that the strains induced by bending do not alter the plate's shape significantly[122-124].

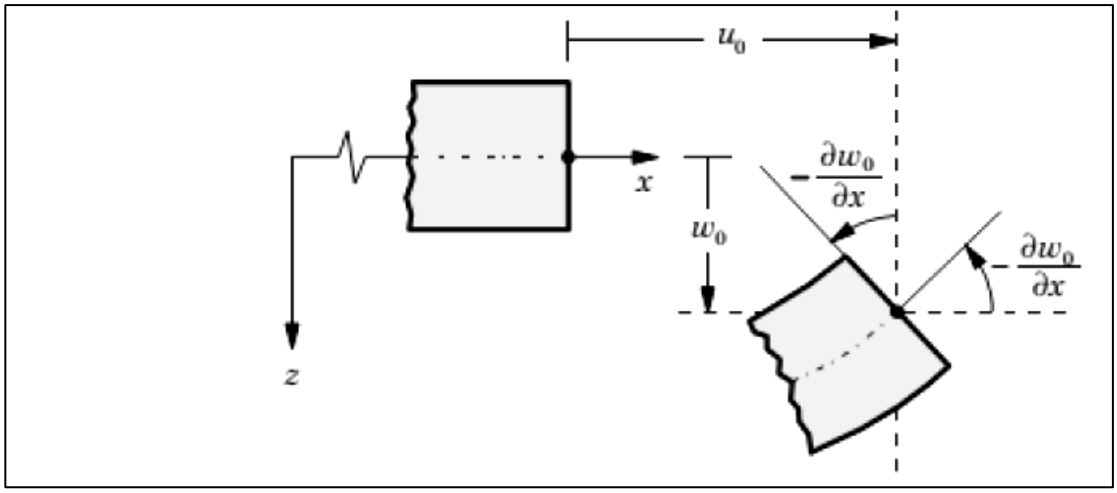

Figure III. 1: Illustration of love-Kirchhoff model

Based on the assumptions above the displacement field can be written as[118]:

$$\begin{aligned} u(x,y,z) &= u_0(x,y) - z\frac{dw_0(x,y)}{dx} \\ v(x,y,z) &= v_0(x,y) - z\frac{dw_0(x,y)}{dy} \\ w(x,y,z) &= w_0(x,y) \end{aligned} \tag{01}$$

The CPT is a useful model for thin FG plates, but it's useless for thick ones because it doesn't take into consideration the shear effect, so it has not ensured accurate results for the response of the behavior of FG plates. Compared with the CPT, the first-order shear deformation theory (FSDT) considers the effects of shear deformation

III.2.2. First shear deformation theory

First-order shear deformation theory, commonly known developed by Mindlin and Reissner for the linear variation of the shear deformation effect [125]. However, the Reissner theory is not similar to the Mindlin theory, like erroneous perception of many researchers through the use of misleading descriptions such as "Reissner-Mindlin plates" and "FSDT of Reissner".[120],[119]. The FSDT was developed by including transverse shear in the kinematic field of the classical theory, so the plan sections that are perpendicular to the neutral layer before bending remain plan but not necessarily perpendicular to the neutral layer after bending. In other words, the displacement w is constant through the thickness of the plate while u and v are varying linearly. In both CPT and FSDT, if the transverse deflection varies through the thickness, the inextensibility of the transverse normal is removed, and this leads to full three-dimensional constitutive equations[126].

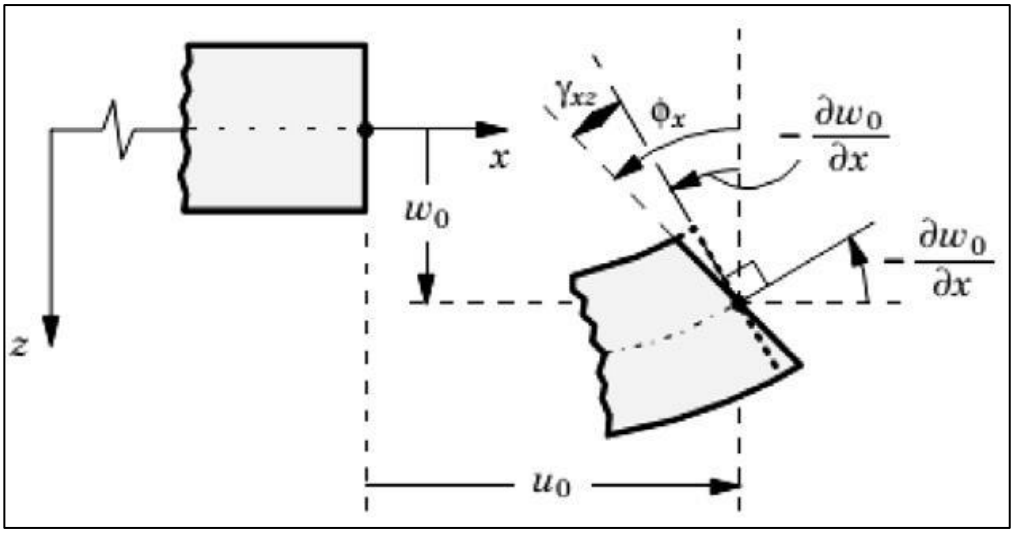

Figure III. 2: Illustration of Reissner-Mindlin model

Then the displacement field can be written as[120],[119]:

$$\begin{aligned} u(x,y,z) &= u_0(x,y) + z\phi_x(x,y) \\ v(x,y,z) &= v_0(x,y) + z\phi_y(x,y) \\ w(x,y,z) &= w_0(x,y) \end{aligned} \tag{02}$$

Shear correction factors are typically needed to account for nonlinear distributions of transverse shear stress fields since the linear in-plane displacement assumptions of the FSDT produce constant transverse shear stress fields.[127]. Nonetheless, boundary conditions, loadings, and cross-sectional geometries all affect shear correction factors. Additionally, graded differences in the properties of the FG material make solving the problem even more challenging.

III.2.3. High shear deformation theory

The limitation of CPT and FSDT led to the development of HSDT; the HSDT used polynomial shape functions or nonpolynomial shape functions[128]. To avoid the use of correction factor in FSDT and to develop a hypothesis more realistic from the one's love-Kirchhoff. The HSDT introduces additional variables that are often difficult to interpret in physical terms., the HSDT was proposed by several researchers, by Reddy [121, 123, 129, 130], Naghdi [131], Iyengar et al.[132]. Generally, these theories were developed by using the Taylor series across the thickness presented as:

$$u(x,y,z) = u_0(x,y,z) + z\phi_\alpha(x,y) + z^2\phi_\alpha^2(x,y) + \ldots\ldots + z^n\phi_\alpha^n(x,y) \tag{03}$$

For love-Kirchhoff theory n=0

For Reissner-Mindlin theory, n=1 in the case of the plane displacement and n=0 for normal displacement

According to Reddy[133]and Mallikarjuna and Kant [134], the assumption to develop these theories are :

-The effect of transverse shear is not negligible

-The displacement is too small if compared with the thickness of the plates

-The plan section doesn't perpendicular to the neutral layer after bending and it takes shape through polynomial shape functions or nonpolynomial shape functions

-The nonlinear stress varied according to thickness.

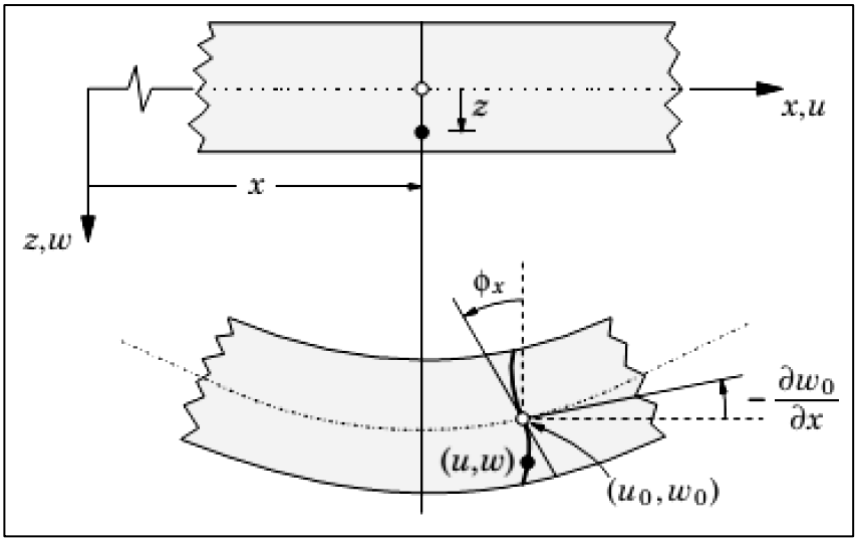

Figure III. 3: illustration of high-order shear deformation theory model

The most common (HSDT) theories are presented based on Reissner[120], Mindlin[119] and Reddy[135] and the displacement is:

$$\begin{aligned} u(x,y,z) &= u_0(x,y) - z\frac{\partial w_0(x,y)}{dx} + f(z)\phi_x(x,y) \\ v(x,y,z) &= v_0(x,y) - z\frac{\partial w_0(x,y)}{dy} + f(z)\phi_y(x,y) \\ w(x,y,z) &= w_0(x,y) \end{aligned} \tag{04}$$

When, u_0, v_0 and w_0 are the axial displacement and ϕ is a rotational displacement

F(z) is the shape function,

-for love-Kirchhoff theory (CPT), f(z)=0

-for Reissner-Mindlin theory (FSDT) f(z)=z.

The present table shows the most common theories and their shape functions.

Table III. 1: different shape function for high-order shear deformation theory

Theory	Shape function
Reddy[136]	$f(z)=z\left(1-\frac{4}{3h^2}z^2\right)$
Touratier[137]	$f(z)=\frac{h}{\pi}\sin\left(\frac{\pi z}{h}\right)$
Karama[138]	$f(z)=ze^{-2(z/h)^2}$
Reissner[139]	$f(z)=\frac{5z}{4}\left(1-\frac{4}{3h^2}z^2\right)$
Soldatos[140]	$f(z)=h\sinh\left(\frac{z}{h}\right)-z\sinh\left(\frac{1}{2}\right)$
Mantari[141]	$f(z)=\sin\left(\frac{\pi z}{h}\right)e^{m\cos\left(\frac{\pi z}{h}\right)}+m\left(\frac{\pi z}{h}\right)$
Ait Atmane[142]	$f(z)=\frac{\cosh\left(\frac{\pi}{2}\right)}{\left[\cosh(\pi/2)-1\right]^z}z-\frac{(\pi/z)\sinh\left(\frac{\pi}{h}z\right)}{\left[\cosh(\pi/2)-1\right]}$
Nguyen[143]	$f(z)=\sinh^{-1}\left(\frac{3z}{h}\right)-z\left(\frac{6}{h\sqrt{13}}\right)$

III.2.4. Refined plate theory RPT

In order to eliminate the number of unknowns used in the higher-order shear deformation theory, the refined model was developed by Shimpi in 2002 for isotropic plates, known as refined plate theory [144], The following are the assumptions involved in the refined plate theory (RPT):

1. The strains are tiny, on the reason of the displacements are small,
2. The transversal displacement has two constituents: wb for bending displacement and ws for shear displacement, and both are functions of (x, y),
3. The transverse normal stress σ_z is infinitesimal compared with σ_x and σ_y, while σ_x and σ_y are related to strains ε_x and ε_y based on generated behavior law,
4. The displacement u varies in the x direction and v varies in the y direction; however, each consists of two components.

The displacement of this theory is given by[144]:

$$\begin{aligned} u(x,y,z) &= u_0(x,y) - z\frac{\partial w_b(x,y)}{\partial x} + f(z)\frac{\partial w_s(x,y)}{\partial x} \\ v(x,y,z) &= v_0(x,y) - z\frac{\partial w_b(x,y)}{\partial y} + f(z)\frac{\partial w_s(x,y)}{\partial y} \\ w(x,y,z) &= w_b(x,y) + w_s(x,y) \end{aligned} \tag{05}$$

III.2.5. Modified 3D quasi HSDT

Quasi-3D theories are HSDTs with higher-order variations of in-plane and transverse displacement through the thickness, on the other hand, the shear deformation effect and the thickness stretching effect are considered. In general, quasi-3D theories initially proposed by Carrera[145, 146] and recently extended by Demasi[147-152]. Quasi-3D theories have been proposed in the literature. Thai and Kim proposed quasi-3d theory as first-order shear deformation theory with six variables [153]. Hebali and Tounsi[154], Tounsi and Houari[155], the effect of variation of shape functions on quasi-3d theory with five unknowns was studied by Hamidi and Tounsi[156], zenkour has proposed a new quasi-3d theory with only four variables [157, 158].

Therefore, there is a need to simplify the existing HSDTs and quasi-3D theories or to develop simple theories with fewer unknowns.

The displacement field of this theory is presented below:

For RPT QUASI-3D

$$\begin{aligned} u(x,y,z) &= u_0(x,y) - z\frac{\partial w_b(x,y)}{\partial x} + f(z)\frac{\partial w_s(x,y)}{\partial x} \\ v(x,y,z) &= v_0(x,y) - z\frac{\partial w_b(x,y)}{\partial y} + f(z)\frac{\partial w_s(x,y)}{\partial y} \\ w(x,y,z) &= w_b(x,y) + w_s(x,y) + g(z)\phi_z \end{aligned} \tag{06}$$

And quasi-3d theory with integral terms:

$$\begin{aligned} u(x,y,z) &= u_0(x,y) - z\frac{\partial w(x,y)}{\partial x} + f(z)\int_a \theta(x,y) \\ v(x,y,z) &= v_0(x,y) - z\frac{\partial w(x,y)}{\partial y} + f(z)\int_b \theta(x,y) \\ w(x,y,z) &= w(x,y) + g(z)\phi_z \end{aligned} \tag{07}$$

III.3. 3D elasticity theory

The analysis of functionally graded plates under mechanical and thermal loads remains a three-dimensional problem with a that 3-D elasticity theory able to provide an exact solution and are often employed to validate the accuracy of ELS models[133].

Over the years, a number research studies have been proposed to assess the validity and establish the accuracy of 3D-elasticity models, an elasticity solution for a simply supported functionally graded plate under cylindrical bending was obtained by Sankar[159]. Zhong and Shang[160] developed a three-dimensional analysis for a rectangular plate made of an orthotropic functionally graded piezoelectric material. Three-dimensional elasticity solution for bending of functionally graded rectangular plates by Kashtalyan[161], Three-dimensional elasticity solution of functionally graded rectangular plates with variable thickness[162].

III.4. Layerwise theory

The layerwise theories have been developed under the assumption that the displacement field is only C0-continuous over the laminate thickness, in contrast to the equivalent single-layer theories.[121]

Thus, the displacement components are continuous through the laminate thickness. Still, the transverse derivatives of the displacements may be discontinuous at various points through the thickness, thereby allowing for the possibility of continuous transverse stresses at interfaces separating dissimilar materials. Layerwise displacement fields provide a much more kinematically correct representation of moderate to severe cross-sectional warping associated with the deformation of moderately thick to very thick laminates[163]

III.5. Zig-zag theory

In fact, the ZZ models seem to be a reasonable balance between economy and solution accuracy, making them appropriate for the precise deflection and stress analysis of laminates under bending. The ZZ models seem to have limited validity due to their neglect of the effects of transverse normal strain and stress. In addition, the ZZ models' constitutive equations predict transverse shear stresses that are getting progressively less accurate when the thickness-to-length ratio decreases and for layers with varying elastic moduli.[149]

Closed-form methods use the integration of local differential equilibrium equations to get around the issue. This is difficult to do with finite element models because they need shape functions that have a higher-order interpolation in the element's plane. Furthermore, ZZ models require C1

interpolation. This renders them undesirable for use in general-purpose finite element algorithms due to their computational inefficiency. [164].

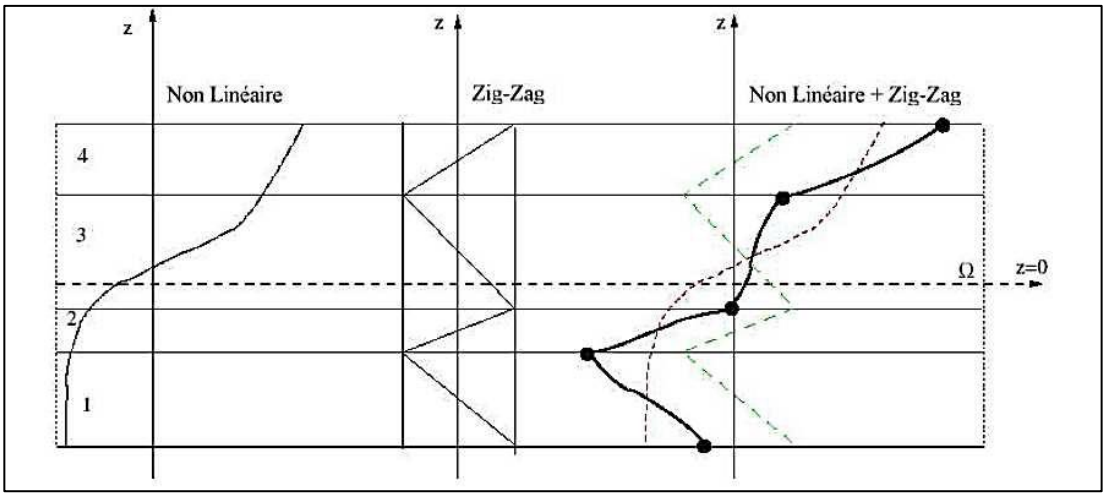

Figure III. 4: illustration of zz theory

III.6. Conclusion

The present study focused on a review of the literature on modeling techniques and solution methods for the bending, buckling, and vibration analysis of FG single layer and sandwich plates based on both lower-order and higher-order shear deformation theories.

CHAPTER IV

THEORETICAL FORMULATION

CHAPTER IV: THEORETICAL FORMULATION

IV.1. Introduction:

Functionally graded materials are basically advanced composite Materials that retain the strengths and eliminate the weaknesses existing in traditional stratifies, as the concentration of the stress between discrete materials, specifically under high thermal loads[165]. FGMs present a homogeneous structure made up of two different constituents, usually ceramic and metal, ceramic with its high thermal resistance and metal with high mechanical resistance in which final proprieties vary gradually across the thickness.

Studies related to FG structures have received too much attention from existing literature. Various theories have been developed in order to provide more useful analysis methods with lower computational costs. Drici et al. studied the free vibration of viscoelastic FGM nano-size beam by proposing the first-order shear deformation theory with the shear correction factor using the finite element method[166]. Lu et al. studied the nonlinear energy transfer of a flexible plate using a various approach to solve the mathematical equations, via the Lagrange, Fourier series, and Rayleigh-ritz method, and then the analytical results were validate using a finite element simulation [167]. Hu, Zhou et al. sought a new analytic free vibration solution non- for Lévy-type functionally graded (FG) doubly curved shallow shells under complicated boundary conditions by using an analytic simplistic superposition method (SSM) [168]. Zahari et al. compared the different kinematics theories for the buckling of FGM plates using the Finite element method[169]. Milazzo et al. used a single-domain Ritz approach based on the FSDT with nonlinear von Karman strain–displacement to study the buckling and post-buckling behavior of variable angles lightweight plates with cut-outs[170]. Alam et al. investigated the post-buckling behavior of a piezoelectric, NLSG thin cylindrical shell with a functional gradation of elastic properties under thermal, mechanical, and electrical load based on Donnell's approach, including the pre-buckling nonlinearity.[171]. J Wang et al. used the Lyapunov theory to analyze the stability of the closed-loop system confirmed by MATLAB software simulation[172]. Based on layer-wise theory, Kiarasi et al investigated the effect of the hydrothermal environment on the natural frequencies of FGM annular piezo-magneto-electro-elastic thick plate[173]. J.R. Hong et al. studied the dynamic of thick FGM plate and shell under thermal vibration by using a generalized differential quadrature technique[174].

Mouaici et al. Analyzed the effect of porosity on the free vibration analysis of functionally graded material plates using shear deformation plate theory based on neutral surface position [175]. Chang

et al. examined the static buckling and post-buckling dynamic of porous functionally graded pipelines resting on the Pasternak foundation based on the Euler-Bernoulli beam theory[176]. Zhou et al. analyzed the influence of multiphase flow on the nonlinear system vibration of FGM pipelines with pores under generalized boundary conditions[177]. Wang et al. used simple, refined plate theory (S-RPT) to analyze the bending and buckling, and free vibration of functionally graded porous plates reinforced with graphene platelets[178]. Babaei H et al. analyzed the effect and consequences of porosity on the behavior buckling of four types of FGM sandwich plates under a nonuniform in-plane edge load based on higher-order shear deformation theory. They concluded that the effect of even is much more severe than the uneven porosity distribution porosity on the buckling response[179]. Vasara et al. used numerically the first-order shear deformation theory to examine the effect of uniform, O-shape, and X-shape porosity distributions on fundamental frequencies of functionally graded circular and annular plates. They concluded that the natural frequency decreases with an increase in porosity factor in cases of clamped support. In contrast, the natural frequency increases with an increase in porosity factor in the case of support. The evaluation of the influence of porosity in this case is weakening the stiffness of the structure[180].

Based on the three-dimensional shear deformation theory. Lieu et al. employed a NURBS process for the free vibration and buckling problems of IBFG plates using a quasi-3D hyperbolic HSDT and different boundary conditions.[181] Wu et al. studied the bending of two-directional functionally graded (FG) circular plates using quasi-three-dimensional (3D) theory under various boundary conditions[182]. Akbaş extended a three-dimensional 3D elastic theory to analyze the vibration response of single-layered thick FG rectangular porous plates subject to arbitrary boundary conditions using the Rayleigh-Ritz process and Fourier cosine series[183]. Mashat, D.S et al. examined the effect of porosity on the statics and free vibration behavior of FG plates using a quasi-3D hyperbolic HSDT, taking into account the transverse shear and normal deformation[184]. Zenkour et al. studied the effect of porosity on the natural frequencies of functionally graded plates based on a new quasi-3-D refined theory[185].

Singh et al. investigated the effect of even, symmetric, and non-symmetric uneven porosity shapes on stability and vibration of thick FGM sandwich plate Galerkin Vlasov's method subjected to various boundary conditions[8]. Long et al. analyzed the effect of various types of porosity in the buckling behavior of thick FGM shells under thermo-mechanical load based on higher-order shear deformation theory[186]. Mekerbi et al. Studied the effect of thermal and porosity on the buckling behavior of FGM plate using quasi-3D [187]. Kumar et al. proposed a new hyperbolic shape function

based on higher-order shear deformation theory to compute the stability (FGM) of sandwich plates under the influence of medium pores using A meshfree approach[188]. Using a new refined quasi-3-D theory, Zenkour et al. analyzed the effect of porosity on the buckling of single-layered and three-layered FG plates [189]. A ceramic core with two different FGM face sheets, considered a new shape of the sandwich plate, is studied by Van Vinh et al. for static, free vibration, and buckling under the effect of porosity using finite element method-based high shear deformation theory[190].

There are few works on estimating sandwich constructions with metal foam cores. . T Wei, et al. Proposed a perfect design of modified nickel foam derived from metal–organic framework-derived Co3O4 to implant Li metal for Li batteries.[191].The effect of the non-uniform porosity distribution (foam) on the free and forced vibration of the functionally graded beam by including Ritz trial functions and Lagrange equation is studied by Chen et al. based on Timoshenko beam theory.[192]. Also, he analyzed the free vibration and post-bulking of sandwich nanobeam containing foam metallic core and reinforced by graphene platelets (GPLs) based on Timoshenko beam theory and von Kármán type nonlinearity.[193]. Such as, the FG sandwich plate with closed-cell Aluminium foam core is studying bending and buckling behavior using the Chebyshev-Ritz method by Chen et al. [194]. Garg et al. analyzed the effect of three different porosity distributions of the metal foam core in the stability and free vibration of sandwich FGM plate basing finite element method using zigzag theory formulation. [195]. Wang, Y.Q., and Z.Y. Zhang Studying the bending and buckling of 3D graphene foam plate using refined shear deformation theory without considering the shear correction factor [196].

However, to the best of the author's knowledge, a few researchers are interested in studying the buckling behavior of porous FG sandwich plates using a high-order shear deformation theory, and no prior studies have analyzed the buckling behavior of FG porous sandwich plates and a sandwich plate containing metal foam core with the consideration of the influence of the thickness stretching on the structure, especially for thick plate investigation. Therefore, this paper will use quasi-3D high deformation theory to investigate the effect of porosity on the buckling of sandwich FG plates subjected to various boundary conditions and Pasternak and Winkler elastic foundations under axial and biaxial in-plane loads with different shapes. The thickness stretching effect is considered in this theory. Two configurations of FG models are analyzed here: FG faces with the ceramic core when The FG material with microvoids varies smoothly in the thickness direction-based power law distribution. FG faces with metal foam core presented for the second model. The stability equations are obtained by Hamilton's principal, then it's solved by Navier solution for supported plate. The

numerical results are validated with the existing literature, the variation of the critical buckling of the FG sandwich plate vis-a-vis the effect of geometric parameters, power-law index k, different shapes of porosity distribution, metal foam coefficients, various boundary conditions, elastic foundations and types of in-plane loads are thoroughly reported.

IV.2. Plate construction

FG sandwich plate is considered in this work with uniform thickness h linked to a coordinate system (x, y, z). The vertical position of sandwich layers: two skins in the bottom and the top covers the core in the middle layer are denoted by h0, h1, h2, and h3; two different models of the sandwich are presented here based on power-law distribution. The porosity distribution projected in the FGM layer across the thickness direction for model I with four different shapes, metal foam is considered in model II with three different geometries.

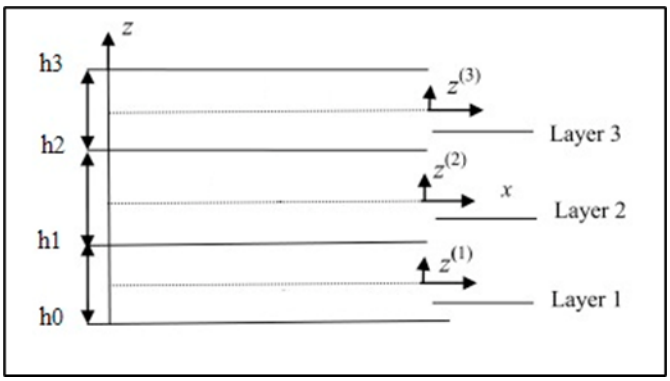

Figure IV. 1:FGM Sandwich plate

Porosity-dependent functionally graded sandwich plates

Various types of porosity distribution are presented here as[197]:

Porosity distribution I (imperfect I):

The porosity can be functionally varied in the thickness direction of the FG layers as indicated below:

$$\begin{cases} E^{(1)}(z) = (Ec - Em) * V^{(1)}(z) + Em - \dfrac{\zeta}{2}(Ec + Em)\left[1 - \dfrac{\left|2z - (h_0 + h_1)\right|}{h_1 - h_0}\right] \\ E^{(2)}(z) = (Ec - Em) * V^{(2)}(z) + Em \\ E^{(3)}(z) = (Ec - Em) * V^{(3)}(z) + Em - \dfrac{\zeta}{2}(Ec + Em)\left[1 - \dfrac{\left|2z - (h_3 + h_2)\right|}{h_3 - h_2}\right] \end{cases} \quad (1.a)$$

Porosity distribution II (imperfect II):

This model is common when the porosities vary uniformly along the thickness of the FG layer

$$\begin{cases} E^{(1)}(z) = (Ec - Em) * V^{(1)}(z) + Em - \dfrac{\zeta}{2}(Ec + Em) \\ E^{(2)}(z) = (Ec - Em) * V^{(2)}(z) + Em \\ E^{(3)}(z) = (Ec - Em) * V^{(3)}(z) + Em - \dfrac{\zeta}{2}(Ec + Em) \end{cases} \quad (1.b)$$

Porosity distribution III (imperfect III):

The third model is based on a logarithmic function, and it is expressed as:

$$\begin{cases} E^{(1)}(z) = (Ec - Em) * V^{(1)}(z) + Em - \log\left(1 + \dfrac{\zeta}{2}\right)(Ec - Em)\left[1 - \dfrac{\left|2z - (h_0 + h_1)\right|}{h_1 - h_0}\right] \\ E^{(2)}(z) = (Ec - Em) * V^{(2)}(z) + Em \\ E^{(3)}(z) = (Ec - Em) * V^{(3)}(z) + Em - \log\left(1 + \dfrac{\zeta}{2}\right)(Ec - Em)\left[1 - \dfrac{\left|2z - (h_3 + h_2)\right|}{h_3 - h_2}\right] \end{cases} \quad (1.c)$$

Porosity distribution IV (imperfect IV):

In this model, the porosity is low at the exterior surfaces of the sandwich and high at the two interface positions:

$$\begin{cases} E^{(1)}(z) = (Ec - Em) * V^{(1)}(z) + Em + \dfrac{\zeta}{2}(Ec + Em)\left[1 - \dfrac{z - h_1}{h_0 - h_1}\right] \\ E^{(2)}(z) = (Ec - Em) * V^{(2)}(z) + Em \\ E^{(3)}(z) = (Ec - Em) * V^{(3)}(z) + Em + \dfrac{\zeta}{2}(Ec + Em)\left[1 - \dfrac{z - h_1}{h_0 - h_1}\right] \end{cases} \quad (1.d)$$

Where E_C and Em are the ceramic and metal Young's modulus, respectively, ζ is porosity coefficient

Power-law FGM plate

In this paper, three FGM plate models are considered, an isotropic plate, a sandwich plate with a ceramic core, and a sandwich plate with a metal foam core [198, 199]:

Single layered:

$$V(z) = \left(\frac{2z + h}{2h}\right)^k \quad (2)$$

Sandwich plate

The model I sandwich plate is made of ceramic core and porous FGM face layers.

$$V1(z)=\left(\frac{z-h_0}{h_1-h_0}\right)^k, \quad \lambda_1=1, \quad z\in[h_0...h_1]$$
$$V2(z)=1 \qquad \lambda_2=0, \quad z\in[h_1...h_2] \tag{3}$$
$$V3(z)=\left(\frac{z-h_3}{h_2-h_3}\right)^k, \quad \lambda_3=1, \quad z\in[h_2...h_3]$$

Sandwich FGM plate containing metal foam core.

The distribution of the modulus young for a sandwich plate with a metal foam core is described in three models below [195, 196]:

Foam I:

$$E1(z)=E_f+(E_c-E_f)*\left(\frac{z-h_1}{h_0-h_1}\right)^k \quad z\in[h_0...h_1]$$
$$E2(z)=E_f*\left(1-\eta\cos(\frac{\pi z}{h_c})\right) \qquad z\in[h_1...h_2] \tag{6}$$
$$E3(z)=E_f+(E_c-E_f)*\left(\frac{z-h_2}{h_3-h_2}\right)^k \quad z\in[h_2...h_3]$$

Foam II:

$$E1(z)=E_f+(E_c-E_f)*\left(\frac{z-h_1}{h_0-h_1}\right)^k \quad z\in[h_0...h_1]$$
$$E2(z)=E_f*\left(1-\eta^*\left[1-\cos(\frac{\pi z}{h_c})\right]\right) \quad z\in[h_1...h_2] \tag{7}$$
$$E3(z)=E_f+(E_c-E_f)*\left(\frac{z-h_2}{h_3-h_2}\right)^k \quad z\in[h_2...h_3]$$

Foam III

$$E1(z)=E_f+(E_c-E_f)*\left(\frac{z-h_1}{h_0-h_1}\right)^k \quad z\in[h_0...h_1]$$
$$E2(z)=E_f*\gamma \qquad z\in[h_1...h_2] \tag{8}$$
$$E3(z)=E_f+(E_c-E_f)*\left(\frac{z-h_2}{h_3-h_2}\right)^k \quad z\in[h_2...h_3]$$

Where E_f and E_c are the young modulus of metal foam and ceramic, respectively, η,η^{*} *and* γ are metal foam coefficients for Foam I, foam II, and foam III, respectively.

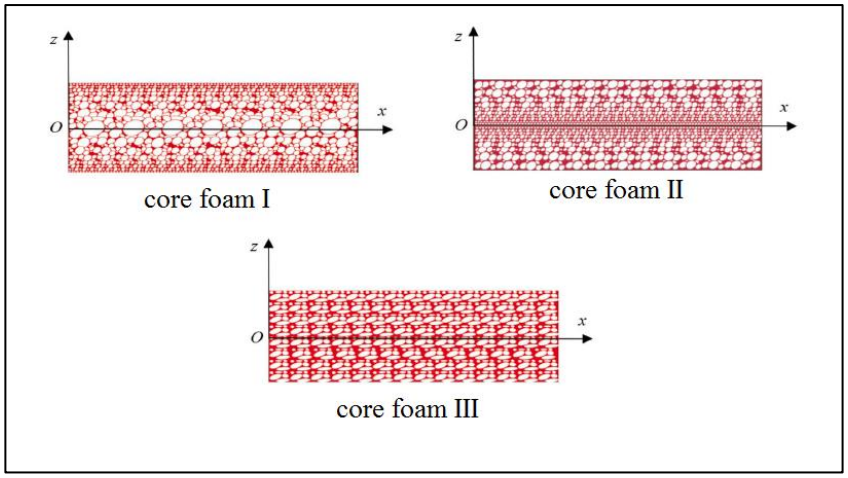

Figure IV. 2: Geometry of a metallic foam core (Foam I, Foam II and Foam III)

IV.3. **Basic mathematical equations**

The displacement field using quasi-3D high shear deformation theory can be given as follows[200]:

$$\begin{aligned} u(x,y,z) &= u_0(x,y,t) - z\frac{dw_0(x,y,t)}{dx} + f(z)K_1\int\theta_x(x,y,t)dx \\ v(x,y,z) &= v_0(x,y,t) - z\frac{dw_0(x,y,t)}{dy} + f(z)K_2\int\theta_y(x,y,t)dy \\ w(x,y,z) &= w_0(x,y,t) + g(z)\varphi((x,y,t)) \end{aligned} \tag{9}$$

The polynomial function *f(z)* accounts for the distribution of shear stresses, that satisfy the shear stress on the top and the bottom equal zero

$$f(z) = z\left(\frac{1}{\pi} - \frac{5}{37}\pi z^2\right) \tag{10.a}$$

Where:

$$g(z) = \frac{df(z)}{dz} \tag{10.b}$$

Strain field

The deformations associated with the displacements are on the form:

$$\begin{Bmatrix}\varepsilon_{xx}\\ \varepsilon_{yy}\\ \gamma_{xy}\end{Bmatrix} = \begin{Bmatrix}\dfrac{\partial u}{\partial x}\\ \dfrac{\partial v}{\partial y}\\ \dfrac{\partial v}{\partial x}+\dfrac{\partial u}{\partial y}\end{Bmatrix}, \begin{Bmatrix}\gamma_{xz}\\ \gamma_{yz}\\ \varepsilon_{zz}\end{Bmatrix} = \begin{Bmatrix}\dfrac{\partial u}{\partial z}+\dfrac{\partial w}{\partial x}\\ \dfrac{\partial v}{\partial z}+\dfrac{\partial w}{\partial y}\\ \dfrac{\partial w}{\partial z}\end{Bmatrix} \tag{11}$$

$$\varepsilon_{xx} = \frac{\partial u_0}{\partial x} - z\frac{\partial^2 w_0}{\partial x^2} + K_1 f(z)\theta_x$$
$$\varepsilon_{yy} = \frac{\partial v_0}{\partial y} - z\frac{\partial^2 w_0}{\partial y^2} + K_2 f(z)\theta_y$$
$$\varepsilon_{yy} = g'(z)\phi_z$$
$$\gamma_{xy} = \frac{\partial u_0}{\partial y} + \frac{\partial v_0}{\partial x} - 2z\frac{\partial^2 w_0}{\partial x \partial y} + AK_1 f(z)\frac{\partial^2 \theta_x}{\partial x \partial y} + BK_2 f(z)\frac{\partial^2 \theta_y}{\partial x \partial y} \quad (12.a)$$
$$\gamma_{xz} = AK_1 f'(z)\frac{\partial \theta_x}{\partial x} + g(z)\frac{\partial \phi_z}{\partial x}$$
$$\gamma_{yz} = BK_2 f'(z)\frac{\partial \theta_y}{\partial y} + g(z)\frac{\partial \phi_z}{\partial y}$$

Where:

$$\int \theta dx = A\frac{\partial \theta}{\partial x}, \quad \int \theta dy = B\frac{\partial \theta}{\partial y} \quad (12.b)$$

Where the coefficients A and B are expressed according to the type of solution used, in this case, the Navier solution was used, with A and B expressed as follows:

$$A = -\frac{1}{\lambda^2}, \quad B = -\frac{1}{\mu^2} \text{ and } k_1 = \lambda^2, \qquad k_2 = \mu^2, \quad (12.c)$$

Where:

$\lambda = m\pi / a$ and $\mu = n\pi / b$

The relationship stress-strain of the porous plate when $(\varepsilon_z \neq 0)$ can be written as:

$$\begin{Bmatrix} \sigma_{xx} \\ \sigma_{yy} \\ \sigma_{zz} \\ \tau_{xz} \\ \tau_{yz} \\ \tau_{xy} \end{Bmatrix}^n = \begin{bmatrix} C_{11} & C_{12} & C_{13} & 0 & 0 & 0 \\ C_{12} & C_{22} & C_{23} & 0 & 0 & 0 \\ C_{13} & C_{23} & C_{33} & 0 & 0 & 0 \\ 0 & 0 & 0 & C_{44} & 0 & 0 \\ 0 & 0 & 0 & 0 & C_{55} & 0 \\ 0 & 0 & 0 & 0 & 0 & C_{66} \end{bmatrix} \begin{Bmatrix} \varepsilon_{xx} \\ \varepsilon_{yy} \\ \varepsilon_{zz} \\ \gamma_{xz} \\ \gamma_{yz} \\ \gamma_{xy} \end{Bmatrix}^n \quad (13)$$

The computation of the elastic constants Cij $\varepsilon_z \neq 0$ are given by:

$$C_{11} = C_{22} = C_{33} = \frac{E(z)(1-\nu)}{(1-2\nu)(1+\nu)}$$
$$C_{12} = C_{13} = C_{23} = \frac{\nu E(z)}{(1-2\nu)(1+\nu)} \quad (14)$$
$$C_{44} = C_{55} = C_{66} = \frac{E(z)}{2(1+\nu)}$$

IV.3.1. The stability equations

The virtual work principle is applied here to obtain the stability equations of the FG sandwich plate:

$$\int_V (\delta U + \delta V + \delta U_f) dV = 0 \tag{15}$$

Where *U, V, and Uf* are the strain energy, the potential energy of the applied loads, and the elastic foundation energy of the FG sandwich plate, respectively.

The variation of the strain energy of the plate is written as:

$$\delta U = \int_V \left[\sigma_{xx}\, \varepsilon_{xx} + \sigma_{yy}\, \varepsilon_{yy} + \tau_{xy}\, \gamma_{xy} + \tau_{yz}\ \gamma_{yz} + \tau_{xz}\ \gamma_{xz} + \sigma_{zz}\ \varepsilon_{zz} \right] dV \tag{16.a}$$

$$\delta U = \int_\Omega \begin{bmatrix} N_{xx}\,\delta u_{0,x} + M_{xx}\,\delta w_{0,xx} + P_{xx}\,\delta\theta_x + N_{yy}\,\delta v_{0,y} + M_{yy}\,\delta w_{0,xx} + P_{yy}\,\delta\theta_y + \\ N_{zz}\,\delta\varepsilon^0_{zz} + N_{xy}\,\delta u_{0,y} + N_{xy}\,\delta v_{0,x} + 2M_{xy}\,\delta w_{0,xy} + Q_{yz}\delta\phi_{z,y} + Q_{xz}\,\delta\phi_{z,x} \\ P_{xy}\,(AK_1\delta\theta_{x,xy} + BK_2\delta\theta_{y,xy}) + S_{yz}K_2B\delta\theta_{y,y} + S_{xz}\,K_1A\delta\theta_{x,x} \end{bmatrix} dA \tag{16.b}$$

Substituting equations (12. a) and (12. b) into the equation (16. b), the governing equations of stability can be expressed as follows:

$$\begin{aligned}
&\delta u_0 : \frac{\partial N_{xx}}{\partial x} + \frac{\partial N_{xy}}{\partial y} = 0, \quad \delta v_0 : \frac{\partial N_{xy}}{\partial x} + \frac{\partial N_{yy}}{\partial y} = 0 \\
&\delta w_0 : \frac{\partial^2 M_{xx}}{\partial x^2} + 2\frac{\partial^2 M_{xy}}{\partial x \partial y} + \frac{\partial^2 M_{yy}}{\partial y^2} + \bar{N} + f_e = 0 \\
&\delta\theta_x : -K_1A\frac{\partial^2 R_{xx}}{\partial x^2} - K_1A\frac{\partial^2 R_{xy}}{\partial x \partial y} + K_1A\frac{\partial S_{xz}}{\partial x} = 0 \\
&\delta\theta y : K_2B\frac{\partial^2 R_{yy}}{\partial y^2} - K_2B\frac{\partial^2 R_{xy}}{\partial x \partial y} + K_2B\frac{\partial S_{yz}}{\partial y} = 0 \\
&\delta\varphi : \frac{\partial Q_{xz}}{\partial x} + \frac{\partial Q_{yz}}{\partial y} - N_{zz} + g(z)^2\bar{N} = 0
\end{aligned} \tag{17}$$

The resultants (N_{xx}, N_{yy}, N_{xy}) and moment resultants (M_{xx}, M_{yy}, M_{xy}) are defined below:

$$\begin{Bmatrix} N_{xx} \\ N_{yy} \\ Nxy \end{Bmatrix} = \int_{-h/2}^{h/2} \begin{Bmatrix} \sigma_{xx} \\ \sigma_{yy} \\ \tau_{xy} \end{Bmatrix} d\,z, \quad \begin{Bmatrix} M_{xx} \\ M_{yy} \\ Mxy \end{Bmatrix} = \int_{-h/2}^{h/2} \begin{Bmatrix} \sigma_{xx} \\ \sigma_{yy} \\ \tau_{xy} \end{Bmatrix} z\,d\,z \tag{18}$$

The resultants of stress couples (R_{xx}, R_{yy}, R_{xy}) and (Q_{yz}, Q_{xz} , S_{xz} , S_{yz}) associated with the in-plane normal and tangential stress and effects transverse shear stress are defined as :

$$\begin{Bmatrix} R_{xx} \\ R_{yy} \\ Rxy \end{Bmatrix} = \int_{-h/2}^{h/2} \begin{Bmatrix} \sigma_{xx} \\ \sigma_{yy} \\ \tau_{xy} \end{Bmatrix} f(z)\,d\,z, \quad \begin{Bmatrix} Q_{xz} \\ Q_{yz} \end{Bmatrix} = \int_{-h/2}^{h/2} \begin{Bmatrix} \tau_{xz} \\ \tau_{yz} \end{Bmatrix}^{(n)} g(z)\,d\,z \tag{19}$$

$$\begin{Bmatrix} S_{xz} \\ S_{yz} \end{Bmatrix} = \int_{-h/2}^{h/2} \begin{Bmatrix} \tau_{xz} \\ \tau_{yz} \end{Bmatrix}^{(n)} \frac{\partial f(z)}{\partial z} d\,z, \quad \{N_{zz}\} = \int_{-h/2}^{h/2} \{\sigma_{zz}\}^{(n)} g'(z) d\,z,$$

$$\delta V = -\int_A \bar{N}\delta w\, dA = -\int_A \bar{N}(\delta w_0 + g(z)\delta\varphi)\, dA \tag{20}$$

With:

$$\bar{N} = \left[N_x^0 \frac{\partial^2 w}{\partial x^2} + N_{xy}^0 \frac{\partial^2 w}{\partial x \partial y} N_y^0 \frac{\partial^2 w}{\partial y^2} \right] \tag{20}$$

Where *fe* is the density of the reaction force of the foundation. For the elastic foundation model:

$$\delta U_f = \int_A f_e \delta w.dA = K_w w_0 - Kp\nabla^2 w_0$$

Where: K_p and K_w are Pasternak and Winkler elastic foundation parameters.

The equilibrium equations can be expressed in terms of displacement by Substituting equations (12.a), (12.b), (18), and (19) into equation (17), as:

$$\begin{aligned} \delta u_0 : \quad & A_{11}\frac{\partial^2 u_0}{\partial x^2} + A_{66}\frac{\partial^2 u_0}{\partial y^2} + (A_{12}+A_{66})\frac{\partial^2 v_0}{\partial x \partial y} - B_{11}\frac{\partial^3 w_0}{\partial x^3} - (B_{12}+2B_{66})\frac{\partial^3 w_0}{\partial x \partial y^2} \\ & + Bs_{11}K_1 A\frac{\partial^3 \theta}{\partial x^3} + (Bs_{12}K_2 B + Bs_{66}(K_1 A + K_2 B))\frac{\partial^3 \theta}{\partial x \partial y^2} + A_{13}\frac{\partial \varphi}{\partial x} = 0 \end{aligned} \tag{21.a}$$

$$\begin{aligned} \delta v_0 : \quad & (A_{12}+A_{66})\frac{\partial^2 u_0}{\partial x \partial y} + A_{22}\frac{\partial^2 v_0}{\partial y^2} + A_{66}\frac{\partial^2 v_0}{\partial x^2} - B_{22}\frac{\partial^3 w_0}{\partial y^3} - (B_{12}+2B_{66})\frac{\partial^3 w_0}{\partial x^2 \partial y} \\ & + Bs_{22}K_2 B\frac{\partial^3 \theta}{\partial y^3} + (Bs_{12}K_1 A + Bs_{66}(K_1 A + K_2 B))\frac{\partial^3 \theta}{\partial x^2 \partial y} + A_{23}\frac{\partial \varphi}{\partial y} = 0 \end{aligned} \tag{21.b}$$

$$\begin{aligned} \delta w_0 : \quad & B_{11}\frac{\partial^3 u_0}{\partial x^3} + (B_{12}+2B_{66})\frac{\partial^3 u_0}{\partial x \partial y^2} + B_{22}\frac{\partial^3 v_0}{\partial y^3} + (B_{12}+2B_{66})\frac{\partial^3 v_0}{\partial x^2 \partial y} \\ & - D_{11}\frac{\partial^4 w_0}{\partial x^4} - D_{22}\frac{\partial^4 w_0}{\partial y^4} - 2(D_{12}+2D_{66})\frac{\partial^4 w_0}{\partial x^2 \partial y^2} + Ds_{11}K_1 A\frac{\partial^4 \theta}{\partial x^4} + Ds_{22}K_2 B\frac{\partial^4 \theta}{\partial y^4} \\ & + (Ds_{12}+2Ds_{66})(K_1 A + K_2 B)\frac{\partial^4 \theta}{\partial x^2 \partial y^2} + B_{13}\frac{\partial^2 \varphi}{\partial x^2} + B_{23}\frac{\partial^2 \varphi}{\partial y^2} \\ & + N_x^0\frac{\partial^2 w}{\partial x^2} + N_{xy}^0\frac{\partial^2 w}{\partial x \partial y} + N_y^0\frac{\partial^2 w}{\partial y^2} + K_w w_0 - Kp\left(\frac{\partial^2 w_0}{\partial^2 x} + \frac{\partial^2 w_0}{\partial^2 y}\right) = 0 \end{aligned} \tag{21.c}$$

$$\delta\theta_x: \quad -Bs_{12}K_2\frac{\partial u_0}{\partial x}-Bs_{66}K_2B\frac{\partial^3 u_0}{\partial x\partial y^2}-Bs_{22}K_2\frac{\partial v_0}{\partial y}-Bs_{66}(K_1A)\frac{\partial^3 v_0}{\partial x^2\partial y}$$
$$+Ds_{11}K_2\frac{\partial^2 w_0}{\partial x^2}+Ds_{22}K_2\frac{\partial^2 w_0}{\partial y^2}+2K_2B(2Dss_{66})\frac{\partial^4 w_0}{\partial x^2\partial y^2}+Hs_{12}K_1K_2\theta x+$$
$$Hs_{22}K\theta y-Hs_{66}BK_2(AK1)\frac{\partial^4\theta x}{\partial x^2\partial y^2}-Hs_{66}(BK_2)^2\frac{\partial^4\theta y}{\partial x^2\partial y^2}-As_{44}(K_2B)^2\frac{\partial^2\theta y}{\partial y^2}$$
$$+Bs_{22}K_2\phi_z+As_{44}K_2B\frac{\partial^2\phi_z}{\partial y^2} \qquad (21.d)$$

$$\delta\theta_y: \quad Bs_{11}K_1\frac{\partial u_0}{\partial x}+Bs_{66}AK_1\frac{\partial^3 u_0}{\partial x\partial y^2}+Bs_{12}K_1\frac{\partial v_0}{\partial y}-Bs_{66}AK_1\frac{\partial^3 v_0}{\partial x^2\partial y}$$
$$-Ds_{11}K_1\frac{\partial w_0}{\partial x^2}-Ds_{12}K_1\frac{\partial^2 w_0}{\partial y^2}+2Ds_{66}AK_1\frac{\partial^4 w_0}{\partial x^2\partial y^2}+Hs_{11}K_1^2\theta_x$$
$$-Hs_{66}(AK_1)^2\frac{\partial^4\theta x}{\partial x^2\partial y^2}+Hs_{12}K_1K_2\theta_y-Hs_{66}AK_1BK_2\frac{\partial^4\theta y}{\partial x^2\partial y^2}$$
$$+(AK_1)^2As_{55}\frac{\partial^2\theta_x}{\partial x^2}+Bs_{13}K_1\phi_z+As_{55}AK_1\frac{\partial_2\phi_z}{\partial x^2} \qquad (21.e)$$

$$\delta\varphi: \quad A_{13}\frac{\partial u_0}{\partial x}+A_{23}\frac{\partial v_0}{\partial y}+B_{13}\frac{\partial^2 w_0}{\partial x^2}+B_{23}\frac{\partial^2 w_0}{\partial y}-(Bs_{13}+As_{44})K_1A\frac{\partial^2\theta}{\partial x^2}$$
$$-(Bs_{23}+As_{55})K_2B\frac{\partial^2\theta}{\partial y^2}+As_{44}K_2B\frac{\partial^2\varphi}{\partial x^2}+As_{55}\frac{\partial^2\varphi}{\partial y^2} \qquad (21.f)$$
$$-A_{33}+N_x^0\frac{\partial^2 w}{\partial x^2}+N_{xy}^0\frac{\partial^2 w}{\partial x\partial y}+N_y^0\frac{\partial^2 w}{\partial y^2}=0$$

where A_{ij}, $B_{ij,}$ . . ., are defined by

$$\begin{Bmatrix} A_{11} & B_{11} & D_{11} & Bs_{11} & Ds_{11} & Hs_{11} \\ A_{12} & B_{12} & D_{12} & Bs_{12} & Ds_{12} & Hs_{12} \\ A_{66} & B_{66} & D_{66} & Bs_{66} & Ds_{66} & Hs_{66} \end{Bmatrix} = \int_{-h/2}^{h/2}[1, z, z^2, f(z), z\,f(z), f^2(z)]\begin{Bmatrix} C_{11} \\ C_{12} \\ C_{66} \end{Bmatrix} dz \qquad (22)$$

$$As_{44}^0 = As_{55}^0 = \int_{-h/2}^{h/2} C_{44}g(z)^2 dz$$

IV.3.2. Exact solutions for FGMs sandwich plates resting boundary conditions

The exact solution of equations (21) for the FGMs sandwich plate under various boundary conditions can be constructed:

$$\begin{Bmatrix} u_0(x,y) \\ v_0(x,y) \\ w_0(x,y) \\ \theta_x(x,y) \\ \theta_y(x,y) \\ \phi(x,y) \end{Bmatrix} = \begin{Bmatrix} U_{mn} & X'_m(x)Y_n(y) \\ V_{mn} & X_m(x)Y'_n(y) \\ W_{mn} & X_m(x)Y_n(y) \\ \theta_{xmn} & X_m(x)Y_n(y) \\ \theta_{ymn} & X_m(x)Y_n(y) \\ \phi_{mn} & X_m(x)Y_n(y) \end{Bmatrix} \tag{23}$$

Where U_{mn}, V_{mn}, W_{mn}, θx_{mn}, θy_{mn} *and* ϕ_{mn} are arbitrary parameters. The functions Xm(x) and Yn(y) are suggested here to satisfy at least the geometric boundary conditions given in equations (23) and represent approximate shapes of the deflected surface of the plate. These functions for the different cases of boundary conditions are listed in Table 1 and presented in figures IV (3,4,5 and 6).

Tableau IV. 1: The admissible functions Xm(x) and Yn(y).

	Boundary conditions		**The functions X_m and Y_n**	
	At $x = 0, a$	At $y = 0, b$	$X_m(x)$	$Y_n(y)$
SSSS	$X_m(0) = X''_m(0) = 0$ $X_m(a) = X''_m(a) = 0$	$Y_n(0) = Y''_n(0) = 0$ $Y_n(b) = Y''_n(b) = 0$	$\sin(\lambda x)$	$\sin(\mu y)$
CSSS	$X_m(0) = X'_m(0) = 0$ $X_m(a) = X''_m(a) = 0$	$Y_n(0) = Y''_n(0) = 0$ $Y_n(b) = Y''_n(b) = 0$	$\sin(\lambda x)\left[\cos(\lambda x) - 1\right]$	$\sin(\mu y)$
CSCS	$X_m(0) = X'_m(0) = 0$ $X_m(a) = X''_m(a) = 0$	$Y_n(0) = Y'_n(0) = 0$ $Y_n(b) = Y''_n(b) = 0$	$\sin(\lambda x)\left[\cos(\lambda x) - 1\right]$	$\sin(\mu y)\left[\cos(\mu y) - 1\right]$
CCSS	$X_m(0) = X'_m(0) = 0$ $X_m(a) = X'_m(a) = 0$	$Y_n(b) = Y''_n(b) = 0$ $Y_n(b) = Y''_n(b) = 0$	$\sin^2(\lambda x)$	$\sin(\mu y)$
CCCC	$X_m(0) = X'_m(0) = 0$ $X_m(a) = X'_m(a) = 0$	$Y_n(0) = Y'_n(0) = 0$ $Y_n(b) = Y'_n(b) = 0$	$\sin^2(\lambda x)$	$\sin^2(\mu y)$
FFCC	$X''_m(0) = X'''_m(0) = 0$ $X''_m(a) = X'''_m(a) = 0$	$Y_n(0) = Y'_n(0) = 0$ $Y_n(b) = Y'_n(b) = 0$	$\cos^2(\lambda x)\left[\sin^2(\lambda x) + 1\right]$	$\sin^2(\mu y)$
FFSS	$X''_m(0) = X'''_m(0) = 0$ $X''_m(a) = X'''_m(a) = 0$	$Y_n(b) = Y''_n(b) = 0$ $Y_n(b) = Y''_n(b) = 0$	$\cos^2(\lambda x)\left[\sin^2(\lambda x) + 1\right]$	$\sin(\mu y)$

Denotes the derivative with respect to the corresponding coordinates.

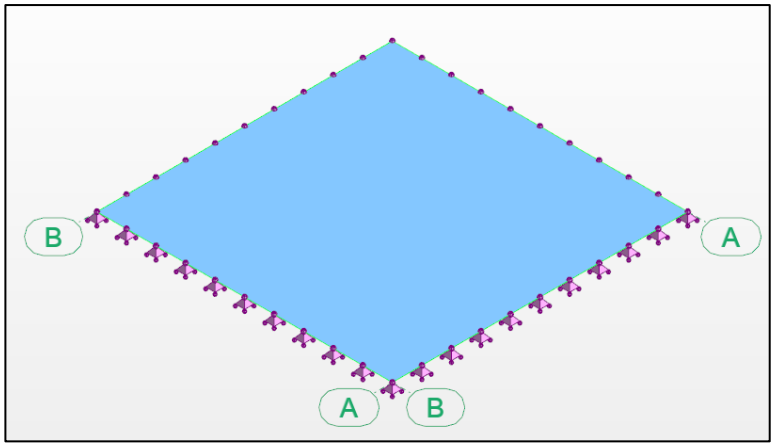

Figure IV. 3: simply supported plate

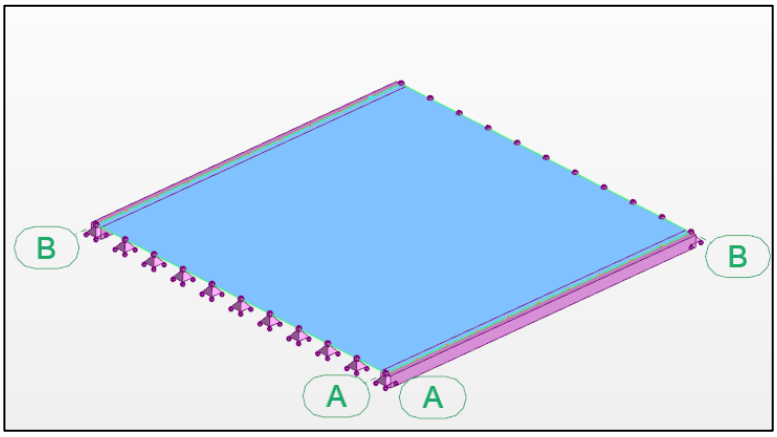

Figure IV. 4:: plate resting on clamped-clamped, simple-simple edges

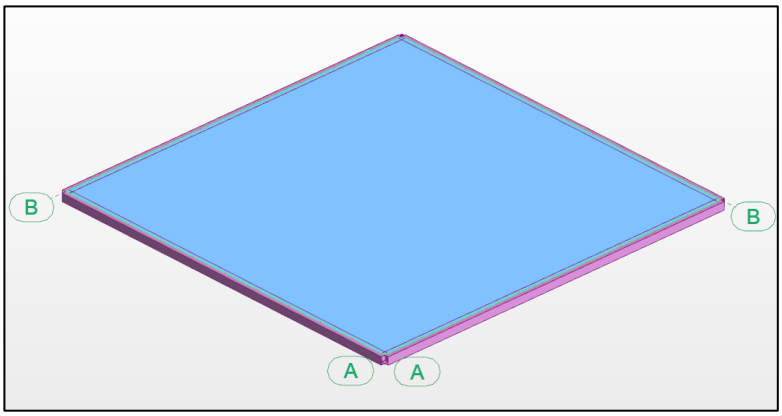

Figure IV. 5: plate resting on clamped-clamped-clamped-clamped edges

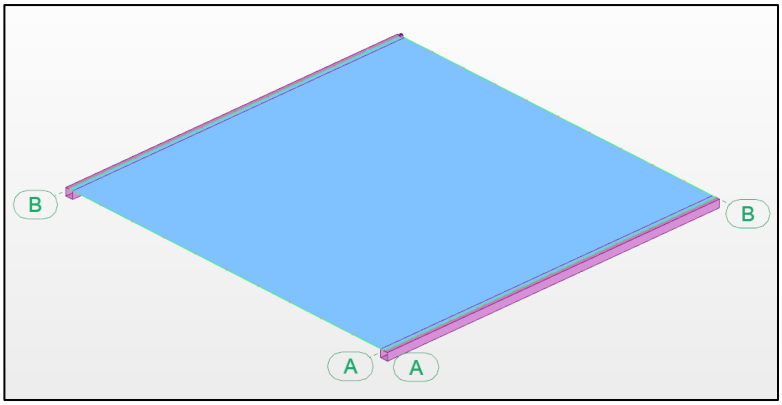

Figure IV. 6: plate resting on free-free, clamped-clamped edges

Substituting an expression (23) into the governing equations (21) and multiplying each equation by the corresponding eigenfunction, then integrating over the domain of solutions, we can obtain, after some mathematical manipulations, the following equations

$$[K]\{\Delta\} = \{0\} \tag{24}$$

Where:

$$\begin{bmatrix} a_{11} & a_{12} & a_{13} & a_{14} & a_{15} & a_{16} \\ a_{12} & a_{22} & a_{23} & a_{24} & a_{25} & a_{26} \\ a_{13} & a_{23} & a_{33} & a_{34} & a_{35} & a_{36} \\ a_{14} & a_{24} & a_{34} & a_{44} & a_{45} & a_{46} \\ a_{15} & a_{25} & a_{35} & a_{45} & a_{55} & a_{56} \\ a_{16} & a_{26} & a_{36} & a_{46} & a_{56} & a_{66} \end{bmatrix} \begin{Bmatrix} U_{mn} \\ V_{mn} \\ W_{mn} \\ \theta x_{mn} \\ \theta y_{mn} \\ \phi_{mn} \end{Bmatrix} = 0 \tag{25}$$

in which

$$\begin{aligned} a_{11} &= A_{11}L_{12} + A_{66}L_8 \\ a_{12} &= (A_{12} + A_{66})L_8 \\ a_{13} &= -B_{11}L_{12} - (B_{12} + 2B_{66})L_8 \\ a_{14} &= Bs_{66}(K_1A)L_8 + Bs_{11}K_1A\ L_{12} \\ a_{15} &= (Bs_{12} + Bs_{66})K_2BL_8 \\ a_{16} &= A_{13}\ L_6 \end{aligned} \tag{26.a}$$

$$\begin{aligned} a_{21} &= (A_{12} + A_{66})L_{10} \\ a_{22} &= A_{22}L_4 + A_{66}L_{10} \\ a_{23} &= -B_{11}L_4 - (B_{12} + 2B_{66})L_{10} \\ a_{24} &= (Bs_{12} + Bs_{66})K_1AL_{10} \\ a_{25} &= Bs_{22}K_2B\ L_4 + Bs_{66}(K_2B)\ L_{10} \\ a_{26} &= A_{13}L_2 \end{aligned} \tag{26.b}$$

$$
\begin{aligned}
a_{31} &= B_{11}L_{13} + (B_{12} + 2B_{66})L_{11} \\
a_{32} &= B_{11}L_5 + (B_{12} + 2B_{66})L_{11} \\
a_{33} &= -D_{11}L_{13} - D_{22}L_5 - 2(D_{12} + 2D_{66})L_{11} - N_x^0 L_9 - N_y^0 L_3 - K_w - K_p(L_9 + L_3) \\
a_{34} &= Ds_{11}K_1 A\, L_{13} + (Ds_{12} + 2Ds_{66})(K_1 A)L_{11} \\
a_{35} &= (Ds_{12} + 2Ds_{66})(K_2 B)L_{11} + Ds_{22}K_2 B L_5 \\
a_{36} &= B_{13}L_9 + B_{23}L_3 - g(z)(N_x^0 L_9 + N_y^0 L_3)
\end{aligned}
\tag{26.c}
$$

$$
\begin{aligned}
a_{41} &= -(Bs_{12}K_2 B + Bs_{66}(K_1 A + K_2 B))\; L_{11} - Bs_{11}K_1 A\; L_{13} \\
a_{42} &= -Bs_{22}K_2\; L_5 - (Bs_{12}K_1 A + Bs_{66}(K_1 A + K_2 B))L_{11} \\
a_{43} &= Ds_{11}K_1 A L_{13} + (Ds_{12} + 2Ds_{66})(K_1 A + K_2 B))L_{11} + Ds_{22}K_2 B\, L_5 \\
a_{44} &= -(K_1 A)^2 Hs_{11}L_{13} - Hs_{22}(K_2 B)^2 L_5 + (As_{55}(K_1 A)^2)L_9 + \\
&\quad (As_{44}(K_2 B)^2)L_3 + Hs_{66}(K_1 A)^2 L_{11} - (Hs_{12}K_1 A K_2 B)L_{11} \\
a_{45} &= Hs_{66}(K_1 A * K_2 B)^2)L_{11} - (Hs_{12}K_1 K_2)L_{11} \\
a_{46} &= (As_{55}K_1 A - Bs_{13}K_1 A)L_9
\end{aligned}
\tag{26.d}
$$

$$
\begin{aligned}
a_{51} &= (Bs_{12} + Bs_{66})K_2 B L_8 \\
a_{52} &= Bs_{22}K_2 B\; L_4 + Bs_{66}(K_2 B)\, L_{10} \\
a_{53} &= (Ds_{12} + 2Ds_{66})(K_2 B)L_{11} + Ds_{22}K_2 B L_5 \\
a_{54} &= Hs_{66}(K_1 A * K_2 B)^2)L_{11} - (Hs_{12}K_1 K_2)L_{11} \\
a_{55} &= -Hs_{66}(K_2 B)^2 L_{11} + As_{44}(K_2 B)^2 L_3 \\
a_{56} &= (As_{44}(BK_2) - Bs_{23}BK_2)L_3
\end{aligned}
\tag{26.e}
$$

$$
\begin{aligned}
a_{61} &= A_{13}L_6 \\
a_{62} &= A_{23}L_2 \\
a_{63} &= B_{13}L_9 + B_{23}L_3 - g(z)(N_x^0 L_9 + N_y^0 L_3) \\
a_{64} &= (As_{55}K_1 A - Bs_{13}K_1 A)L_9 \\
a_{65} &= (As_{44}(BK_2) - Bs_{23}BK_2)L_3 \\
a_{66} &= As_{55}L_3 + As_{44}L_9 - A_{33} - g(z)^2(N_x^0 L_9 + N_y^0 L_3)
\end{aligned}
\tag{26.f}
$$

And

$$
\begin{aligned}
&\left(L_1, L_2, L_3, L_4\right) = \int_0^a \int_0^b \left(X_m''' Y_n, X_m' Y_n'', X_m' Y_n, X_m' Y_n''\right) X_m' Y_n \, dxdy \;\; , \left(L_5, L_6, L_7\right) = \int_0^a \int_0^b \left(X_m'' Y_n', X_m Y_n''', X_m Y_n'\right) X_m Y_n' \, dxdy \\
&\left(L_8, L_9, L_{10}\right) = \int_0^a \int_0^b \left(X_m''' Y_n, X_m'' Y_n'', X_m'' Y_n\right) X_m Y_n \, dxdy \;\; , \left(L_{11}, L_{12}, L_{13}\right) = \int_0^a \int_0^b \left(X_m Y_n''', X_m Y_n'', X_m Y_n\right) X_m Y_n \, dxdy
\end{aligned}
\tag{30}
$$

IV.3.3. Expression of in-plane load

The in-plane compressive load applied is of the form[179]:

Case 1 triangular load

$$N_{xx} = N_0\left(1-\gamma\frac{y}{b}\right) \qquad \gamma = 1 \tag{31.a}$$

Case 2: exponential load

$$N_{xx} = N_0 e^{\frac{\gamma y}{b}} \tag{31.b}$$

Case 3: sinusoidal load

$$N_{xx} = N_0 \sin\left(\frac{\pi y}{b}\right) \tag{31.c}$$

Case 4: uniform load

$$N_{xx} = N_0\left(1-\gamma\frac{y}{b}\right) \qquad \gamma = 0 \tag{31.d}$$

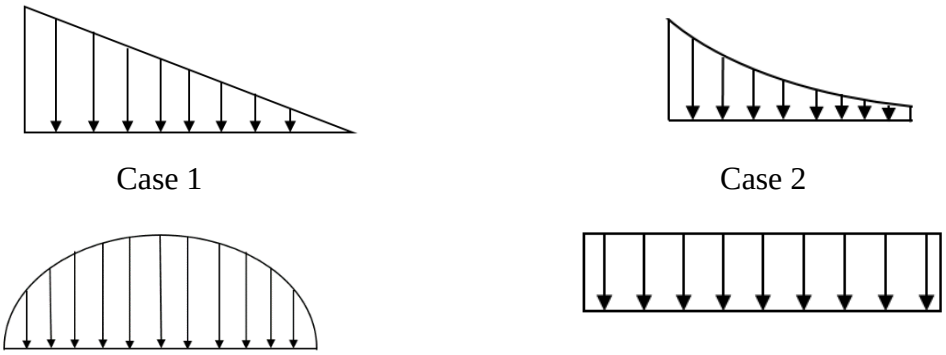

Case 1 Case 2

Case 3 Case 4

Figure 1:Schematic representation of different types of in-plane compressive

IV.4. Conclusion

In this chapter, quasi-3D high deformation theory is used to investigate the effect of porosity on the buckling of sandwich FG plates subjected to various boundary conditions and Pasternak and Winkler elastic foundation under axial and biaxial in-plane loads with different shapes. The thickness stretching effect is considered in this theory. Two configurations of FG models are analyzed here: FG faces with the ceramic core when The FG material with micro voids varies smoothly in the thickness direction-based power law distribution. FG faces with metal foam core presented for the second model. Hamilton's principle obtains the stability equations, and then it's solved by Navier solution for the supported plate.

CHAPTER V

RESULTS AND DISCUSSION

CHAPTER V: RESULTS AND DISCUSSION

V.1. Introduction:

This chapter presents the numerical results of the analysis of the effect of porosity on the buckling of sandwich FG plates subjected to various boundary conditions and Pasternak and Winkler elastic foundations under axial and biaxial in-plane loads with different shapes. Two configurations of FG models are analyzed here: FG faces with the ceramic core when The FG material with microvoids varies smoothly in the thickness direction-based power law distribution. The present model validated with those from the literature, then the effect of different parameters: porosity parameters, foam cell distribution, boundary conditions, elastic foundation, power law index, ratio aspect, side to thickness, and different in-plane load on the variation of the buckling behavior are demonstrated.

V.2. Numerical results

The present sandwich plate is made of a mixture of metal and ceramic and subjected to in-plane load in two directions $\left(\overline{N}_{xx}^{0} = N_{cr},\ \overline{N}_{yy}^{0} = RN_{cr}\right)$,the properties of both metal (Aluminum-Al) and ceramic (Alumina-Al2O3) materials are represented as

-Alumina, Al_2O_3: $E_c = 380\times10^9\ \mathrm{N/m^2}$;
-Aluminum, Al: $E_m = 70\times10^9\ \mathrm{N/m^2}$;

-Metal foam E_f= 200 * 10 ^9 N/m^2

The Poisson's ratio is assumed to be a constant for all results $(\upsilon = 0,3)$.
It is to be noted that several kinds of sandwich plates are considered[189]

The (1-0-1) FG Sandwich Porous Plate

The structure is composed of two skin layers

$$h1 = h2 = 0. \tag{1.a}$$

The (1-1-1) FG Sandwich Porous Plate

The structure is composed of three equal skin layers

$$h_1 = -\frac{h}{6},\ h_2 = \frac{h}{6} \tag{1.b}$$

The (1-2-1) FG Sandwich Porous Plate

The structure is in three skin layers, has a core with double thickness than face layers:

$$h_1 = -\frac{h}{4},\ h_2 = \frac{h}{4} \tag{1.c}$$

The (2-1-2) FG Sandwich Porous Plate

The structure is in three skin layers, and has a core with half the thickness than face layers:

$$h_1 = -\frac{h}{10},\ h_2 = \frac{h}{10} \tag{1.d}$$

The (2-2-1) FG Sandwich Porous Plate

The non-symmetric scheme sandwich plate has an upper skin sheet with the same thickness as half of the core and bottom skin layer.

$$h_1 = -\frac{h}{10},\ h_2 = \frac{3h}{10} \tag{1.e}$$

The (2-1-1) FG Sandwich Porous Plate

The non-symmetric scheme sandwich plate has a lower skin sheet with the same thickness as half of the core and upper skin layer.

$$h_1 = 0,\ h_2 = \frac{h}{4} \tag{1.f}$$

The (1-3-1) FG Sandwich Porous Plate

The structure is in three skin layers, and has a core with triple the thickness than face layers:

$$h_1 = -\frac{3h}{10},\ h_2 = \frac{3h}{10} \tag{1.g}$$

The following non-dimensional parameters are used:

$$\begin{gathered} \overline{N}_{cr} = \frac{Na^2}{bh^3E_m},\quad \hat{N} = \frac{Nb}{Dc} \\ D_c = \frac{E_c h^3}{12(1-\nu^2)},\ D_m = \frac{E_m h^3}{12(1-\nu^2)} \end{gathered} \tag{2}$$

V.2.1. Comparison studies

To validate our present work, the mechanical buckling load of FGM isotropic and sandwich plate is compared with the paper of A. Zenkour and A. Radwan, who worked on the effect of elastics foundation on Hygrothermo-mechanical buckling of FGM plate using a quasi-3D theory [201], H. Akhavan et al., examined Exact solutions for FGM rectangular plates under loads resting on Pasternak elastic foundation [202] and A. Neves et al., when they studied the static and dynamic of

FGM sandwich plate basing quasi-3D theory and a meshless technique [203]. In comparison with N. El Meiche et al., they used A new hyperbolic shear deformation theory to analyze the buckling and vibration of functionally graded sandwich plate [204], H.-T. Thai et al., analyzed the behavior of FGM sandwich plate-based first shear deformation theory [205], R. Meksi et al., used an analytical solution for bending, buckling and free vibration response of FGM sandwich plates [206] and with A. A. Daikh and A. M. Zenkour for the effect of porosity on the buckling and free vibration FG sandwich plate using high shear deformation theory [165], for various configuration of sandwich under uni-axial and bi-axial loads. Table V.1 presents a comparison results for the buckling behavior of FG square and rectangular plat resting on Pasternak and Winkler foundation for different values of thickness ratio a/h under mechanical load. It can be seen that with the decrease of a/h and a/b, the critical buckling decreases, and it increases with the inclusion of elastic foundation coefficients. Furthermore, the hyperbolic shear deformation theory (HPT) presents a good agreement.

a/b	(K*w*, K*p*)	a/h = 1000			a/h= 100			a/h= 10		
		[202]	[201]	Present	[202]	[201]	Present	[202]	[201]	Present
0.5	0,0	61.6848	61.6848	61.6848	61.6641	61.6698	61.6619	59.6629	60.1915	59.4376
	100, 10	152.213	152.2130	152.213	152.1930	152.1980	152.178	150.1910	150.7190	148.783
	1000,100	704.589	704.5890	704.588	704.386	704.4410	704.128	686.1710	690.5500	-
1	0,0	39.4782	39.4782	39.4781	39.4570	39.4628	39.4546	37.4477	37.9661	37.2303
	100,10	69.6103	69.6103	69.6102	69.5891	69.5949	69.5803	67.5798	68.0982	66.7463
	1000,100	212.014	212.014	212.014	210.1610	211.9540	211.843	204.6510	206.3610	-
2	0,0	39.4776	39.4778	39.4775	39.3930	39.4162	39.3829	32.4414	33.9285	31.7932
	100,10	45.1108	45.1111	45.1106	45.0262	45.0494	45.0115	37.5182	40.3313	37.0239
	1000,100	85.2563	85.2567	85.2557	85.0952	85.1392	85.0229	72.8290	75.9736	-

Table V.1 : Comparison of normalized Uni-axial buckling load Ncr of rectangular FG plates

The next comparison results are shown in both Tables V.2 and V.3 for the buckling load of square FGM plate under Uni-axial and bi-axial load successively with three different sandwich shapes and various values of k. It can bet noted that increasing index k decreased the critical buckling; for the validation of our results, the present theory agrees well with those given by [203].

Table V.2: Uni-axial buckling load of the simply supported plate (Ncr)

Shape	Theory	K			
		0	1	5	10
1-0-1	Present	12.955558	5.1499270	2.6479672	2.4773691
	[203]	12.95287	5.06137	2.63652	2.47216
1-1-1	Present	12.955558	6.4440096	3.5680855	3.1839136
	[203]	12.95287	6.31500	3.53005	3.18391
2-1-2	Pres	12.955558	5.8210420	3.0317930	2.7359379
	[203]	12.95287	5.71135	3.00791	2.72046

Table V. 3:Bi-axial buckling load of simply supported plate (Ncr).

Scheme	Theory	K			
		0	1	5	10
1-0-1	Present	6.4777791	2.5749635	1.3239836	1.2386846
	[203]	6.47643	2.53069	1.31826	1.23608

1-1-1	Present	6.4777791	3.2220048	1.7840428	1.5919568
	[203]	6.47643	3.15750	1.76502	1.57880
2-1-2	Pres	6.4777791	2.9105210	1.5158965	1.3679690
	[203]	6.47643	2.85568	1.50395	1.36023

Table V. 4: . Dimensionless buckling load Ncr of square plates under uniaxial compression (γ1 =-1, γ2= 0, a/h = 10).

k	Theory	1-0-1	2-1-2	1-1-1	2-2-1	1-2-1
0	El Meiche et al[204]	13.0055	13.0055	13.0055	13.0055	13.0055
	Huu-Tai T et al.[205]	13.0045	13.0045	13.0045	13.0045	13.0045
	Meksi et al. [206]	13.0236	13.0236	13.0236	13.0236	13.0236
	Present 2D	13.0051	13.0051	13.0051	13.0051	13.0051
0.5	El Meiche et al[204]	7.3638	7.9405	8.4365	8.8103	9.2176
	Huu-Tai T et al. [205]	7.3634	7.9403	8.4361	8.8095	9.2162
	Meksi et al. [206]	7.3664	7.9442	8.4423	8.8182	9.2277
	Present 2D	7.3648	7.9412	8.4366	8.8100	9.2166
1	El Meiche et al[204]	5.1663	5.8394	6.4645	6.9495	7.5072
	Huu-Tai T et al.[205]	5.1648	5.8387	6.4641	6.9485	7.5056
	Meksi et al. [206]	5.1651	5.8392	6.4664	6.9536	7.5138
	Present 2D	5.1676	5.8405	6.4649	6.9495	7.5063
5	El Meiche et al [204]	2.6568	3.0414	3.5787	4.1116	4.7346
	Huu-Tai T et al.[205]	2.6415	3.0282	3.5710	4.1024	4.7305
	Meksi et al. [206]	2.6518	3.0369	3.5756	4.1103	4.7351
	Present 2D	2.6590	3.0408	3.5800	4.1124	4.7347
10	El Meiche et al[204]	2.4857	2.7450	3.1937	3.7069	4.2796
	Huu-Tai T et al.[205]	2.4666	2.7223	3.1795	3.6901	4.2728
	Meksi et al. [206]	2.4808	2.7397	3.1898	3.7048	4.2789
	Present 2D	2.4881	2.7470	3.1952	3.7079	4.2800

Table V 5: Dimensionless buckling load Ncr of square plates under biaxial compression (γ1 =-1, γ2= -1, a/h = 10)

k	Theory	1-0-1	2-1-2	1-1-1	2-2-1	1-2-1
0	Huu-Tai T et al.[205]	6.5022	6.5022	6.5022	6.5022	6.5022
	Meksi et al. [206]	6.5118	6.5118	6.5118	6.5118	6.5118
	Daikh et al.[165]	6.5026	6.5026	6.5026	6.5026	6.5026
	Present 2D	6.5026	6.5026	6.5026	6.5026	6.5026

0.5	Huu-Tai T et al.[205]	3.6817	3.9702	4.2181	4.4047	4.6081
	Meksi et al. [206]	3.6832	3.9721	4.2212	4.4091	4.6138
	Daikh et al. [165]	3.6825	3.9706	4.2183	4.4050	4.6083
	Present 2D	3.6824	3.9706	4.2183	4.4050	4.6083
1	Huu-Tai T et al.[205]	2.5824	2.9193	3.2320	3.4742	3.7528
	Meksi et al. [206]	2.5826	2.9196	3.2332	3.4768	3.7569
	Daikh et al. [165]	2.5839	2.9203	3.2325	3.4748	3.7531
	Present 2D	2.5838	2.9202	3.2325	3.4748	3.7532
5	Huu-Tai T et al. [205]	1.3208	1.5141	1.7855	2.0512	2.3652
	Meksi et al. [206]	1.3259	1.5185	1.7878	2.0551	2.3676
	Daikh et al. [165]	1.3296	1.5216	1.7900	2.0562	2.3673
	Present 2D	1.3295	1.5216	1.7900	2.0562	2.3673
10	Huu-Tai T et al.[205]	1.2333	1.3612	1.5897	1.8450	2.1364
	Meksi et al. [206]	1.2404	1.3699	1.5949	1.8524	2.1395
	Present 2D	1.2441	1.3735	1.5976	1.8539	2.1400

Tables V.4 and V.5 present the non-dimensional values of the critical buckling load, N_{cr}, for various types of supported sandwich square plates under uniaxial and biaxial compression, respectively, and different values of index k. The results obtained from the present theory are compared with those presented by Meiche et al. [204], Huu-Tai Thai et al. [205], Daikh et al. [165], and Meksi et al. [206]. It is to be noted that the critical buckling decreases with increasing index k. Furthermore, the present hyperbolic shear deformation theory (HPT) gives a very good accuracy

V.2.2. parametric results

The effect of the aspect ratio, side-to-thickness ratio, index gradient, different configurations of sandwich scheme, and boundary conditions in the buckling of porous FG sandwich plate and sandwich plate containing metal foam core is shown in tables and figures below.

Table V. 6: The critical buckling load Ncr of an FG square sandwich plate (R = 0) under the effect porosity distribution

Load	Bcs	a/h	Scheme								
			Perfect			Imperfect I			Imperfect II		
			1-0-1	1-1-1	1-2-1	1-0-1	1-1-1	1-2-1	1-0-1	1-1-1	1-2-1
Case 1	SSSS	5	6.6728	8.3200	9.5793	5.3941	7.0186	8.4034	3.7254	5.5655	7.1463
		10	7.3570	9.2057	10.690	5.9014	7.6811	9.2851	4.0220	6.0196	7.8170
		100	7.6151	9.5414	11.116	6.0907	7.9284	9.6187	4.1306	6.1863	8.0671
	CCSS	5	10.714	13.299	15.165	8.7450	11.364	13.449	6.1281	9.1320	11.563

		10	12.962	16.190	18.724	10.436	13.577	16.337	7.1517	10.694	13.815
		100	13.986	17.524	20.414	11.187	14.563	17.666	7.5873	11.363	14.817
	CCCC	5	15.936	19.676	22.153	13.141	17.056	19.929	9.3357	13.883	17.346
		10	20.551	25.647	29.604	16.577	21.560	25.887	11.388	17.023	21.936
		100	22.577	28.287	32.951	18.059	23.507	28.517	12.248	18.343	23.919
	FFCC	5	19.821	24.468	27.550	16.355	21.221	24.781	11.631	17.291	21.574
		10	26.096	32.546	37.511	21.083	27.414	32.856	14.516	21.687	27.887
		100	29.244	36.640	42.680	23.391	30.449	36.936	15.866	23.761	30.981
Case 2	SSSS	5	7.8614	9.8021	11.286	6.3548	8.2686	9.9007	4.3889	6.5568	8.4193
		10	8.6673	10.845	12.593	6.9524	9.0491	10.939	4.7383	7.0916	9.2091
		100	8.9713	11.241	13.095	7.1754	9.3406	11.332	4.8663	7.2880	9.5039
	CCSS	5	12.622	15.666	17.866	10.302	13.388	15.844	7.2193	10.759	13.622
		10	15.270	19.073	22.059	12.295	15.996	19.247	8.4254	12.599	16.274
		100	16.477	20.646	24.050	13.179	17.156	20.813	8.9386	13.387	17.456
	CCCC	5	18.772	23.179	26.095	15.482	20.094	23.476	10.999	16.356	20.436
		10	24.213	30.216	34.877	19.530	25.401	30.499	13.417	20.054	25.843
		100	26.599	33.326	38.820	21.274	27.694	33.596	14.430	21.610	28.179
	FFCC	5	23.353	28.824	32.464	19.269	25.004	29.195	13.703	20.372	25.419
		10	30.744	38.341	44.191	24.837	32.296	38.707	17.100	25.550	32.854
		100	34.451	43.166	50.281	27.557	35.873	43.514	18.691	27.993	36.500
Case 3	SSSS	5	11.001	13.718	15.794	8.8936	11.571	13.856	6.1421	9.1757	11.783
		10	12.130	15.177	17.624	9.7299	12.664	15.309	6.6311	9.9246	12.888
		100	12.555	15.731	18.327	10.042	13.072	15.859	6.8101	10.199	13.300
	CCSS	5	17.664	21.926	25.003	14.418	18.735	22.173	10.103	15.056	19.064
		10	21.370	26.693	30.870	17.207	22.386	26.936	11.791	17.631	22.777
		100	23.060	28.893	33.657	18.444	24.010	29.126	12.509	18.734	24.429
	CCCC	5	26.274	32.441	36.527	21.668	28.121	32.856	15.392	22.890	28.601
		10	33.883	42.286	48.809	27.330	35.547	42.683	18.776	28.066	36.167
		100	37.223	46.639	54.329	29.773	38.757	47.016	20.194	30.243	39.434
	FFCC	5	32.678	40.342	45.426	26.966	34.989	40.854	19.177	28.509	35.571
		10	43.026	53.657	61.840	34.757	45.197	54.169	23.931	35.757	45.977
		100	48.214	60.409	70.367	38.566	50.203	60.897	26.159	39.176	51.080

Table V.6 analyzed the effect of two different shapes of porosity (imperfect I and II) in the buckling behavior of FG sandwich plate with various schema under three cases of in-plane load subjected to various boundary conditions and ratio a/h, the critical buckling was in the maximum value with FFCC boundary condition than the other for all the cases of load, and it is observed that the critical buckling increased with the including of porosity when the results obtained for imperfect II is smaller than imperfect I.

Table V. 7: Variation of critical buckling load for perfect and imperfect FG sandwich plates under uni-axial and bi-axial in plane load

k	Porosity	ζ	Scheme						
			1-0-1	1-1-1	1-2-1	2-1-2	2-1-1	2-2-1	1-3-1
Uni-axial									
0	Perfect	0	7.3871	7.3871	7.3871	7.3871	7.3871	7.3871	7.3871
	imperfect III	0.1	7.2079	7.1936	7.2079	7.1914	7.2036	7.2086	7.2257
		0.3	6.8744	6.8321	6.8744	6.8272	6.8624	6.8752	6.9248
	Imperfect VI	0.1	7.2714	7.2421	7.2400	7.2521	7.2557	7.2500	7.2471
		0.3	7.0395	6.9528	6.9450	6.9833	6.9931	6.9751	6.9669
1	Perfect	0	2.9111	3.6445	4.2370	3.2905	3.5071	3.9331	4.6876

	imperfect III	0.1	2.7231	3.4469	4.0546	3.0919	3.3145	3.7447	4.5234
		0.3	2.3722	3.0779	3.7136	2.7210	2.9529	3.3910	4.2167
	Imperfect VI	0.1	2.7993	3.4981	4.0872	3.1562	3.3739	3.7905	4.5454
		0.3	2.5754	3.2054	3.7871	2.8876	3.1068	3.5039	4.2603
5	Perfect	0	1.4946	2.0094	2.6625	1.7074	1.9407	2.3394	3.2396
	imperfect III	0.1	1.3061	1.8096	2.4778	1.5069	1.7381	2.1416	3.0736
		0.3	0.95386	1.4359	2.1326	1.1318	1.3535	1.7680	2.7634
	Imperfect VI	0.1	1.3829	1.8619	2.5110	1.5724	1.8024	2.1904	3.0958
		0.3	1.1595	1.5661	2.2076	1.3021	1.5229	1.8894	2.8076
Bi-axial									
0	Perfect	0	4.9246	4.9246	4.9246	4.9246	4.9246	4.9246	4.9246
	imperfect III	0.1	4.7999	4.7956	4.8055	4.7944	4.8026	4.8057	4.8172
		0.3	4.5673	4.5547	4.5829	4.5515	4.5749	4.5836	4.6166
	Imperfect VI	0.1	4.8476	4.8281	4.8264	4.8349	4.8371	4.8331	4.8314
		0.3	4.6930	4.6351	4.6300	4.6556	4.6621	4.6501	4.6446
1	Perfect	0	1.9408	2.4296	2.8247	2.1937	2.3381	2.6221	3.1251
	imperfect III	0.1	1.8154	2.2979	2.7030	2.0613	2.2096	2.4965	3.0156
		0.3	1.5814	2.0519	2.4757	1.8140	1.9686	2.2607	2.8111
	Imperfect VI	0.1	1.8662	2.3321	2.7248	2.1041	2.2492	2.5270	3.0302
		0.3	1.7170	2.1369	2.5248	1.9251	2.0712	2.3359	2.8402
5	Perfect	0	0.99643	1.3396	1.7750	1.1382	1.2939	1.5596	2.1597
	imperfect III	0.1	0.87071	1.2064	1.6519	1.0046	1.1588	1.4278	2.0491
		0.3	0.63592	0.95729	1.4218	0.75457	0.90236	1.1787	1.8423
	Imperfect VI	0.1	0.92200	1.2412	1.6740	1.0482	1.2016	1.4603	2.0639
		0.3	0.77300	1.0440	1.4717	0.86807	1.0153	1.2596	1.8717

The variations of critical buckling loads for perfect and imperfect (III and VI) FG sandwich plate under Uni-axial and bi-axial in-plane load and various values of index k (0, 1 and 2) is presented in table V.7, the porosity coefficient (ζ = 0.1, 0.3). It is observed that the non-dimensional critical buckling load for Uni-axial and bi-axial loading decreases with the increase of index k and the value of the porosity coefficient. This is due to the effect of the porosity distribution on the inertia and the stiffness of the plate during the increase of the number and size of porosity cells.

Table V 8: Variation of non-dimensional critical buckling load for SSSS and CCSS sandwich plates containing three different types of metal foam core 1-3-1

a/b	SSSS						CCSS					
	Foam I		Foam II		Foam III		Foam I		Foam II		Foam III	
	η	$\overline{N}_{cr}$	η^*	$\overline{N}_{cr}$	γ	$\overline{N}_{cr}$	η	$\overline{N}_{cr}$	η^*	$\overline{N}_{cr}$	γ	$\overline{N}_{cr}$
0.5	0.1	1.8766	0.1738	1.8906	0.9361	1.8817	0.1	5.4758	0.1738	5.5492	0.9360	5.5028
	0.2	1.8482	0.3442	1.8774	0.8716	1.8586	0.2	5.3510	0.3442	5.5065	0.8713	5.4082
	0.3	1.8188	0.5103	1.8645	0.8064	1.8348	0.3	5.2175	0.5065	5.4648	0.8058	5.3082
	0.4	1.7878	0.6708	1.8520	0.7404	1.8101	0.4	5.0720	0.6708	5.4240	0.7391	5.2030
	0.5	1.7549	0.8231	1.8401	0.6733	1.7843	0.5	4.9112	0.8231	5.3855	0.6711	5.0898
	0.6	1.7192	0.9612	1.8293	0.6047	1.7569	0.6	4.7292	0.9612	5.3500	0.6012	4.9660
1	0.1	4.6657	0.1738	4.7074	0.9361	4.6808	0.1	7.8145	0.1738	7.9175	0.9360	7.8520
	0.2	4.5864	0.3442	4.6735	0.8716	4.6177	0.2	7.6400	0.3442	7.8560	0.8713	7.7190
	0.3	4.5029	0.5103	4.6404	0.8064	4.5520	0.3	7.4540	0.5065	7.7965	0.8058	7.5795
	0.4	4.4140	0.6708	4.6084	0.7404	4.4836	0.4	7.2520	0.6708	7.7390	0.7391	7.4320
	0.5	4.3176	0.8231	4.5780	0.6733	4.4112	0.5	7.0300	0.8231	7.6835	0.6711	7.2740
	0.6	4.2110	0.9612	4.5504	0.6047	4.3336	0.6	6.7815	0.9612	7.6340	0.6012	7.1030

2	0.1	25.798	0.1738	26.214	0.9361	25.952	0.1	24.795	0.1738	25.192	0.9360	24.940
	0.2	25.117	0.3442	26.003	0.8716	25.446	0.2	24.147	0.3442	24.989	0.8713	24.458
	0.3	24.368	0.5103	25.794	0.8064	24.907	0.3	23.440	0.5065	24.788	0.8058	23.945
	0.4	23.530	0.6708	25.592	0.7404	24.326	0.4	22.654	0.6708	24.595	0.7391	23.396
	0.5	22.561	0.8231	25.402	0.6733	23.690	0.5	21.763	0.8231	24.411	0.6711	22.798
	0.6	21.407	0.9612	25.227	0.6047	22.980	0.6	20.715	0.9612	24.243	0.6012	22.134

Table V. 8 shows the non-dimensional critical buckling load for SSSS and CCSS sandwich plates containing three different types of metal foam core under mechanical load with different values of aspect ratio a/b (0.5, 1, and 2). As we can see, the critical buckling obtained with SSSS boundaries is smaller than CCSS; this may prove the effect of various boundary conditions on the rigidity of the plate. Furthermore, the increase in foam coefficient η , η^* and γ decreased the critical buckling

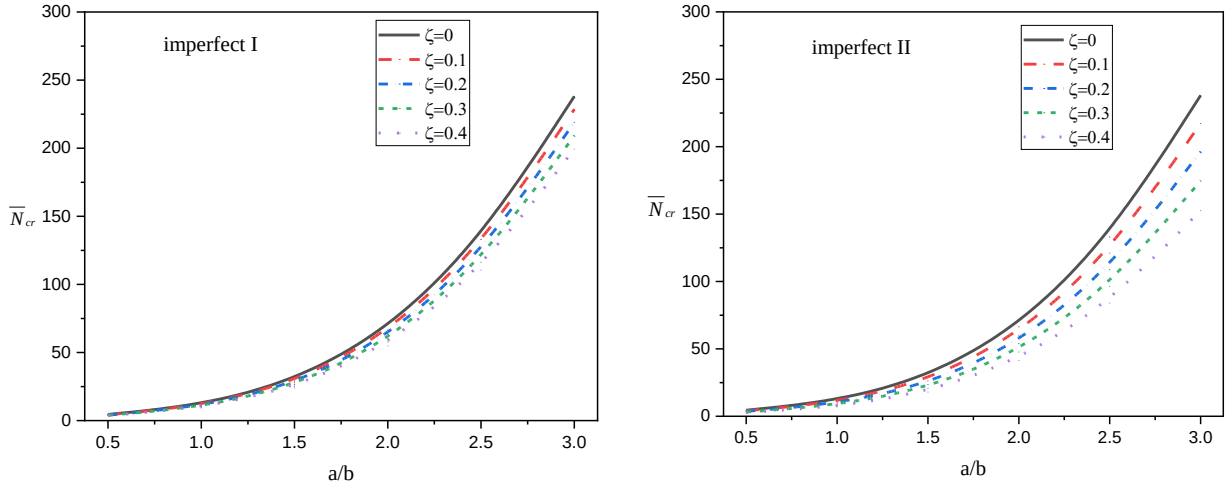

(a) (b)

Figure V. 1:non-dimensional critical buckling load N versus axial compression ratio a/b for different pore distributions values (, a/h=10, k =0.5): (a) imperfect I; (b) imperfect II.

Figures V. 1-a and V.1-b show the critical buckling load for the FG sandwich plate (1-2-1), with the aspect ratio a/b under the effect of two different shapes of porosity, imperfect I in 3-a and imperfect II in 3-b. The critical buckling increases with the augmentation of the aspect ratio a/b; the inclusion of porosity reduces the critical buckling. Also, the second shape of porosity (imperfect II) made the plate weaker than the first shape (imperfect I).

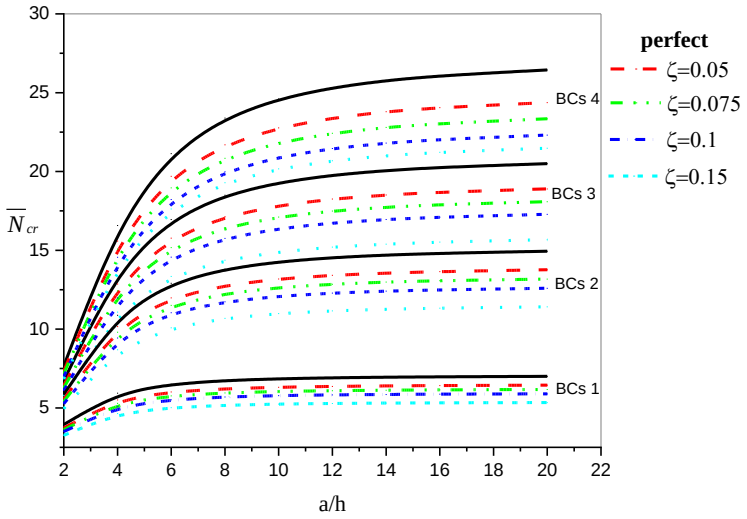

Figure V. 2:non-dimensional critical buckling load N versus length-to-thickness ratio a/h under different boundary conditions for various values of porosity (a=b) k= 2*

Figure V. 2 illustrates the variation of non-dimensional critical buckling load with thickness ratio a/h subjected to various boundary conditions, which is BCs1 is SSSS, BCs2 is CSCS, BCs3 is CCC, and BCs FFCC, under the effect of porosity (imperfect II). The critical buckling increasing with the increase of a/h, such as the including of the porosity, reduces the value of the critical buckling when the porosity coefficient increases, and this is because of its effect on the stiffness of the plate.

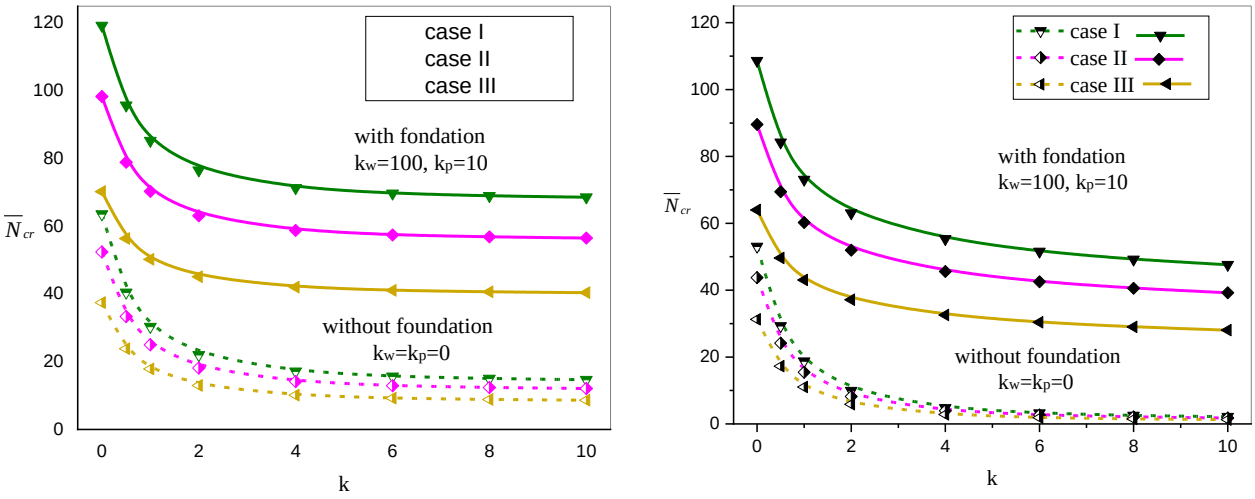

Figure V. 3: Comparison of the critical buckling loads (Ncr) for different types of in-plane load of FG sandwich plate supported with (a/h=5, a/b=1)

Figures V. 3(a) and V.3(b) show the effect of various in-plane loads, elastic foundation, and the porosity on the critical buckling of FG sandwich plate with index k. With increasing of index power k, there is decreasing in buckling load the highest critical buckling is always under case 1 loading which is triangular load when the minimum values are shown with case 3 sinusoidal load also the elastic foundation augment the critical buckling which means increase the stiffness and

inertia of the plate. The inclusion of the porosity in Figure V.3 (b) reduces the critical buckling with and without elastic foundation.

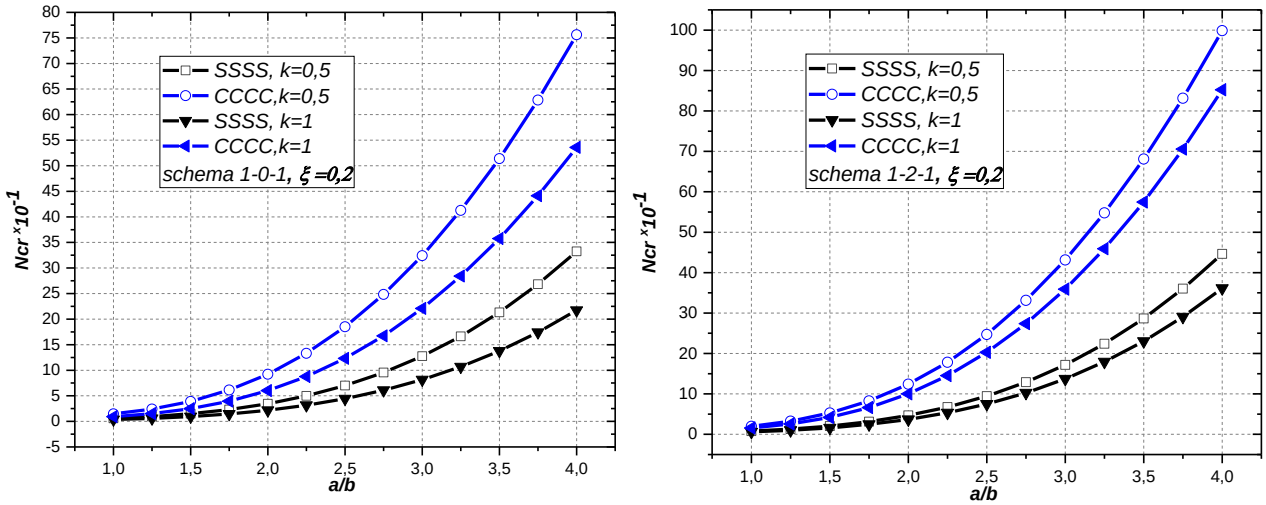

Figure V 4: Critical buckling load Ncr versus the ratio a/b of the (1–2-1)/ (1–0–1) porous square FGM sandwich plates with various boundary conditions under uniaxial loads

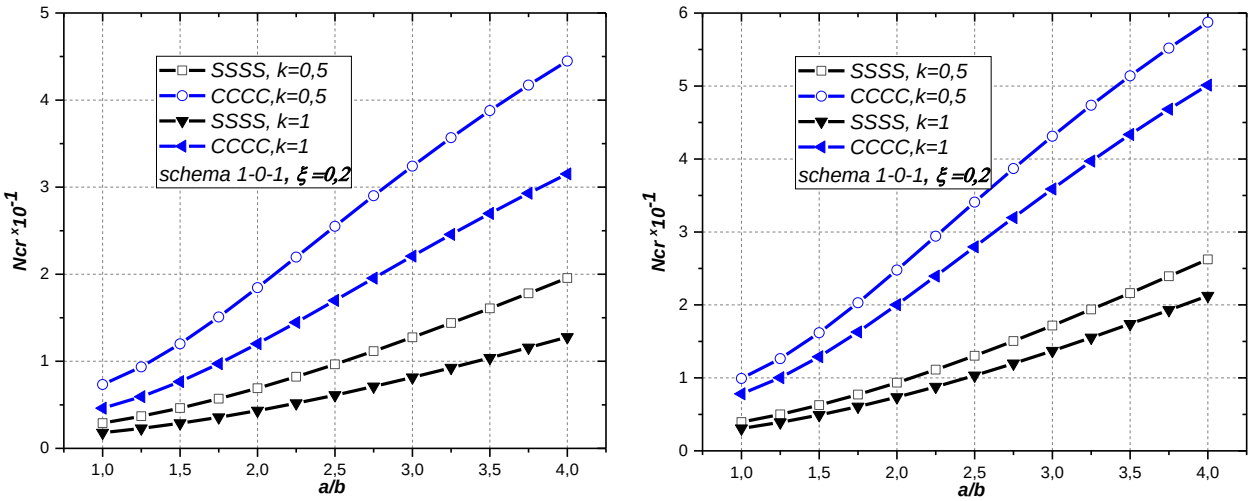

Figure V 5: Critical buckling load Ncr versus the ratio a/b of the (1–2-1)/ (1–0–1) porous square FGM sandwich plates with various boundary conditions under bi-axial loads

Figure V.4 and Figure V.5 present the variation of the Critical buckling load Ncr of FG plates with ratio a/b resting on different boundary conditions under uniaxial and bi-axial compression loads. The plate with a higher volume fraction of ceramics has a significantly higher Critical buckling load Ncr than the plate with a higher metal volume fraction, particularly for plates with a larger a/b aspect ratio. Notably, the plate with all edges clamped boundary condition shows the highest non-dimensional Critical buckling load, owing to the more significant constraint at the edges, as depicted in Figure. V. 4 and V. 5.

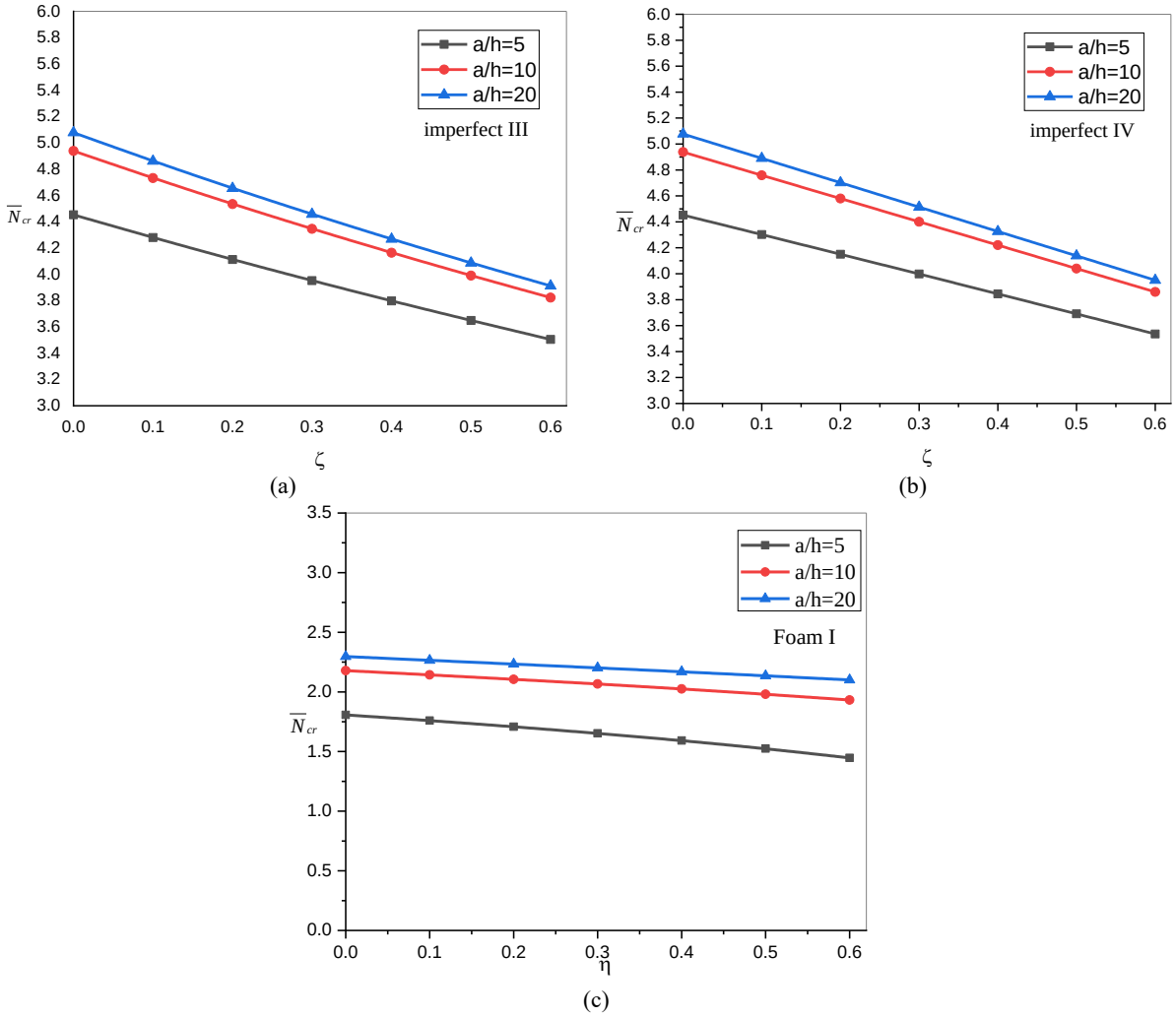

Figure V. 6: buckling load versus side-to-thickness a/h, porosity and foam metal coefficient for FG sandwich plate (1-3-1), under bi-axial loading

Figures V. 6(a, b, and c) describe the variation of critical buckling versus the porosity and foam coefficient presented with two shapes (imperfect III and IV) and metal foam I with different values of the side-to-thickness ratio a/h (a/h = 5, 10 and 20). When the porosity parameter increased, the critical buckling of the FG porous plates for different a/h decreased for all index k values. Also, the critical buckling decreased with the increasing metal foam coefficient.

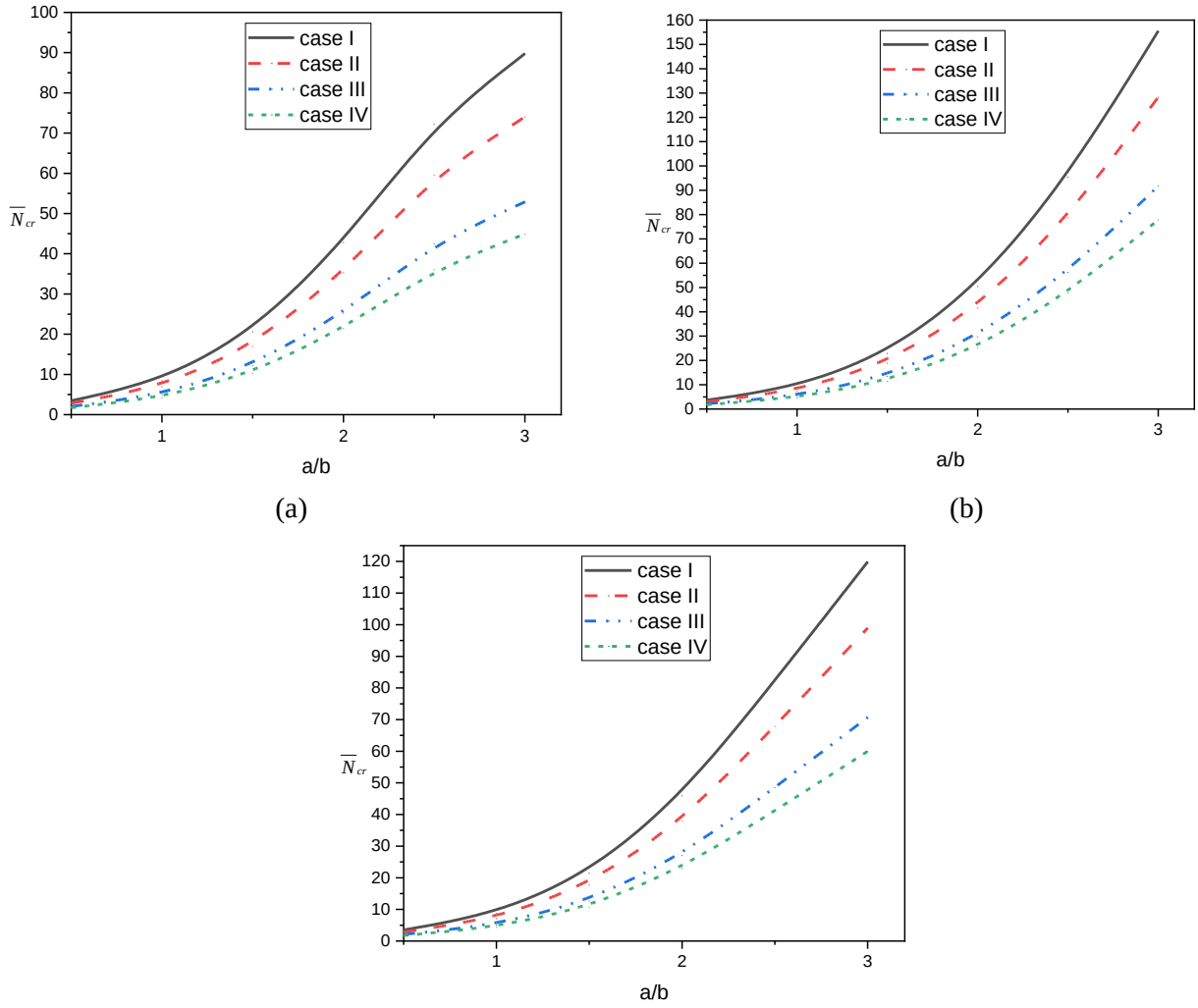

Figure V. 7: Comparison of the critical buckling loads (Ncr) for different types of in-plane load of FG sandwich plate containing meal foam core with (a/h=5, k=1) (a) Foam I, (b) Foam II, (c) Foam III,

Figures V. 7(a, b, and c) show the variation of critical buckling beside the ratio a/b for FG sandwich plate containing three types of metal foam core under triangular, exponential, sinusoidal, and uniform mechanical load. It can be seen that the critical buckling increases when the index k increases and the maximum value is always the triangular load for the three cases.

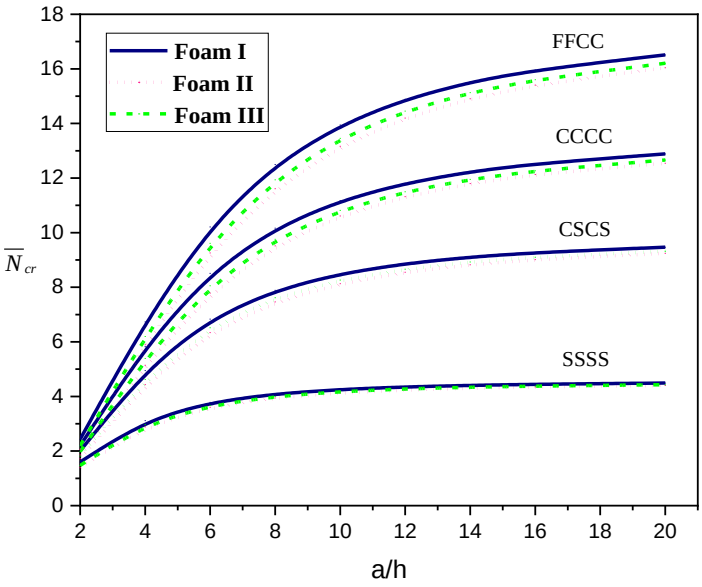

Figure V. 8: variation of critical buckling load Ncr versus length-to-thickness ratio a/h for FG sandwich plate resting on different boundary conditions for (foam I, foam II, and Foam III, a=b, k= 2)

Figure V.8 shows the change in critical buckling behavior with the length-to-thickness ratio of two FG layers of the face and three types of metal foam core. It can be noted that increasing a/h increases critical buckling. The FFCC and SSSS have the highest and lowest critical buckling, respectively.

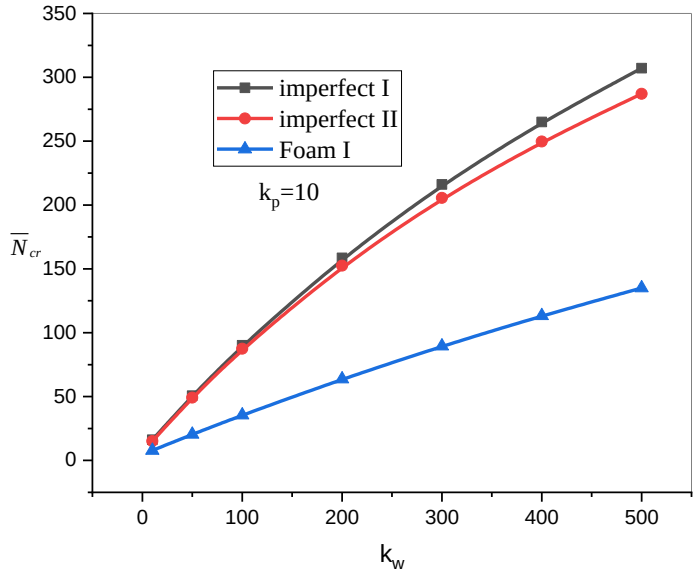

Figure V 9: Effect of the elastic foundation parameter Kw on the critical buckling load (ˆN) for a simply supported FG sandwich plate (imperfect I, II and containing foam core)

The effect of the Winkler elastic foundation parameters on the critical buckling load is shown in Figure V. 9; the increase in the Kw parameter leads to an increase in the critical buckling load. This can be explained by the fact that the increase in the parameters of the elastic foundation leads to an increase in the rigidity of the plate and, consequently, the increase in the critical buckling loads.

Also, the effect of micro-voids on the variation of mechanical buckling is shown; the imperfect has the highest value when the metal foam I have the lowest, and this explains the effect of micro-voids on the stiffness and inertia of the FG structures.

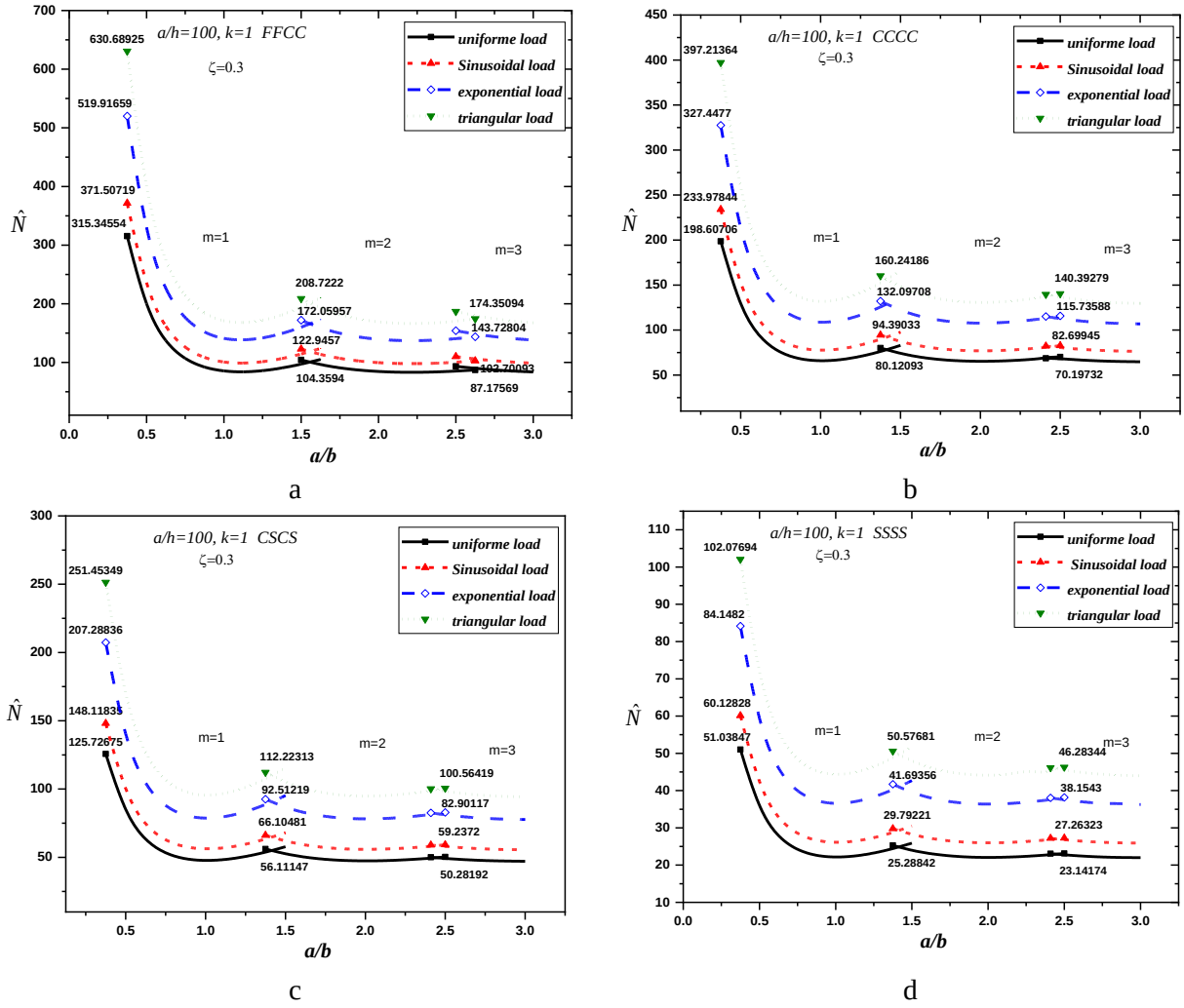

Figure V 10: Buckling load and modes shapes for rectangular FG porous sandwich plate subjected to linearly varying uniaxial in plane compressive load

Figure V.10 analyzed the buckling load for three modes and four types of loads for rectangular porous FG sandwich plates subjected to various boundary conditions. It can be noted that the critical buckling decreases due to the increase of side-to-thickness a/b vis-a-vis the transition of the modes. Furthermore, the maximum and minimum values of critical buckling are always shown with (triangular load, FFCC Boundary condition) and (uniform load, SSS Boundary condition), respectively.

V.3. Conclusion

Quasi-3D high deformation theory is used here to analyze the effect of porosity in the mechanical behavior of FG sandwich plate resting on various boundary conditions and elastic foundations under

uniform, triangular, sinusoidal, and exponential in-plane loading. The mathematical formulation was constructed by including the indeterminate integral terms in the displacement field; Hamilton's principal proposed to obtain the governing equations, which were then solved by Navier's solution for support. Four shapes of porosity distribution are used in the FG face sheet layers for FG sandwich model I. Another important model of the sandwich plate containing a metal foam core is investigated here.

The following conclusions from the numerical computations were drawn.

- ✓ Increase in inhomogeneity parameter k of FGM sandwich plate decreases the critical buckling loads
- ✓ The aspect ratio a/b and side-to-thickness ratio a/h have a significant influence on the buckling loads, where the increasing of these geometrical parameters increases the buckling
- ✓ The buckling loads are maximum for a perfect FG sandwich plate and decrease when the porosity
- ✓ An excellent agreement can be seen between the current theory and previous theories
- ✓ The effect of metal foam is reducing the stiffness of the sandwich plate and decreasing the critical buckling.
- ✓ The critical buckling of the FGM sandwich plate under a uniaxial load had the highest value than a biaxial buckling load

The critical buckling load has the highest values with FFCC boundary condition, the triangular in-plan load, uniaxial load

GENERAL CONCLUSION

General conclusion

Sandwich plates have extensive applications in the production of mechanical constructions. One significant factor is their exceptional light weight, which is doubled in some configurations of a mechanically robust sign. As a result, they enable the industry to manufacture both light and sturdy structures. Sandwich plates with FGM offer a rich field of application and a promising subject for future research since their composition and design may be freely altered to achieve the desired qualities of the materials. The creation of analytical tools tailored to the geometrical and material specificities of these materials is necessary for their design and development.

The mechanical behavior of FG sandwich plate on buckling is intimately linked to the geometric shape, the properties of the constituent materials, the boundary conditions, various porosities distributions, and the multiple environmental effects and theories applied to model the phenomenon. In addition, choosing the right resolution method is crucial to the reliability of the prediction of the behavior.

This study employs a novel analytical performance model grounded in quasi-3D high shear deformation plate theory to examine the influence of varying porosity distributions on the mechanical behavior of thick functionally graded sandwich plates subjected to uniform, triangular, and sinusoidal mechanical loads. The porosity analyzed is based on two sandwich models: the first model features four types of functionally graded porous face sheets. In contrast, the second model incorporates three types of metal foam cores, representing a significant aspect of our research's innovation. To validate our model, we compared it with existing literature utilizing a displacement field with six unknowns that distinguishes rotation in the x and y axes and incorporates the effects of stretching to ensure an accurate and precise solution.

According to the results of the study, the following can be drawn:

- ✓ Increase in inhomogeneity parameter k of FGM sandwich plate decreases the critical buckling loads
- ✓ The aspect ratio a/b and side-to-thickness ratio a/h have a significant influence on the buckling loads, where the increasing of these geometrical parameters increases the buckling
- ✓ The buckling loads are maximum for a perfect FG sandwich plate and decrease when the porosity
- ✓ An excellent agreement can be seen between the current theory and previous theories
- ✓ The effect of metal foam is reducing the stiffness of the sandwich plate and decreasing the critical buckling.

- ✓ The critical buckling of the FGM sandwich plate under a uniaxial load had the highest value than a biaxial buckling load
- ✓ The critical buckling load has the highest values with FFCC boundary condition, the triangular in-plan load, and the uniaxial load.

REFERENCES

References

[1] Z. Zhang, Y. Li, H. Wu, H. Zhang, H. Wu, S. Jiang, G. Chai, Mechanical analysis of functionally graded graphene oxide-reinforced composite beams based on the first-order shear deformation theory, *Mechanics of Advanced Materials and Structures,* Vol. 27, No. 1, pp. 3-11, 2020.

[2] M. Bever, P. Duwez, Gradients in composite materials, *Materials Science and Engineering,* Vol. 10, pp. 1-8, 1972.

[3] A. S. Sayyad, Y. M. Ghugal, Modeling and analysis of functionally graded sandwich beams: A review, *Mechanics of Advanced Materials and Structures,* Vol. 26, No. 21, pp. 1776-1795, 2019.

[4] M. Koizumi, Recent progress of functionally gradient materials in Japan, in *Proceeding of,* 333.

[5] A. Edwin, V. Anand, K. Prasanna, Sustainable development through functionally graded materials: An overview, *Rasayan Journal of Chemistry,* Vol. 10, No. 1, pp. 149-152, 2017.

[6] G. Udupa, S. S. Rao, K. Gangadharan, Functionally graded composite materials: an overview, *Procedia Materials Science,* Vol. 5, pp. 1291-1299, 2014.

[7] M. A. A. Meziane, H. H. Abdelaziz, A. Tounsi, An efficient and simple refined theory for buckling and free vibration of exponentially graded sandwich plates under various boundary conditions, *Journal of Sandwich Structures & Materials,* Vol. 16, No. 3, pp. 293-318, 2014.

[8] S. Singh, S. Harsha, Analysis of porosity effect on free vibration and buckling responses for sandwich sigmoid function based functionally graded material plate resting on Pasternak foundation using Galerkin Vlasov's method, *Journal of Sandwich Structures & Materials,* Vol. 23, No. 5, pp. 1717-1760, 2021.

[9] P. K. Masjedi, A. Maheri, P. M. Weaver, Large deflection of functionally graded porous beams based on a geometrically exact theory with a fully intrinsic formulation, *Applied Mathematical Modelling,* Vol. 76, pp. 938-957, 2019.

[10] Q.-M. Xiong, Z. Chen, J.-T. Huang, M. Zhang, H. Song, X.-F. Hou, X.-B. Li, Z.-J. Feng, Preparation, structure and mechanical properties of Sialon ceramics by transition metal-catalyzed nitriding reaction, *Rare metals,* Vol. 39, No. 5, pp. 589-596, 2020.

[11] J. Chen, H. Tong, J. Yuan, Y. Fang, R. Gu, Permeability Prediction Model Modified on Kozeny-Carman for Building Foundation of Clay Soil, *Buildings,* Vol. 12, No. 11, pp. 1798, 2022.

[12] D. K. Rajak, D. D. Pagar, R. Kumar, C. I. Pruncu, Recent progress of reinforcement materials: A comprehensive overview of composite materials, *Journal of Materials Research and Technology,* Vol. 8, No. 6, pp. 6354-6374, 2019.

[13] T. W. Clyne, D. Hull, 2019, *An introduction to composite materials*, Cambridge university press,

[14] Q. Qin, *Introduction to the composite and its toughening mechanisms*, in: *Toughening mechanisms in composite materials*, Eds., pp. 1-32: Elsevier, 2015.

[15] D. Gay, 2022, *Composite materials: design and applications*, CRC press,

[16] T. P. Dolen, Historical development of durable concrete for the Bureau of Reclamation, in *Proceeding of,* 135.

[17] F. C. Campbell, 2010, *Structural composite materials*, ASM international,

[18] M. W. Hyer, S. R. White, 2009, *Stress analysis of fiber-reinforced composite materials*, DEStech Publications, Inc,

[19] S. Chand, Review carbon fibers for composites, *Journal of materials science,* Vol. 35, pp. 1303-1313, 2000.

[20] K. Li, X. Ni, Q. Wu, C. Yuan, C. Li, D. Li, H. Chen, Y. Lv, A. Ju, Carbon-based fibers: fabrication, characterization and application, *Advanced Fiber Materials,* Vol. 4, No. 4, pp. 631-682, 2022.
[21] A. K. Kaw, 2005, *Mechanics of composite materials*, CRC press,
[22] A. Cevahir, *Glass fibers*, in: *Fiber Technology for Fiber-Reinforced Composites*, Eds., pp. 99-121: Elsevier, 2017.
[23] L. Markovičová, V. Zatkalíková, Composite materials based on pa reinforced glass fibers, *Materials Today: Proceedings,* Vol. 3, No. 4, pp. 1056-1059, 2016.
[24] N. Chawla, Y. L. Shen, Mechanical behavior of particle reinforced metal matrix composites, *Advanced engineering materials,* Vol. 3, No. 6, pp. 357-370, 2001.
[25] R. Hsissou, R. Seghiri, Z. Benzekri, M. Hilali, M. Rafik, A. Elharfi, Polymer composite materials: A comprehensive review, *Composite structures,* Vol. 262, pp. 113640, 2021.
[26] Y. X. Gan, Effect of interface structure on mechanical properties of advanced composite materials, *International journal of molecular sciences,* Vol. 10, No. 12, pp. 5115-5134, 2009.
[27] D. A. Børsting, Q. Zhou, J. J. Van Der Zee, R. Rajamani, Method of applying gelcoat and an arrangement performing said method, Google Patents, 2014.
[28] G. N. Bullen, Unified Structures, *MANUFACTURING ENGINEERING,* Vol. 144, No. 3, pp. 47-+, 2010.
[29] A. B. Strong, 2008, *Fundamentals of composites manufacturing: materials, methods and applications*, Society of manufacturing engineers,
[30] B. Morey, Composites challenge cutting tools, *Manufacturing Engineering Magazine, Society of Manufacturing Engineer Editor,* Vol. 138, No. 4, 2007.
[31] B. Morey, Innovation Drives Composites Production, *Manufacturing Engineering,* Vol. 142, No. 3, pp. 49-+, 2009.
[32] N. Minsch, F. Herrmann, T. Gereke, A. Nocke, C. Cherif, Analysis of filament winding processes and potential equipment technologies, *Procedia CIRP,* Vol. 66, pp. 125-130, 2017.
[33] P. D. Rufe, 2013, *Fundamentals of manufacturing*, Society of Manufacturing Engineers,
[34] P. P. Adrian, B. M. Gheorghe, Manufacturing process and applications of composite materials, *Fascicle Manag. Technol. Eng,* Vol. 9, No. 19, pp. 3.1-3.6, 2010.
[35] Y. Leong, S. Thitithanasarn, K. Yamada, H. Hamada, *Compression and injection molding techniques for natural fiber composites*, in: *Natural Fibre Composites*, Eds., pp. 216-232: Elsevier, 2014.
[36] V. M. Werner, R. Krumpholz, C. Rehekampff, T. Scherzer, M. Eblenkamp, Thermoplastic encapsulations of a sensor platform by high-temperature injection molding up to 360° C, *Polymer Engineering & Science,* Vol. 59, No. 7, pp. 1315-1331, 2019.
[37] M. González-López, A. Pérez-Fonseca, R. Manríquez-González, M. Arellano, D. Rodrigue, J. Robledo-Ortíz, Effect of surface treatment on the physical and mechanical properties of injection molded poly (lactic acid)-coir fiber biocomposites, *Polymer Composites,* Vol. 40, No. 6, pp. 2132-2141, 2019.
[38] C. M. González-Henríquez, M. A. Sarabia-Vallejos, J. Rodriguez-Hernandez, Polymers for additive manufacturing and 4D-printing: Materials, methodologies, and biomedical applications, *Progress in Polymer Science,* Vol. 94, pp. 57-116, 2019.
[39] G. D. Goh, Y. L. Yap, S. Agarwala, W. Y. Yeong, Recent progress in additive manufacturing of fiber reinforced polymer composite, *Advanced Materials Technologies,* Vol. 4, No. 1, pp. 1800271, 2019.
[40] M. Knight, D. Curliss, Composite Materials, Encyclopedia of Physical Science and Technology, Academic Press: Cambridge, MA, USA, 2003.
[41] A. K. Kaw, 2006, *MECHANICS OF Composite Materials*, 2nd.ed.

[42] C. Borsellino, L. Calabrese, A. Valenza, Experimental and numerical evaluation of sandwich composite structures, *Composites Science and Technology,* Vol. 64, No. 10-11, pp. 1709-1715, 2004.
[43] A. Petras, *Design of sandwich structures*, Thesis, University of Cambridge, 1999.
[44] F. Hassanpour Roudbeneh, G. Liaghat, H. Sabouri, H. Hadavinia, High-velocity impact loading in honeycomb sandwich panels reinforced with polymer foam: a numerical approach study, *Iranian Polymer Journal,* Vol. 29, pp. 707-721, 2020.
[45] R. Nasirzadeh, A. R. Sabet, Study of foam density variations in composite sandwich panels under high velocity impact loading, *International Journal of Impact Engineering,* Vol. 63, pp. 129-139, 2014.
[46] X. Liu, X. Tian, T. Lu, B. Liang, Sandwich plates with functionally graded metallic foam cores subjected to air blast loading, *International Journal of Mechanical Sciences,* Vol. 84, pp. 61-72, 2014.
[47] X. Xue, C. Zhang, W. Chen, M. Wu, J. Zhao, Study on the impact resistance of honeycomb sandwich structures under low-velocity/heavy mass, *Composite Structures,* Vol. 226, pp. 111223, 2019.
[48] M. Basha, A. Wagih, A. Melaibari, G. Lubineau, A. Abdraboh, M. Eltaher, Impact and post-impact response of lightweight CFRP/wood sandwich composites, *Composite Structures,* Vol. 279, pp. 114766, 2022.
[49] B. Han, K.-K. Qin, B. Yu, Q.-C. Zhang, C.-Q. Chen, T. J. Lu, Design optimization of foam-reinforced corrugated sandwich beams, *Composite Structures,* Vol. 130, pp. 51-62, 2015.
[50] D. Guedra-Degeorges, P. Thevenet, S. Maison, Damage tolerance of aeronautical sandwich structures, in *Proceeding of,* Springer, pp. 29-36.
[51] H. Lee, H. Park, Study on structural design and manufacturing of sandwich composite floor for automotive structure, *Materials,* Vol. 14, No. 7, pp. 1732, 2021.
[52] F. Tarlochan, F. Samer, A. Hamouda, S. Ramesh, K. Khalid, Design of thin wall structures for energy absorption applications: Enhancement of crashworthiness due to axial and oblique impact forces, *Thin-Walled Structures,* Vol. 71, pp. 7-17, 2013.
[53] I. E. Elishakoff, D. Pentaras, C. Gentilini, 2015, *Mechanics of functionally graded material structures*, World Scientific,
[54] J. Zhu, Z. Lai, Z. Yin, J. Jeon, S. Lee, Fabrication of ZrO2–NiCr functionally graded material by powder metallurgy, *Materials chemistry and physics,* Vol. 68, No. 1-3, pp. 130-135, 2001.
[55] M. Shen, M. Bever, Gradients in polymeric materials, *Journal of Materials science,* Vol. 7, pp. 741-746, 1972.
[56] M. Niino, A. Kumakawa, R. Watanabe, Y. Doi, Fabrication of a high pressure thrust chamber by the CIP forming method, in *Proceeding of,* 1227.
[57] T. Hirai, Functional gradient materials, *Materials science and technology*, pp. 293-341, 1996.
[58] M. Koizumi, M. Niino, Overview of FGM research in Japan, *Mrs Bulletin,* Vol. 20, No. 1, pp. 19-21, 1995.
[59] Y. Miyamoto, M. Niino, M. Koizumi, *FGM research programs in Japan—from structural to functional uses*, in: *Functionally Graded Materials 1996*, Eds., pp. 1-8: Elsevier, 1997.
[60] D. T. Do, S. Thai, T. Q. Bui, Long short-term memory for nonlinear static analysis of functionally graded plates, *Journal of Science and Technology in Civil Engineering (STCE)-HUCE,* Vol. 16, No. 3, pp. 1-17, 2022.
[61] I. Bharti, N. Gupta, K. Gupta, Novel applications of functionally graded nano, optoelectronic and thermoelectric materials, *International Journal of Materials, Mechanics and Manufacturing,* Vol. 1, No. 3, pp. 221-224, 2013.
[62] J. Dossett, G. Totten, Introduction to surface hardening of steels, *ASM Handbook,* Vol. 4, pp. 389-398, 2013.

[63] G. Bao, L. Wang, Multiple cracking in functionally graded ceramic/metal coatings, *International Journal of Solids and Structures,* Vol. 32, No. 19, pp. 2853-2871, 1995.

[64] M. Mahinzare, M. J. Alipour, S. A. Sadatsakkak, M. Ghadiri, A nonlocal strain gradient theory for dynamic modeling of a rotary thermo piezo electrically actuated nano FG circular plate, *Mechanical Systems and Signal Processing,* Vol. 115, pp. 323-337, 2019.

[65] E. Pei, G. H. Loh, D. Harrison, H. Almeida, M. Domingo, M. Verona, R. Paz, Exploring the concept of functionally graded additive manufacturing, *Assem. Autom,* Vol. 37, No. 2, pp. 147-153, 2017.

[66] A. Boccaccio, A. E. Uva, M. Fiorentino, G. Mori, G. Monno, Geometry design optimization of functionally graded scaffolds for bone tissue engineering: A mechanobiological approach, *PloS one,* Vol. 11, No. 1, pp. e0146935, 2016.

[67] V. Popovich, E. Borisov, A. Popovich, V. S. Sufiiarov, D. Masaylo, L. Alzina, Functionally graded Inconel 718 processed by additive manufacturing: Crystallographic texture, anisotropy of microstructure and mechanical properties, *Materials & Design,* Vol. 114, pp. 441-449, 2017.

[68] P. Popoola, G. Farotade, O. Fatoba, O. Popoola, Laser engineering net shaping method in the area of development of functionally graded materials (FGMs) for aero engine applications-a review, *Fiber Laser,* Vol. 2, pp. 64, 2016.

[69] R. Gabbrielli, I. Turner, C. R. Bowen, Development of modelling methods for materials to be used as bone substitutes, *Key Engineering Materials,* Vol. 361, pp. 903-906, 2008.

[70] R. M. Mahamood, E. T. Akinlabi, M. Shukla, S. L. Pityana, Functionally graded material: an overview, 2012.

[71] S. Kaushal, D. Gupta, H. Bhowmick, An approach for functionally graded cladding of composite material on austenitic stainless steel substrate through microwave heating, *Journal of Composite Materials,* Vol. 52, No. 3, pp. 301-312, 2018.

[72] S. N. S. Jamaludin, F. Mustapha, D. M. Nuruzzaman, S. N. Basri, A review on the fabrication techniques of functionally graded ceramic-metallic materials in advanced composites, *Scientific Research and Essays,* Vol. 8, No. 21, pp. 828-840, 2013.

[73] Y. Miyamoto, W. Kaysser, B. Rabin, A. Kawasaki, R. G. Ford, 2013, *Functionally graded materials: design, processing and applications*, Springer Science & Business Media,

[74] P. Zhao, S. Wang, S. Guo, Y. Chen, Y. Ling, J. Li, Bonding W and W–Cu composite with an amorphous W–Fe coated copper foil through hot pressing method, *Materials & Design,* Vol. 42, pp. 21-24, 2012.

[75] X. Gong, L. Wang, Y. Mou, H. Wang, X. Wei, W. Zheng, L. Yin, Improved Four-channel PBTDPA control strategy using force feedback bilateral teleoperation system, *International Journal of Control, Automation and Systems,* Vol. 20, No. 3, pp. 1002-1017, 2022.

[76] W. Pompe, H. Worch, M. Epple, W. Friess, M. Gelinsky, P. Greil, U. Hempel, D. Scharnweber, K. Schulte, Functionally graded materials for biomedical applications, *Materials Science and Engineering: A,* Vol. 362, No. 1-2, pp. 40-60, 2003.

[77] T. Shi, Y. Liu, Z. Hu, M. Cen, C. Zeng, J. Xu, Z. Zhao, Deformation Performance and Fracture Toughness of Carbon Nanofiber-Modified Cement-Based Materials, *ACI Materials Journal,* Vol. 119, No. 5, 2022.

[78] M. Gu, X. Cai, Q. Fu, H. Li, X. Wang, B. Mao, Numerical Analysis of Passive Piles under Surcharge Load in Extensively Deep Soft Soil, *Buildings,* Vol. 12, No. 11, pp. 1988, 2022.

[79] J. Groves, H. Wadley, Functionally graded materials synthesis via low vacuum directed vapor deposition, *Composites Part B: Engineering,* Vol. 28, No. 1-2, pp. 57-69, 1997.

[80] S. Chu, H. Wang, R. Wu, Investigation on the properties of carbon fibre with C-Si functionally graded coating, *Surface and Coatings Technology,* Vol. 88, No. 1-3, pp. 38-43, 1997.

[81] U. Leushake, U. Schulz, T. Krell, M. Peters, W. Kaysser, *Al2O3-ZrO2 graded thermal barrier coatings by EB-PVD-concept, microstructure and phase stability*, in: *Functionally Graded Materials 1996*, Eds., pp. 263-268: Elsevier, 1997.

[82] W. G. French, J. B. MacChesney, P. O'connor, G. Tasker, BSTJ brief: Optical waveguides with very low losses, *The Bell system technical journal,* Vol. 53, No. 5, pp. 951-954, 1974.

[83] R. Gupta, R. Kumar, A. Chaubey, S. Kanpara, S. Khirwadkar, Mechanical and microstructural characterization of W–Cu FGM fabricated by one-step sintering method through PM route, in *Proceeding of,* IOP Publishing, pp. 012042.

[84] A. Tripathy, S. K. Sarangi, R. Panda, Fabrication of functionally graded composite material using powder metallurgy route: an overview, *Int. J. Mech. Prod. Eng. Res. Dev,* Vol. 7, No. 6, pp. 135-145, 2017.

[85] R. Watanabe, A. Kawakasi, H. Takahashi, Mechanics and Mechanisms of Damage in composites and Multi-Materials, *Mechanical Engineering publication, London*, pp. 285-299, 1991.

[86] A. Dehghan, Additive manufacturing as a new technique of fabrication, *J. 3d Print. Appl,* Vol. 1, pp. 3-4, 2018.

[87] H. Bikas, P. Stavropoulos, G. Chryssolouris, Additive manufacturing methods and modelling approaches: a critical review, *The International Journal of Advanced Manufacturing Technology,* Vol. 83, pp. 389-405, 2016.

[88] G. H. Loh, E. Pei, D. Harrison, M. D. Monzón, An overview of functionally graded additive manufacturing, *Additive Manufacturing,* Vol. 23, pp. 34-44, 2018.

[89] J. P. Kruth, P. Mercelis, J. Van Vaerenbergh, L. Froyen, M. Rombouts, Binding mechanisms in selective laser sintering and selective laser melting, *Rapid prototyping journal,* Vol. 11, No. 1, pp. 26-36, 2005.

[90] B. Vandenbroucke, J. P. Kruth, Selective laser melting of biocompatible metals for rapid manufacturing of medical parts, *Rapid Prototyping Journal,* Vol. 13, No. 4, pp. 196-203, 2007.

[91] P. F. Jacobs, 1995, *Stereolithography and other RP&M technologies: from rapid prototyping to rapid tooling*, Society of Manufacturing Engineers,

[92] S. J. Kalita, S. Bose, H. L. Hosick, A. Bandyopadhyay, Development of controlled porosity polymer-ceramic composite scaffolds via fused deposition modeling, *Materials Science and Engineering: C,* Vol. 23, No. 5, pp. 611-620, 2003.

[93] D. W. Hutmacher, T. Schantz, I. Zein, K. W. Ng, S. H. Teoh, K. C. Tan, Mechanical properties and cell cultural response of polycaprolactone scaffolds designed and fabricated via fused deposition modeling, *Journal of Biomedical Materials Research: An Official Journal of The Society for Biomaterials, The Japanese Society for Biomaterials, and The Australian Society for Biomaterials and the Korean Society for Biomaterials,* Vol. 55, No. 2, pp. 203-216, 2001.

[94] P. Diouf, A. Jones, Investigation of bond strength in centrifugal lining of babbitt on cast iron, *Metallurgical and Materials Transactions A,* Vol. 41, pp. 603-609, 2010.

[95] K. Kinoshita, H. Sato, Y. Watanabe, Development of Compositional Gradient Simulation for Centrifugal Slurry-Pouring Methods, in *Proceeding of,* 455.

[96] Y. Watanabe, Y. Inaguma, H. Sato, E. Miura-Fujiwara, A novel fabrication method for functionally graded materials under centrifugal force: The centrifugal mixed-powder method, *Materials,* Vol. 2, No. 4, pp. 2510-2525, 2009.

[97] S. Shahrestani, M. C. Ismail, S. Kakooei, M. Beheshti, Effect of additives on slip casting rheology, microstructure and mechanical properties of Si3N4/SiC composites, *Ceramics International,* Vol. 46, No. 5, pp. 6182-6190, 2020.

[98] J. Zygmuntowicz, P. Wiecińska, A. Miazga, K. Konopka, W. Kaszuwara, Al 2 O 3/Ni functionally graded materials (FGM) obtained by centrifugal-slip casting method, *Journal of Thermal Analysis and Calorimetry,* Vol. 130, pp. 123-130, 2017.

[99] G. Howatt, R. Breckenridge, J. Brownlow, Fabrication of thin ceramic sheets for capacitors, *Journal of the American Ceramic Society,* Vol. 30, No. 8, pp. 237-242, 1947.
[100] R. Mistler, *The principles of tape casting and tape casting applications*, in: *Ceramic processing*, Eds., pp. 147-173: Springer, 1995.
[101] J. W. Phair, N. Lönnroth, M. Lundberg, A. Kaiser, Characteristics of cerium-gadolinium oxide (CGO) suspensions as a function of dispersant and powder properties, *Colloids and Surfaces A: Physicochemical and Engineering Aspects,* Vol. 341, No. 1-3, pp. 103-109, 2009.
[102] F. Ebrahimi, 2016, *Advances in functionally graded materials and structures*, BoD–Books on Demand,
[103] W. Voigt, Ueber die Beziehung zwischen den beiden Elasticitätsconstanten isotroper Körper, *Annalen der physik,* Vol. 274, No. 12, pp. 573-587, 1889.
[104] M. M. Gasik, Micromechanical modelling of functionally graded materials, *Computational Materials Science,* Vol. 13, No. 1-3, pp. 42-55, 1998.
[105] A. Reuß, Berechnung der fließgrenze von mischkristallen auf grund der plastizitätsbedingung für einkristalle, *ZAMM-Journal of Applied Mathematics and Mechanics/Zeitschrift für Angewandte Mathematik und Mechanik,* Vol. 9, No. 1, pp. 49-58, 1929.
[106] A. Akbarzadeh, A. Abedini, Z. Chen, Effect of micromechanical models on structural responses of functionally graded plates, *Composite Structures,* Vol. 119, pp. 598-609, 2015.
[107] R. W. Zimmerman, Behavior of the Poisson ratio of a two-phase composite material in the high-concentration limit, 1994.
[108] M. M. Gasik, B. Zhang, Optimization sintering of zirconia/alumina functionally graded material, in *Proceeding of,* Aedermannsdorf, Switzerland: Trans Tech Publications, 1984-, pp. 183-186.
[109] R. B. Bouiadjra, A. Mahmoudi, S. Benyoucef, A. Tounsi, F. Bernard, Analytical investigation of bending response of FGM plate using a new quasi 3D shear deformation theory: Effect of the micromechanical models, *Structural Engineering and Mechanics, An Int'l Journal,* Vol. 66, No. 3, pp. 317-328, 2018.
[110] J. Ju, T. Chen, Micromechanics and effective moduli of elastic composites containing randomly dispersed ellipsoidal inhomogeneities, *Acta Mechanica,* Vol. 103, No. 1-4, pp. 103-121, 1994.
[111] Y. Benveniste, A new approach to the application of Mori-Tanaka's theory in composite materials, *Mechanics of materials,* Vol. 6, No. 2, pp. 147-157, 1987.
[112] T. Mori, K. Tanaka, Average stress in matrix and average elastic energy of materials with misfitting inclusions, *Acta metallurgica,* Vol. 21, No. 5, pp. 571-574, 1973.
[113] Z. Belabed, M. S. A. Houari, A. Tounsi, S. Mahmoud, O. A. Bég, An efficient and simple higher order shear and normal deformation theory for functionally graded material (FGM) plates, *Composites Part B: Engineering,* Vol. 60, pp. 274-283, 2014.
[114] A. Karakoti, S. Pandey, V. R. Kar, Free vibration response of P-FGM and S-FGM sandwich shell panels: A comparison, *Materials Today: Proceedings,* Vol. 28, pp. 1701-1705, 2020.
[115] Y. Lee, F. Erdogan, Residual/thermal stresses in FGM and laminated thermal barrier coatings, *International Journal of Fracture,* Vol. 69, pp. 145-165, 1994.
[116] Y.-L. Chung, S. Chi, The residual stress of functionally graded materials, 2001.
[117] F. Delale, F. Erdogan, The crack problem for a nonhomogeneous plane, 1983.
[118] A. E. H. Love, XVI. The small free vibrations and deformation of a thin elastic shell, *Philosophical Transactions of the Royal Society of London.(A.)*, No. 179, pp. 491-546, 1888.
[119] R. Mindlin, Influence of rotatory inertia and shear on flexural motions of isotropic, elastic plates, 1951.
[120] E. Reissner, The effect of transverse shear deformation on the bending of elastic plates, 1945.
[121] J. Reddy, D. Robbins Jr, Theories and computational models for composite laminates, 1994.

[122] J. N. Reddy, 2003, *Mechanics of laminated composite plates and shells: theory and analysis*, CRC press,
[123] J. N. Reddy, 1999, *Theory and analysis of elastic plates and shells*, CRC press,
[124] S. Timoshenko, S. Woinowsky-Krieger, 1959, *Theory of plates and shells*, McGraw-hill New York,
[125] L. Euler, 1952, *Methodus inveniendi lineas curvas maximi minimive proprietate gaudentes sive solutio problematis isoperimetrici latissimo sensu accepti*, Springer Science & Business Media,
[126] J. Reddy, C. M. Wang, An overview of the relationships between solutions of the classical and shear deformation plate theories, *Composites Science and Technology,* Vol. 60, No. 12-13, pp. 2327-2335, 2000.
[127] M. Asadijafari, M. Zarastvand, R. Talebitooti, The effect of considering Pasternak elastic foundation on acoustic insulation of the finite doubly curved composite structures, *Composite Structures,* Vol. 256, pp. 113064, 2021.
[128] Z. Wu, R. Chen, W. Chen, Refined laminated composite plate element based on global–local higher-order shear deformation theory, *Composite structures,* Vol. 70, No. 2, pp. 135-152, 2005.
[129] J. Reddy, Analysis of functionally graded plates, *International Journal for numerical methods in engineering,* Vol. 47, No. 1-3, pp. 663-684, 2000.
[130] J. N. Reddy, A simple higher-order theory for laminated composite plates, 1984.
[131] P. Naghdi, On the theory of thin elastic shells, *Quarterly of applied Mathematics,* Vol. 14, No. 4, pp. 369-380, 1957.
[132] K. S. R. Iyengar, K. Chandrashekhara, V. Sebastian, On the analysis of thick rectangular plates, *Ingenieur-Archiv,* Vol. 43, pp. 317-330, 1974.
[133] J. Reddy, On refined computational models of composite laminates, *International Journal for numerical methods in engineering,* Vol. 27, No. 2, pp. 361-382, 1989.
[134] T. Kant, A critical review and some results of recently developed refined theories of fiber-reinforced laminated composites and sandwiches, *Composite structures,* Vol. 23, No. 4, pp. 293-312, 1993.
[135] N. Phan, J. Reddy, Analysis of laminated composite plates using a higher-order shear deformation theory, *International journal for numerical methods in engineering,* Vol. 21, No. 12, pp. 2201-2219, 1985.
[136] J. N. Reddy, Mechanics of laminated composite plates- Theory and analysis(Book), *Boca Raton, FL: CRC Press, 1997.*, 1997.
[137] M. Touratier, An efficient standard plate theory, *International journal of engineering science,* Vol. 29, No. 8, pp. 901-916, 1991.
[138] M. Karama, K. Afaq, S. Mistou, Mechanical behaviour of laminated composite beam by the new multi-layered laminated composite structures model with transverse shear stress continuity, *International Journal of solids and structures,* Vol. 40, No. 6, pp. 1525-1546, 2003.
[139] E. Reissner, On tranverse bending of plates, including the effect of transverse shear deformation, 1974.
[140] K. Soldatos, T. Timarci, A unified formulation of laminated composite, shear deformable, five-degrees-of-freedom cylindrical shell theories, *Composite Structures,* Vol. 25, No. 1-4, pp. 165-171, 1993.
[141] J. Mantari, A. Oktem, C. G. Soares, A new higher order shear deformation theory for sandwich and composite laminated plates, *Composites Part B: Engineering,* Vol. 43, No. 3, pp. 1489-1499, 2012.
[142] H. Ait Atmane, A. Tounsi, I. Mechab, E. A. Adda Bedia, Free vibration analysis of functionally graded plates resting on Winkler–Pasternak elastic foundations using a new

shear deformation theory, *International Journal of Mechanics and Materials in Design,* Vol. 6, pp. 113-121, 2010.
[143] T.-K. Nguyen, K. Sab, G. Bonnet, Shear correction factors for functionally graded plates, *Mechanics of Advanced Materials and Structures,* Vol. 14, No. 8, pp. 567-575, 2007.
[144] R. P. Shimpi, Refined plate theory and its variants, *AIAA journal,* Vol. 40, No. 1, pp. 137-146, 2002.
[145] E. Carrera, A. Ciuffreda, A unified formulation to assess theories of multilayered plates for various bending problems, *Composite Structures,* Vol. 69, No. 3, pp. 271-293, 2005.
[146] E. Carrera, Developments, ideas, and evaluations based upon Reissner's Mixed Variational Theorem in the modeling of multilayered plates and shells, *Appl. Mech. Rev.,* Vol. 54, No. 4, pp. 301-329, 2001.
[147] L. Demasi, ∞ 6 mixed plate theories based on the generalized unified formulation. Part I: governing equations, *Composite structures,* Vol. 87, No. 1, pp. 1-11, 2009.
[148] L. Demasi, ∞ 6 Mixed plate theories based on the generalized unified formulation. Part III: Advanced mixed high order shear deformation theories, *Composite Structures,* Vol. 87, No. 3, pp. 183-194, 2009.
[149] L. Demasi, ∞ 6 Mixed plate theories based on the Generalized Unified Formulation. Part IV: Zig-zag theories, *Composite Structures,* Vol. 87, No. 3, pp. 195-205, 2009.
[150] L. Demasi, ∞ 6 Mixed plate theories based on the Generalized Unified Formulation, *Composite Structures,* Vol. 1, No. 87, pp. 12-22, 2009.
[151] L. Demasi, ∞ 6 Mixed plate theories based on the Generalized Unified Formulation.: Part II: Layerwise theories, *Composite Structures,* Vol. 87, No. 1, pp. 12-22, 2009.
[152] L. Demasi, ∞ 3 Hierarchy plate theories for thick and thin composite plates: the generalized unified formulation, *Composite Structures,* Vol. 84, No. 3, pp. 256-270, 2008.
[153] H.-T. Thai, S.-E. Kim, A simple quasi-3D sinusoidal shear deformation theory for functionally graded plates, *Composite Structures,* Vol. 99, pp. 172-180, 2013.
[154] H. Hebali, A. Tounsi, M. S. A. Houari, A. Bessaim, E. A. A. Bedia, New quasi-3D hyperbolic shear deformation theory for the static and free vibration analysis of functionally graded plates, *Journal of Engineering Mechanics,* Vol. 140, No. 2, pp. 374-383, 2014.
[155] A. Tounsi, M. S. A. Houari, S. Benyoucef, A refined trigonometric shear deformation theory for thermoelastic bending of functionally graded sandwich plates, *Aerospace science and technology,* Vol. 24, No. 1, pp. 209-220, 2013.
[156] A. Hamidi, M. S. A. Houari, S. Mahmoud, A. Tounsi, A sinusoidal plate theory with 5-unknowns and stretching effect for thermomechanical bending of functionally graded sandwich plates, *Steel Compos. Struct,* Vol. 18, No. 1, pp. 235-253, 2015.
[157] A. M. Zenkour, A simple four-unknown refined theory for bending analysis of functionally graded plates, *Applied Mathematical Modelling,* Vol. 37, No. 20-21, pp. 9041-9051, 2013.
[158] A. M. Zenkour, Bending analysis of functionally graded sandwich plates using a simple four-unknown shear and normal deformations theory, *Journal of Sandwich Structures & Materials,* Vol. 15, No. 6, pp. 629-656, 2013.
[159] B. V. Sankar, An elasticity solution for functionally graded beams, *Composites Science and Technology,* Vol. 61, No. 5, pp. 689-696, 2001.
[160] Z. Zhong, E. Shang, Three-dimensional exact analysis of a simply supported functionally gradient piezoelectric plate, *International journal of solids and structures,* Vol. 40, No. 20, pp. 5335-5352, 2003.
[161] M. Kashtalyan, Three-dimensional elasticity solution for bending of functionally graded rectangular plates, *European Journal of Mechanics-A/Solids,* Vol. 23, No. 5, pp. 853-864, 2004.
[162] Y. Xu, D. Zhou, Three-dimensional elasticity solution of functionally graded rectangular plates with variable thickness, *Composite Structures,* Vol. 91, No. 1, pp. 56-65, 2009.

[163] W. Van Paepegem, J. Degrieck, Modelling strategies for fatigue damage behaviour of fibre-reinforced polymer composites, *environment (eg moisture, toxic agents),* Vol. 1, pp. 3, 2001.
[164] J. Oh, M. Cho, A finite element based on cubic zig-zag plate theory for the prediction of thermo-electric-mechanical behaviors, *International Journal of Solids and Structures,* Vol. 41, No. 5-6, pp. 1357-1375, 2004.
[165] A. A. Daikh, A. M. Zenkour, Free vibration and buckling of porous power-law and sigmoid functionally graded sandwich plates using a simple higher-order shear deformation theory, *Materials Research Express,* Vol. 6, No. 11, pp. 115707, 2019.
[166] G. Drici, I. Mechab, H. Abbad, N. Elmeiche, B. Mechab, Investigating the free vibration of viscoelastic FGM Timoshenko nanobeams resting on viscoelastic foundations with the shear correction factor using finite element method, *Mechanics Based Design of Structures and Machines*, pp. 1-26, 2022.
[167] R.-B. Hao, Z.-Q. Lu, H. Ding, L.-Q. Chen, A nonlinear vibration isolator supported on a flexible plate: analysis and experiment, *Nonlinear Dynamics,* Vol. 108, No. 2, pp. 941-958, 2022.
[168] Z. Hu, C. Zhou, X. Zheng, Z. Ni, R. Li, Free vibration of non-Lévy-type functionally graded doubly curved shallow shells: new analytic solutions, *Composite Structures*, pp. 116389, 2022.
[169] K. Zahari, Y. Hilali, S. Mesmoudi, O. Bourihane, Review and comparison of thin and thick FGM plate theories using a unified buckling formulation, in *Proceeding of,* Elsevier*,* pp. 1545-1560.
[170] A. Milazzo, G. Guarino, V. Gulizzi, Buckling and post-buckling of variable stiffness plates with cutouts by a single-domain Ritz method, *Thin-Walled Structures,* Vol. 182, pp. 110282, 2023.
[171] M. Alam, S. K. Mishra, A boundary layer solution for the post-critical thermo-electro-mechanical stability of nonlocal-strain gradient Functionally Graded Piezoelectric cylindrical shells, *European Journal of Mechanics-A/Solids*, pp. 104836, 2022.
[172] J. Wang, J. Tian, X. Zhang, B. Yang, S. Liu, L. Yin, W. Zheng, Control of Time Delay Force Feedback Teleoperation System With Finite Time Convergence, *Frontiers in Neurorobotics,* Vol. 16, 2022.
[173] F. Kiarasi, M. Babaei, K. Asemi, R. Dimitri, F. Tornabene, Free Vibration Analysis of Thick Annular Functionally Graded Plate Integrated with Piezo-Magneto-Electro-Elastic Layers in a Hygrothermal Environment, *Applied Sciences,* Vol. 12, No. 20, pp. 10682, 2022.
[174] C. Hong, Advanced dynamic thermal vibration of thick FGM plates-cylindrical shells, *Ocean Engineering,* Vol. 266, pp. 112701, 2022.
[175] F. Mouaici, S. Benyoucef, H. A. Atmane, A. Tounsi, Effect of porosity on vibrational characteristics of non-homogeneous plates using hyperbolic shear deformation theory, *Wind & structures,* Vol. 22, No. 4, pp. 429-454, 2016.
[176] X. Chang, J. Zhou, Y. Li, Post-buckling characteristics of functionally graded fluid-conveying pipe with geometric defects on Pasternak foundation, *Ocean Engineering,* Vol. 266, pp. 113056, 2022.
[177] J. Zhou, X. Chang, Y. Li, Nonlinear vibration analysis of functionally graded flow pipelines under generalized boundary conditions based on homotopy analysis, *Acta Mechanica*, pp. 1-17, 2022.
[178] Z.-Z. Wang, T. Wang, Y.-m. Ding, L.-s. Ma, A simple refined plate theory for the analysis of bending, buckling and free vibration of functionally graded porous plates reinforced by graphene platelets, *Mechanics of Advanced Materials and Structures*, pp. 1-18, 2022.
[179] B. Adhikari, P. Dash, B. Singh, Buckling analysis of porous FGM sandwich plates under various types nonuniform edge compression based on higher order shear deformation theory, *Composite Structures,* Vol. 251, pp. 112597, 2020.

[180] D. Vasara, S. Khare, H. K. Sharma, R. Kumar, Free Vibration Analysis of Functionally Graded Porous Circular and Annular Plates using Differential Quadrature Method, *Forces in Mechanics*, pp. 100126, 2022.
[181] Q. X. Lieu, D. Lee, J. Kang, J. Lee, NURBS-based modeling and analysis for free vibration and buckling problems of in-plane bi-directional functionally graded plates, *Mechanics of Advanced Materials and Structures,* Vol. 26, No. 12, pp. 1064-1080, 2019.
[182] C.-P. Wu, L.-T. Yu, Quasi-3D static analysis of two-directional functionally graded circular plates, *Steel and Composite Structures, An International Journal,* Vol. 27, No. 6, pp. 789-801, 2018.
[183] Ş. D. Akbaş, Vibration and static analysis of functionally graded porous plates, *Journal of Applied and Computational Mechanics*, 2017.
[184] M. Kaddari, A. Kaci, A. A. Bousahla, A. Tounsi, F. Bourada, E. A. Bedia, M. A. Al-Osta, A study on the structural behaviour of functionally graded porous plates on elastic foundation using a new quasi-3D model: Bending and free vibration analysis, *Computers and Concrete, An International Journal,* Vol. 25, No. 1, pp. 37-57, 2020.
[185] A. M. Zenkour, M. H. Aljadani, Quasi-3D refined theory for functionally graded porous plates: Vibration analysis, *Физическая мезомеханика,* Vol. 24, No. 2, pp. 56-70, 2021.
[186] V. T. Long, H. V. Tung, Mechanical buckling analysis of thick FGM toroidal shell segments with porosities using Reddy's higher order shear deformation theory, *Mechanics of Advanced Materials and Structures*, pp. 1-10, 2021.
[187] M. Mekerbi, S. Benyoucef, A. Mahmoudi, F. Bourada, A. Tounsi, Investigation on thermal buckling of porous FG plate resting on elastic foundation via quasi 3D solution, *Structural Engineering and Mechanics,* Vol. 72, No. 4, pp. 513-524, 2019.
[188] R. Kumar, A. Jain, M. Singh, J. Singh, J. Singh, Porosity-dependent buckling analysis of elastically supported FGM sandwich plate via new tangent HSDT: A meshfree approach, *International Journal of Computational Materials Science and Engineering,* Vol. 12, No. 1, pp. 2250013-319, 2023.
[189] A. M. Zenkour, M. H. Aljadani, Buckling Response of Functionally Graded Porous Plates Due to a Quasi-3D Refined Theory, *Mathematics,* Vol. 10, No. 4, pp. 565, 2022.
[190] P. Van Vinh, N. Van Chinh, A. Tounsi, Static bending and buckling analysis of bi-directional functionally graded porous plates using an improved first-order shear deformation theory and FEM, *European Journal of Mechanics-A/Solids*, pp. 104743, 2022.
[191] T. Wei, J. Lu, P. Zhang, G. Yang, C. Sun, Y. Zhou, Q. Zhuang, Y. Tang, Metal–organic framework-derived Co3O4 modified nickel foam-based dendrite-free anode for robust lithium metal batteries, *Chinese Chemical Letters*, pp. 107947, 2022.
[192] D. Chen, J. Yang, S. Kitipornchai, Free and forced vibrations of shear deformable functionally graded porous beams, *International journal of mechanical sciences,* Vol. 108, pp. 14-22, 2016.
[193] D. Chen, J. Yang, S. Kitipornchai, Nonlinear vibration and postbuckling of functionally graded graphene reinforced porous nanocomposite beams, *Composites Science and Technology,* Vol. 142, pp. 235-245, 2017.
[194] D. Chen, J. Yang, S. Kitipornchai, Buckling and bending analyses of a novel functionally graded porous plate using Chebyshev-Ritz method, *Archives of Civil and Mechanical Engineering,* Vol. 19, No. 1, pp. 157-170, 2019.
[195] A. Garg, H. Chalak, L. Li, M.-O. Belarbi, R. Sahoo, T. Mukhopadhyay, Vibration and Buckling Analyses of Sandwich Plates Containing Functionally Graded Metal Foam Core, *Acta Mechanica Solida Sinica*, pp. 1-16, 2022.
[196] Y. Q. Wang, Z. Y. Zhang, Bending and buckling of three-dimensional graphene foam plates, *Results in Physics,* Vol. 13, pp. 102136, 2019.

[197] A. A. Daikh, A. M. Zenkour, Effect of porosity on the bending analysis of various functionally graded sandwich plates, *Materials Research Express,* Vol. 6, No. 6, pp. 065703, 2019.
[198] L. Hadji, H. A. Atmane, A. Tounsi, I. Mechab, E. Adda Bedia, Free vibration of functionally graded sandwich plates using four-variable refined plate theory, *Applied Mathematics and Mechanics,* Vol. 32, No. 7, pp. 925-942, 2011.
[199] Q. Li, V. Iu, K. Kou, Three-dimensional vibration analysis of functionally graded material sandwich plates, *Journal of Sound and Vibration,* Vol. 311, No. 1-2, pp. 498-515, 2008.
[200] S. Benyoucef, F. Achouri, F. Bourada, R. B. Bouiadjra, A. Tounsi, Robust quasi 3D computational model for mechanical response of FG thick sandwich plate, *Structural Engineering and Mechanics, An Int'l Journal,* Vol. 70, No. 5, pp. 571-589, 2019.
[201] A. Zenkour, A. Radwan, Hygrothermo-mechanical buckling of FGM plates resting on elastic foundations using a quasi-3D model, *International Journal for Computational Methods in Engineering Science and Mechanics,* Vol. 20, No. 2, pp. 85-98, 2019.
[202] H. Akhavan, S. H. Hashemi, H. R. D. Taher, A. Alibeigloo, S. Vahabi, Exact solutions for rectangular Mindlin plates under in-plane loads resting on Pasternak elastic foundation. Part I: Buckling analysis, *Computational Materials Science,* Vol. 44, No. 3, pp. 968-978, 2009.
[203] A. Neves, A. Ferreira, E. Carrera, M. Cinefra, C. Roque, R. Jorge, C. M. Soares, Static, free vibration and buckling analysis of isotropic and sandwich functionally graded plates using a quasi-3D higher-order shear deformation theory and a meshless technique, *Composites Part B: Engineering,* Vol. 44, No. 1, pp. 657-674, 2013.
[204] N. El Meiche, A. Tounsi, N. Ziane, I. Mechab, A new hyperbolic shear deformation theory for buckling and vibration of functionally graded sandwich plate, *International Journal of Mechanical Sciences,* Vol. 53, No. 4, pp. 237-247, 2011.
[205] H.-T. Thai, T.-K. Nguyen, T. P. Vo, J. Lee, Analysis of functionally graded sandwich plates using a new first-order shear deformation theory, *European Journal of Mechanics-A/Solids,* Vol. 45, pp. 211-225, 2014.
[206] R. Meksi, S. Benyoucef, A. Mahmoudi, A. Tounsi, E. A. Adda Bedia, S. Mahmoud, An analytical solution for bending, buckling and vibration responses of FGM sandwich plates, *Journal of Sandwich Structures & Materials,* Vol. 21, No. 2, pp. 727-757, 2019.